Source-Sink Analysis of the Pleistocene sediment routing systems within the Wasatch Mountains, Salt Lake City segment, Utah

Master of Earth Science
Field of study: Petroleum Geology/Sedimentology
Lene Hovda

Abstract:

Source-sink studies consider the sedimentary systems holistically from the erosional hinterland to the depositional basin. Such studies are often challenged by poor constraint on key parameters controlling sediment production, transport and deposition, such as base-level and climate history, drainage catchment area and lithology. The Wasatch Fault is a large active normal fault system in the northern Utah, USA. The fault zone separates the Wasatch Mountains from the Salt Lake Basin, which contained a very large endorheic lacustrine system during the late Pleistocene (Lake Bonneville). Climatic changes caused the lake level to drop in several discrete phases starting at 14.500 years B.P. leaving a series of distinct mappable shorelines. The sediment delivered to these shorelines is derived from a series of drainage catchments linked to seven major canyons that cut across the Wasatch Fault Zone. Each of these catchments drains a specific lithology in the footwall of the fault. The bedrock lithologies, including granite, quartzite, limestone and a soft, Triassic mudstone, were eroded and then deposited as alluvial fans and fan deltas at the mouths of the different canyons. This area is thus well suited for studying source-sink relationships since the recent base-level history, source area geology, climate, catchment area and the subsequent shoreline deposits are all well constrained.

Catchment and fan characteristics were studied using 2 m lidar derived DEM and fieldwork, looking at lithology in the different catchments and fans.
Results illustrate that the largest fans are associated with the most resistant catchment lithologies. This somewhat counter-intuitive result is because the more resistant areas of the catchment were associated with the highest altitudes and were glaciated during the Last Glacial Maximum. Glacial processes significantly increased the production of sediment. Additionally north-south longshore currents during Lake Bonneville times have been suggested to be instrumental in controlling volumes and sediments distribution along the basin. Results also suggest that the BQART model which is commonly used in source-sink studies has, in the present case, significantly underestimated the volumes of sediment supplied from catchments to the basin glaciated and to a lesser extent non-glaciated catchments.

Acknowledgment:

Lene Hovda   Bergen 03.June 2013

Table of Content

1. Introduction

Source-sink studies have a holistic approach on the sedimentary system and aim to understand sediment production, transport and accumulation along the erosional-depositional system (Driscoll and Nittrouer, 2000; Sømme et al., 2009; Martinsen et al., 2011). Several factors including climate, tectonics, bedrock lithology, water discharge, catchment area, slope and relief tends to control the sediment discharge from the catchment area (Milliman and Syvitski, 1992; Summerfield and Hulton, 1994; Syvitski and Milliman, 2007; Martinsen et al., 2011) which influence morphology of the sedimentary systems and sediment volumes deposited in the basin (Harvey, 2005). The factors can be categorized into internal and external controls (Somme et al., 2011). External controls include climatic and tectonic changes, whereas internal controls on sediment supply generally includes catchment characteristics, such as area, shape, relief, slope and bedrock lithology (Blum and Hattier-Womack, 2009).

The source-sink transect can be divided into four linked segments: the upstream catchment, the shelf, the slope, and the deep-marine basin floor (Fig.1.1) (Sømme et al., 2009; Martinsen et al., 2011). The catchment area controls the amount of sediment discharged to the depositional basin floor and is influenced by both climatic and tectonic factors. The shelf segment plays an essential role in liking the sediment transported from the catchment area to the slope and basin floor, where the latter being the ultimate sink (Sømme et al., 2009). Further, the shelf segment shows the greatest variations in accommodation space, which is mainly controlled by the interaction of sediment supply and base level (sea or lake level) changes (Helland-Hansen and Mart, 1996; Muto and Steel, 2002; Sømme et al., 2009).
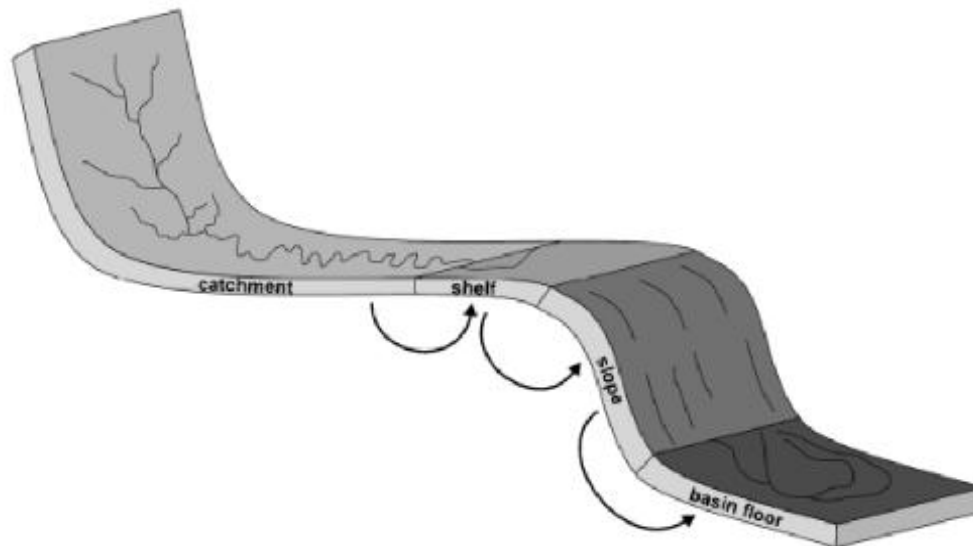
Figure 1.1: *The four linked segments of the sediment transport system, including catchment, shelf, slope and the basin floor, from (Sømme et al., 2009).*

A succession of workers including Bull (1962), Hooke (1968), Bull (1977), Lecce (1991), Milliman and Syvitski (1992), Whipple and Trayler (1996), Eppes and McFadden (2008), and more recent Arzani (2012) have attempted to disentangle the lithological control on bedrock erosion and the associated fan areas. Bull`s (1962) studies of alluvial fans in the Fresno County; California, indicated that the area of fans from erosive catchment lithologies (mudstone and shale) are twice the size of those generated from catchments with lithologies such as quartzite which are most resistant to erosion. In contrast Lecce (1991) reported larger fans in association with resistant catchment lithologies.

The present study is a source-sink study of the Pleistocene sediment routing along the Wasatch Mountains within the Salt Lake City segment of the eastern Salt Lake Basin in Utah, USA. The Wasatch Fault Zone (WFZ), which forms the eastern boundary of the Basin and Range province, is one of the most studied active fault systems in the world (Machette et al., 1991;Stock et al., 2009). The fault dips 50-70º to the west (Cook and Berg, 1961; Smith and Bruhn, 1984; Armstrong et al., 2004) and the fault zone separates the Wasatch Mountains from the Salt Lake Basin. During Pleistocene times, the basin contained Lake Bonneville, a prehistoric lake which fluctuated as a result of climatic changes, leaving distinct shorelines at different elevations. The source to the sediment volumes deposited in the basin and to the shorelines is a series of catchment areas in major canyons that cross cut the Wasatch Fault Zone. There is a significant variety of stratigraphy in the Wasatch Mountains with various

catchments draining different lithologies in the footwall of the fault (Granger et al., 1952; Stock et al., 2009).

The studied drainage systems in the present project are; City Creek Canyon (Fig.1.2), Parleys Canyon, Mill Creek Canyon, Big Cottonwood Canyon and Little Cottonwood Canyon, all of which are located in the Salt Lake City segment on the eastern margin of the Salt Lake Basin. During Lake Bonneville times a series of fan deltas and alluvial fans were deposited at former shoreline positions in front of these catchments as a result of high sediment supply discharged from the Wasatch Mountains (Chan and Milligan, 1994).
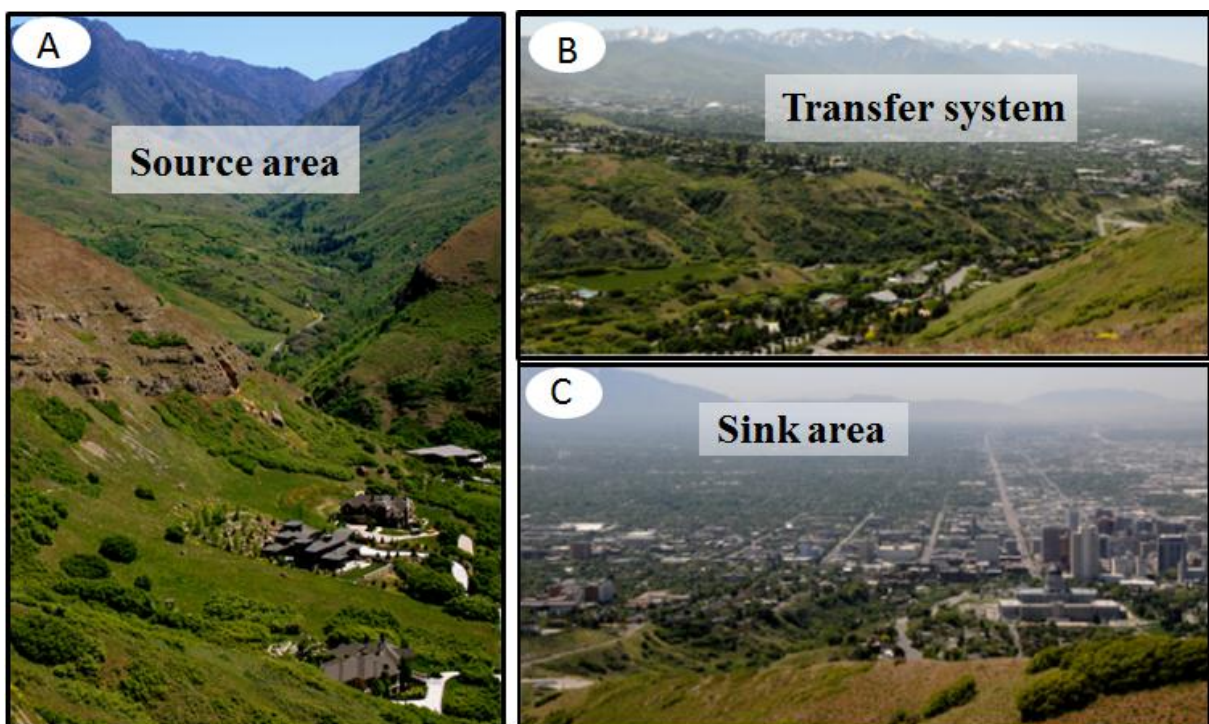
Figure 1.2: *Illustrates typical source-sink segments in the present study area; A) The source area for sediment production and erosion; B) The transfer system of eroded sediments; C) Deposition and accumulation of sediments in the sink area (basin floor). Pictures from the City Creek Canyon (cf. Fig.2.2 for location).*

1.1 Project aims

Calculations of predicted volumes and sediment discharge are standard approaches that are used to understand source-sink systems. In order to understand the link between sediment discharge and accumulation several factors in the sedimentary system, (such as climatic and tectonic history, together with catchment characteristics and lithology) needs to be analyzed.

The main aim of the project is to identify and map different fan deltas within the Salt Lake City segment, and to link these back to the adjacent catchment areas. From this it is possible to investigate how differences in fan volumes and sediment discharge are related to tectonic and climatic factors, along with catchment characteristics and bedrock lithology. An additional aim is to identify how the various bedrock lithologies within the catchments, controls the lithological distribution in the sink area.

The sediment volume calculations were accomplished by a geometrical approach, based on mapping the individual fan delta systems from very high resolution terrain data (from aerial lidar) and then estimating the thicknesses. The BQART model introduced by Syvitski and Milliman (2007), which describes the relationship between catchment area, lithology, climatology, topography and human impact, was used for estimating volumes of sediment discharge from the various catchment areas.

Studies of lithologies within the fans and their source areas were undertaken in the field, with the main focus on the lithology distribution of the clasts deposited in the sink. By detail clast-analysis of these deposits, the lithologies could be traced back to their source, and hence the transport and part of the erosional and depositional system could be interpreted. Additionally a large spit system at the southern boundary of the segment (Point of Mountains spit, cf.Fig.2.2 for location) was studied to establish any possible influence of sediment distribution by longshore currents along the basin during Lake Bonneville times. The key parameters controlling sediment production, transport and deposition are all well illustrated in the study area. This, together with the short distance between the catchment area and the basin, makes it a good location for source-sink studies.

2. Geological setting

2.1 The Wasatch Fault Zone

The study area is in the northern Utah, in the eastern Salt Lake Basin near Salt Lake City. Salt Lake City is located within the hanging wall of the Wasatch Mountain Fault Zone which is a 343 km long, active fault zone (Machette et al., 1991; Lemons et al., 1996; Stock et al., 2009) with up to 11 km of throw (Parry and Bruhn, 1987; Ehlers and Farley, 2003). Fault segmentation in the Wasatch Mountains is well documented by workers such as Cluff et al. (1975), Machette et.al (1991), Schwartz and Coppersmith (1984), Black et al. (1996), DuRoss (2008) and DuRoss et al. (2012). The Salt Lake Basin is bounded by two uplifted blocks called the Wasatch Range and the Oquirrh Mountains (located to the east and west respectively), which has given the basin an asymmetrical horst and graben structure (Gawthorpe and Leeder, 2000). The greatest throw and uplift are on the Wasatch side and the mountain-valley topography is a result of crustal extension and normal faulting which started approximately 16-17 Ma (Lemons et al., 1996; Lemons and Chan, 1999).

The Wasatch fault zone (WFZ) is divided into at least ten seismically independent segments, and evidence of Holocene and Pleistocene surface faulting occurs in five of those segments (Bruhn et al., 1987; Machette, 1992; Lemons and Chan, 1999; DuRoss et al., 2012). The central segments, named Brigham City (36.5 km), Weber (56.5 km), Salt Lake City (40 km), Provo (59 km), Nephi (41.5 km) and Levan (26 km), all shows a curved form in map view indicating a linked extensional fault system (Fig. 2.1). The individual segments of the WFZ ranges in length from 11-17 km up to 60-70 km, where the longest segments with highest slip rate and topography are found in central parts of the WFZ (Machette et al., 1991; Parry and Bruhn, 1987; Gawthorpe and Leeder, 2000). This study focuses on the Salt Lake City segment (marked red in Fig.2.1).
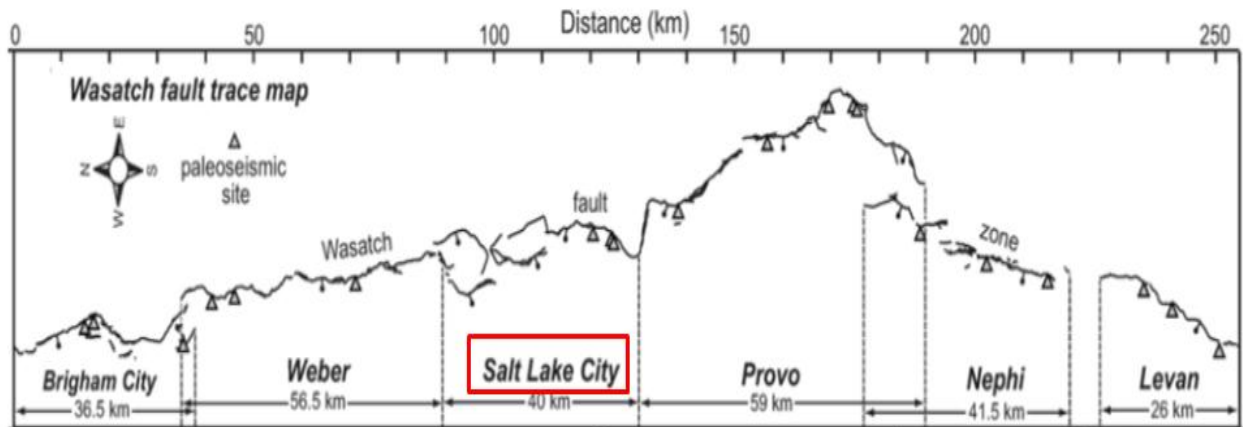
Figure 2.1: *Fault geometry and locations of the central segments within the Wasatch Fault Zone (WFZ). Black vertical lines represent segment boundaries and red marks the study area, the Salt Lake City segment, slightly modified from (DuRoss, 2008).*

2.2 Tectonic activity within the Salt Lake City segment

The Salt Lake City segment (SLC) is a 37.5 km long segment bounded by the Weber segment in the north, and the Provo segment in the south (Fig.2.1) (Machette et al., 1991; Machette, 1992). The segment can be traced from the Traverse Mountains in the south, through the Salt Lake Basin, and up to the Salt Lake Salient in the north (Fig.2.2) (Granger et al., 1952; Machette, 1989; Lund, 1990). The highest water and sediment discharge towards the Salt Lake Basin are by seven major catchments from the eastern side of the Wasatch Mountains (Lund, 1990). The major catchments in the segment are City Creek Canyon, Red Butte Canyon, Emigration Canyon, Parleys Canyon, Mill Creek Canyon in the northern part, and Big Cottonwood Canyon and Little Cottonwood Canyon in the southern part of the segment (Fig.2.2).
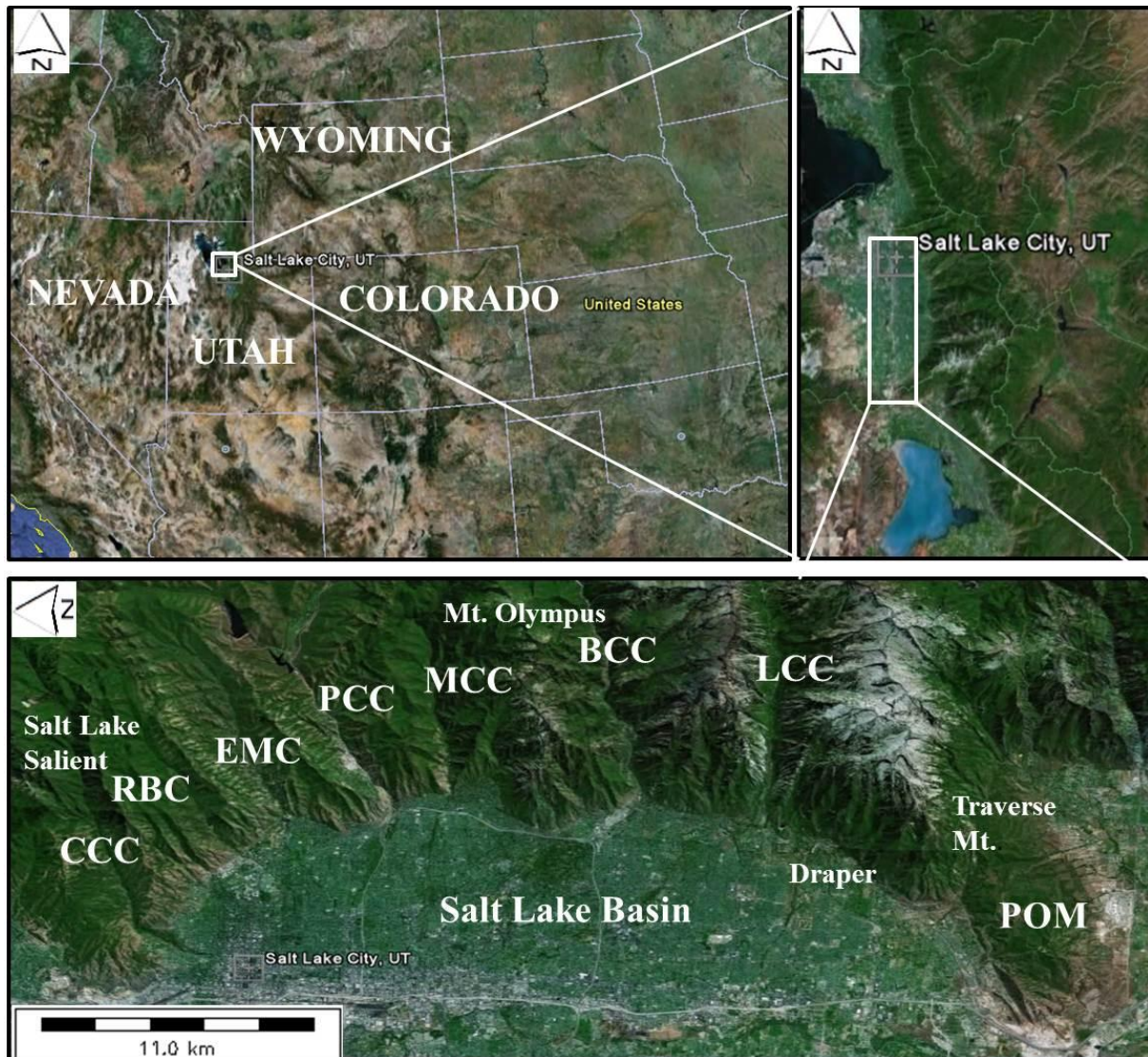
Figure 2.2: *Overview map of study area (Utah, Salt Lake City) and the seven major catchments within the Salt Lake City segment. The major catchments are CCC (City Creek Canyon), RBC (Red Butte Canyon), EMC (Emigration Canyon), PCC (Parleys Canyon), MCC (Mill Creek Canyon), BCC (Big Cottonwood Canyon), LCC (Little Cottonwood Canyon). The spit system is located at the Point of Mountain (POM) in the Traverse Mountains. Base image from Google Earth.*

The present topography in the segment is a result of both uplift of the footwall of the Wasatch Fault and erosion from streams and glaciers (Parry, 2005). Armstrong et al. (2004) documented a long-term exhumation rate of 0.6-1 mm/yr. for the catchments located in the southern parts of the segment, while catchments in the northern parts generally indicated similar exhumation rates as established for the Wasatch Mountains (0.2-0.4 mm/yr.). Using fission track dating of apatite in granite samples from the Little Cottonwood Stock the more rapid uplift in the south has been concluded to have started around 7-11Ma (Kowallis et al., 1990). This resulted in higher topography between the Big Cottonwood Canyon and Little Cottonwood Canyon (BCC and LCC in Fig.2.2 respectively), with peaks ranging between

3300-3400 m. The ridge crests decreases in height towards the north. Peaks dividing the Big Cottonwood Canyon and Mill Creek Canyon (MCC in Fig.2.2) ranges from 2700-3000 m, while the lowest peaks are found in the Parleys Canyon with an maximum elevation of 2500 m. North of the Parleys Canyon (PCC in Fig.2.2) the ridge crest rises up to a maximum altitude of 2700 m (Granger et al., 1952).

Studies of slip rates in a shorter time-scale for the Wasatch Fault Zone have been done by several workers, which suggest a slip rate variation from 0.5-2 mm/yr. along the segments during Pleistocene times (Granger et al., 1952; Machette et al., 1991; Mattson and Bruhn, 2001). Work by Hampel et al. (2010) resulted in a detailed slip rate model for the different fault segments within the Wasatch Fault Zone during the last 40.000 years B.P. (Fig.2.3). This model indicate a slip rate from 0.5-1.41 mm/yr. along the Salt Lake City segment (blue line in Fig.2.3) through time. The highest slip rate is linked to the end of the Bonneville highstand (17.500 years B.P., cf.Fig.2.8), whereas lowest slip rate for the segment is associatied with transgression of the Pleistocene Lake Bonneville (Fig.2.3). The higher slip rate during Bonneville times has established to be related to the ongoing deglaciation after the Last Glacial Maximum (LGM). The deglaciation started slightly after the Bonneville highstand and the accompany variations in water and ice volumes changed the stress field of the crust (Hampel et al., 2010; Karow and Hampel, 2010).
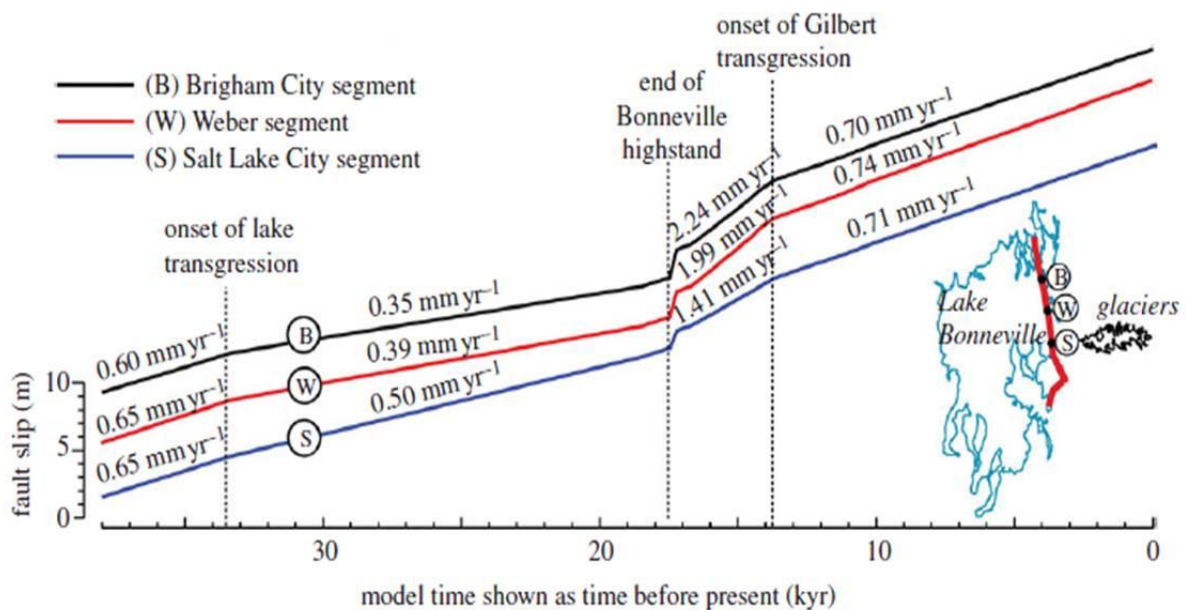
Figure 2.3: *Model illustrating the slip rates in the Bringham City (B), Weber (W) and Salt Lake City (S) segment along the Wasatch Fault Zone (WFZ) through time. Blue line represents the Salt Lake City segment slip rates during the last 40.000 years B.P. The slip rate ranges from 0.65 mm/yr. (40-30.000 years B.P.), 0.5 mm/yr. (30-17.500 years B.P.), 1.41mm/yr. (17.5-14.500 years B.P.) and 0.71mm/yr. (the last 14.500 years B.P.), from (Hampel et al., 2010).*

Active faulting along the segment has formed steep canyons responsible for sediment transport and supply towards the fan deltas. Fault-line scarps, younger than 20.000 years B.P., can be traced throughout the entire SLC segment (Bruhn et al., 1987; Machette, 1989), which indicates multiple surface-faulting earthquakes during Pleistocene times (Lund, 1990; Black et al., 1996). Fault scarps of Bonneville age are observed to be an average of 20-25 m high, while those at the younger Provo level (cf.Fig.2.8) are 10-15 m high (McCalpin, 2002). DuRoss et al. (2012) mapped three major active faults within the Salt Lake City segment, the Warm Springs Fault, the East Bench Fault and the Cottonwood Fault (Fig.2.4). The Warm Springs Fault (Fig.2.4.A) is located in northern parts of the segment situated near the Salt Lake salient (which has according to Gawthorpe and Hurst (1993) been identified as a hanging wall basement high). The East Bench Fault affects catchments such as Mill Creek Canyon, Parleys Canyon, Emigration Canyon and Red Butte Canyon located further south (Fig.2.4.B), and has formed NW-SW tending fault scarps from the Salt Lake City towards the Big Cottonwood Canyon with evidence of 7 m fault scarps in the transgressed Lake Bonneville deposits (cf.Fig.2.8) (Personius and Scott, 1992). The Cottonwood fault has affected Big Cottonwood and Little Cottonwood Canyon, and is found to be a complex fault zone continuing 20 km to the southern end of the segment, and is associated with large scarps and grabens up to 200 m wide (Fig.2.4.C) (Cook and Berg, 1961;Lund, 1990;DuRoss et al., 2012).
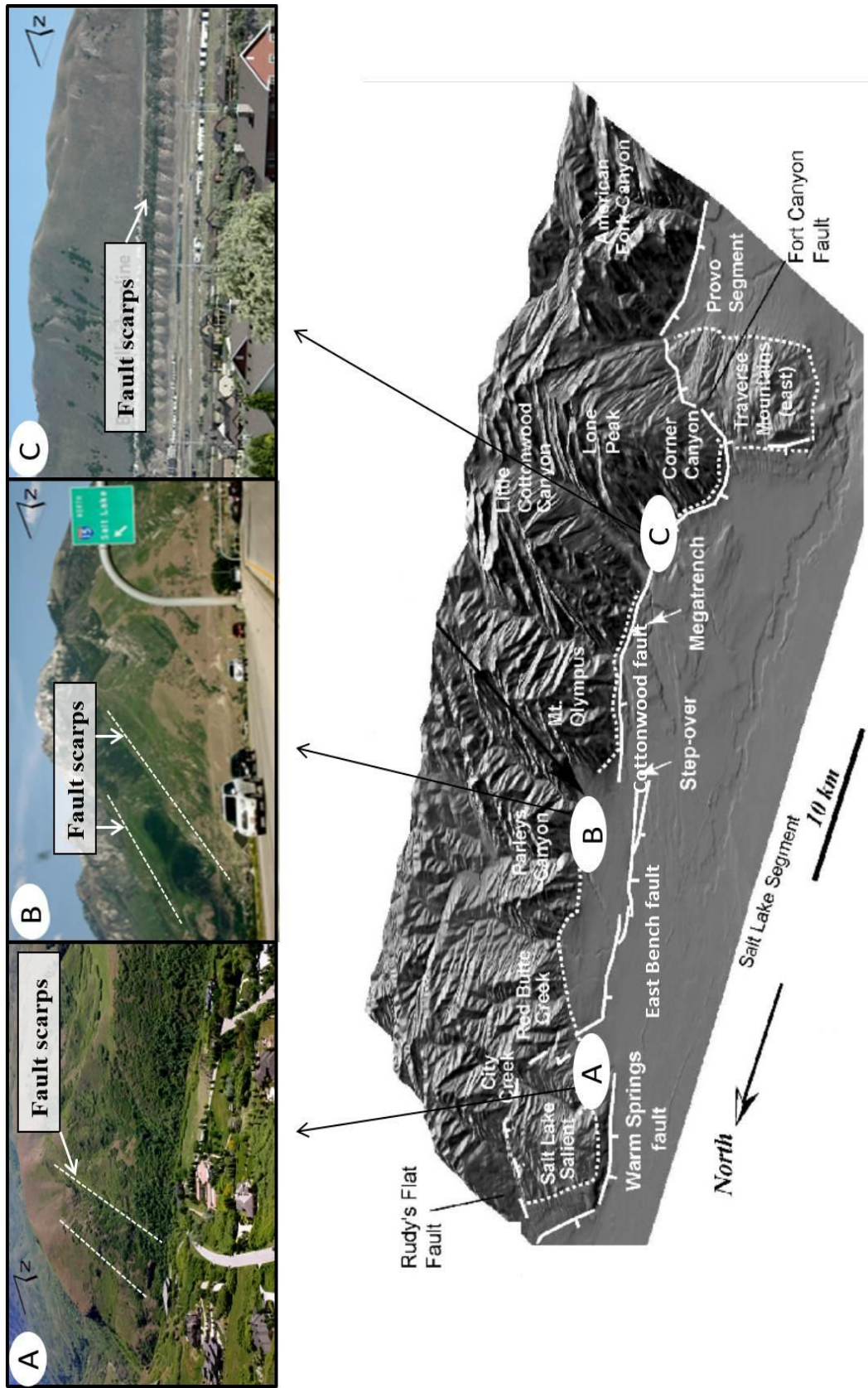
Figure 2.4: *Appearance and location of late Pleistocene faults along the Salt Lake City segment, modified from (Bruhn and Anguita 2013.) A) Fault scarps from the Warm Springs fault, City Creek Canyon, Bonneville level; B) Southern parts of East Bench Fault, Mill Creek Canyon; C) Fault scarps from southern parts of Cottonwood Fault, Little Cottonwood Canyon, Bonneville level.*

2.3 Catchment lithology

Diverse and contrasting bedrock lithologies are exposed along the catchments located in the Salt Lake City segment, including igneous, metamorphic and sedimentary rocks (Case, 1990; Stock et al., 2009; Bryant and Nichols, 1990; Lund, 1990). Work done by Granger et al. (1952) gives a complete study of the catchment lithologies present in the segment. Furthermore, detailed geological maps of Utah and Salt Lake City segment have been completed by Bryant and Nichols (1990) and Hintze et al. (2000), published by the US Geological Survey and the Utah Geological Survey respectively. This section will outline the most dominant lithologies and geological formations in the major catchments surrounding the Wasatch Mountains located in the Salt Lake City segment. A section of the geological map by Hintze et al. (2000) is displayed in Fig.2.5 illustrating the study area. Table 2.1 follows with explanations of the geological formations based on the different color units presented in Fig.2.5.
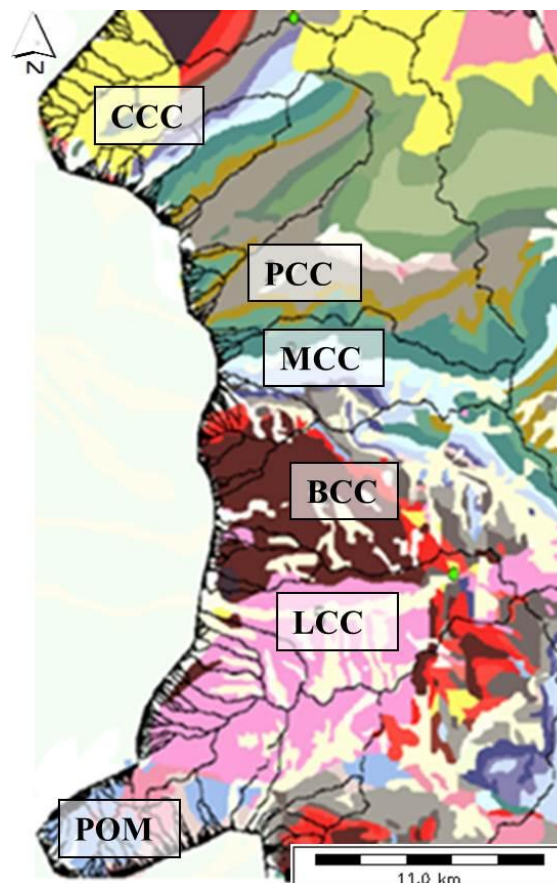
Figure 2.5: *Geological map of the Salt Lake City (SLC) segment slightly modified by Hintze et al. (2000). Major catchments are CCC (City Creek Canyon), PCC (Parleys Canyon) MCC (Mill Creek Canyon) BCC (Big Cottonwood Canyon), and LCC (Little Cottonwood Canyon). POM (Point of Mountain spit, in the Traverse Mountains). Each color represents a geological formation. Explanations of color units and geological formations based on Fig.2.5 follow in Table 2.1.*

Table 2.1: Geological formations and dominant bedrock lithologies extracted based on Fig. 2.5.

Geological time and unit symbols	Formations /bedrock:	Dominant lithology:	Found in:
Proterozoic (Pcs)	Sedimentary and metasedimentary Fm., Big Cottonwood Fm.	Quartzite interbedded with shale	Big Cottonwood Canyon, Little Cottonwood Canyon
Cambrian (C1)	Prospect Mountain, Tintic, Ignacio, Geertsen Canyon, Middle cambrium Fms. St. Charles, Nounan, Bloomington and other Upper Cambrian Fms.	Quartzite, latite, porphyry & tuff, limestone, dolomite	City Creek Canyon, Big Cottonwood Canyon, Little Cottonwood Canyon
Devonian (D)	Pinyon Peak Limestone, Stansbury Quartzite, City Creek Limestone Fms.	Quartzite with nodular limestone	City Creek Canyon, Big Cottonwood Canyon
Carboniferous **(M2)** **(P)**	Great Blue, Humbug, Deseret, Morgan, Round Valley, Honaker Trail, Paradox, Ely, Redwall, Madison, Gardison, Ludgepole Fms.	Limestone with fossils, dolomite, siltstone	City Creek Canyon, Big Cottonwood Canyon, Mill Creek Canyon
Permian (P1) **(P2)**	Toroweap, Park City, Cedar Mesa, Diamond Creek, Arcturus, Kaibab, Opuirrh Group Fms.	Limestone, sandstone	City Creek Canyon, Mill Creek Canyon
Triassic red beds **(Tr1) (Tr2)**	Moenkopi, Dinwoody, Woodside, Chinle, Ankareh, Chainman, Manning Canyon, Doughnut, Thaynes Fms.	Red shale with a smaller amount of limestone, siltstone, sandstone,	Parleys Canyon, Mill Creek Canyon, Big Cottonwood Canyon
Jurassic (J1) **(J2) (Jg)**	Summerville, Entrada, Carmel, Arapien, Twin Creek, Morrison Fm, Glen Canyon Group (Navajo, Kayenta, Wingate, Preuss sst, Moenave Fms and Nugget Sst. Fms.	Limestone, sandstone & siltstone	Parleys Canyon
Cretaceous-Eocene **(K1) (K2)** **(T1)**	Wasatch, Cotton, Flagstaff, Claron, White Sage Indianola, Mancos, Frontier, Straight Cuffs, Iron Springs and other Fms, Dakota, Cedar Mountain, Kelvin, Mesaverde Group, Price River, Kaiparowits, Echo Cyn Fms.	Conglomerate with limestone, sandstone & siltstone	City Creek Canyon, Parleys Canyon, Little Cottonwood Canyon,
Tertiary (Ti)	Little Cottonwood Stock	Intrusive rocks, (Monzogranite)	Big Cottonwood Canyon, Little Cottonwood Canyon
Oligocene (Tov)	Volcanic rocks	Granitic rocks, (rhyolite)	Traverse Mountains, Little Cottonwood Canyon

City Creek Canyon catchment lithologies

The bedrock lithologies in the City Creek Canyon catchment area (CCC in Fig 2.5) are mainly Cenozoic conglomerates (including the Wasatch Fm.), grey, argillaceous limestone (Morgan, Round Valley Fms.) and sandstone (Cedar Mesa, Diamond Creek, Arcturus Fms.) consisting of volcanic clasts and tuff. In addition, conglomerate and sandstone, limestone and quartzite, dolomite and limestone breccia are present (Great Blue, Humbug and Deseret Fms. respectivley) (Granger et al., 1952; Bryant and Nichols, 1990).

Parleys Canyon catcment lithologies

The upper part of the Parleys Canyon catchment (PCC in Fig.2.5) consists of Jurassic/Triassic Nugget Fm., containing pale-grayish-orange, fine-grained sandstone, and white quartz sandstone. Jurassic age Twin Creek Limestone, and red silty sandstone and shale from the Preuss sandstone are also present. The lower basement lithologies are dominated by the early to late Triassic Ankareh Fm. consisting of red sandstone, mudstone and conglomerate (Granger et al., 1952; Bryant and Nichols, 1990).

Mill Creek Canyon catchment lithologies

The dominant bedrock lithology in the Mill Creek Canyon catchment area (MCC in Fig.2.5) consists mainly of dark-grey limestone containing fossil shells from the Park City Fm. and the Thaynes Fm. (Case et al., 2005). In addition, the Weber Sandstone Fm. consisting of pale-yellowish-gray quartzite and calcareous sandstone containing few beds of white limestone and dolomite are present. Moreover, fine-grained sandstone (Nugget Sandstone Fm.), together with a high percentage of red sandstone, mudstone and conglomerate from the Ankareh Fm. are dominant (Granger et al., 1952; Bryant and Nichols, 1990). The Weber Quartzite is also present in the mouth of the canyon.

Big Cottonwood Canyon catchment lithologies

Catchment lithologies in the upper part of the Big Cottonwood Canyon (BCC in Fig.2.5) are characterized by soft sedimentary rocks such as shales, limestone and sandstone, whereas the lower part is dominated by pre-Cambrium quartzite and slates (Hintze, 1914; Bryant and Nichols, 1990). Overall the dominant basement lithology is mainly the Little Willow Fm.

consisting primarily of quartz schist overlain by the Big Cottonwood Fm. consisting of white, green, and gray, pale-reddish-brown weathering quartzite, interbedded with shale and siltstone (Hintze, 1914; Hintze, 1988). Quartz monzo-granite from the Little Cottonwood Stock is observed, together with granodiorite and Jurassic and Permian limestone (Richmond, 1964).

Little Cottonwood Canyon catchment lithologies

The catchment lithologies of the Little Cottonwood Canyon catchment (LCC in Fig.2.5) are dominated by lower Tertiary aged intrusive rocks. These are subdivided into a quartz monzo-granite Little Cottonwood Stock, and a light-gray, biotite-hornblende granodiorite called the Alta Stock. These are separated by white, quartz-sandstone and pale-dark limestone. Little Cottonwood Canyon also includes pre-Cambrium aged folded gneissic quartzite, biotite-muscovite- quartz schist intruded by basic igneous rocks from the Little Willow Fm. (Bryant and Nichols, 1990).

The Traverse Mountains catchment lithologies

The primary catchment lithologies of the Traverse Mountains (POM in Fig.2.5) are from the Oquirrh Fm. consisting of quartzite interbedded with siltstone and shale (Granger et al., 1952; Schofield et al., 2004).

The general pattern of the pre-Tertiary rocks distribution of the Wasatch Mountains along the Salt Lake City segment is an eastwards-pitching syncline with an anticline in the middle. The youngest rocks of Jurassic time are exposed in the Emigration Canyon (EMC in Fig.2.5) just east of the Salt Lake City. Progressively older units are observed towards the south with pre-Cambrian Big Cottonwood series and the Little Willow Fm. in the southern parts of the segment (Jones and Marsell, 1955).

2.4 Pleistocene climate control on catchment glaciations and lake-level fluctuations

Colder climate during late Pleistocene times resulted in glacial appearance in the high-topographic catchments. Climatic changes caused the lake level to drop in several discrete phases leaving a series of distinct mappable shorelines along the Salt Lake Basin. For understanding of the climatic control of the lacustrine system, the next section will focus on the glacial record established in the catchments followed by the hydrography of the Pleistocene Lake Bonneville.

2.4.1   Glacial record in the catchments

Studies of glaciation in the Wasatch Mountains have been undertaken by a succession of workers, including Gilbert (1890), Atwood (1909), Ives (1950), Richmond (1964) and Madsen and Currey (1979). Gilbert (1890) was the first to describe the glacial deposits in the Salt Lake City segment in details, whereas Atwood (1909) studies resulted in a complementary map over the whole area affected by glaciers during Pleistocene time (black area in Fig.2.6). Evidences for two major glaciations in the Pleistocene time have been found, the Bull Lake Glaciation and the Pinedale Glaciation (Madsen and Currey, 1979; Lemons et al.,1996). According to Kaufman (2003) the temperature in the southern part of the Bonneville basin had an average of 1.1±2.5°C during the glacial period until 12.000 years B.P., whereas temperature from 12.000-5.800 years B.P., was an average of 6.6±1.9°C, increasing towards an average of 10.9±1.3°C from 5.800 years B.P. to present time.

Upper parts of Big Cottonwood Canyon and Mill Creek Canyon and whole Little Cottonwood Canyon were covered by glaciers during the full-glaciated period (Ives, 1950; Atwood, 1909; Granger et al., 1952). Canyons located further to the north were not glaciated due to lower elevation and insignificantly snow accumulation (Case et al., 2005). Canyons associated with glaciation, such as the Little Cottonwood Canyon, have a characteristics U-shaped valley formed by ice erosion (Fig.2.6.C). This contrast to the V-shaped canyons formed by stream erosion, such as lower parts of the Mill Creek Canyon (Fig.2.6.B) (Atwood, 1909; Hintze, 1914; Ives, 1950; Madsen and Currey, 1979). No evidence for glaciation occurs in lower part of Big Cottonwood Canyon, which also has a V-shaped morphology. However significant evidence for ice-sheets is observed in the upper part covering approximately 25% of the catchment area (Lemons and Chan, 1999). A large system of moraine deposit is found in the

mouths of both Big Cottonwood Canyon and Little Cottonwood Canyon (Fig.2.6.C) consisting mainly of Archean rocks and monzo-granite from the Little Cottonwood Stock (Atwood, 1909; Eldredge, 2010). Recent work suggests that the ice-sheet in the Little Cottonwood Canyon reached all the way down to the mouth of the canyon and into the Pleistocene Lake Bonneville, with a depth between approximately 140-260 m. A deglaciation of the thick glacial cover began shortly after the Bonneville highstand, approximately 17.500 years B.P. (Laabs et al., 2011).
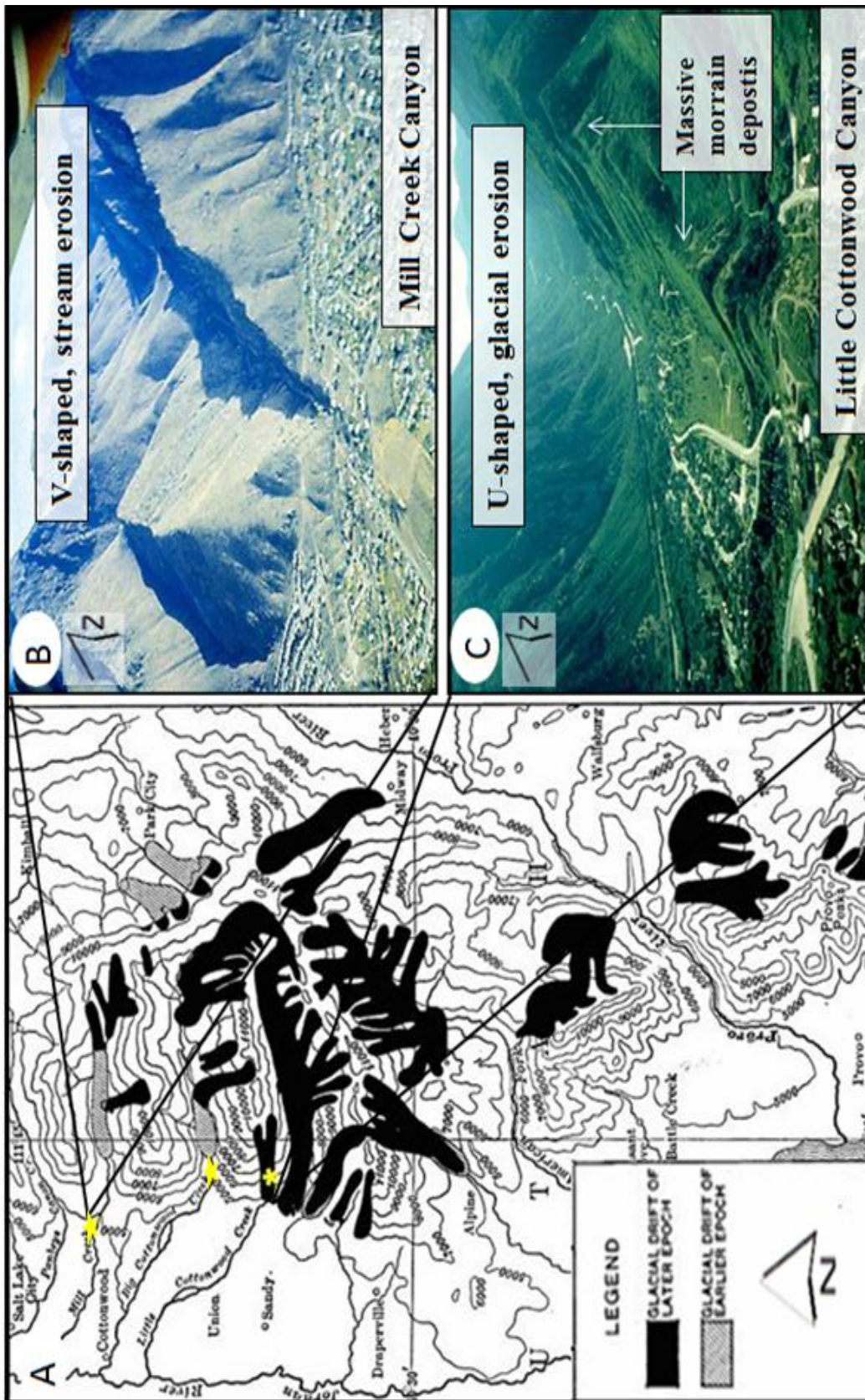
Figure 2.6: *A) Map showing the extent of Pleistocene glaciations (black area) within the Salt Lake City segment, mapped by Atwood (1909). Glacial cover was present in whole Little Cottonwood Canyon catchment and upper Mill Creek Canyon and Big Cottonwood Canyon catchments (marked by yellow stars); B) Lower part of Mill Creek V-shaped canyon after stream erosion; C) Lower parts of Little Cottonwood, U-shaped canyon after glacier erosion, slightly modified from Eldredge, S. (2010).*

2.4.2   Hydrology of Lake Bonneville and paleoclimate

Studies of the correlations between paleoclimate and Lake Bonneville fluctuations have been undertaken by several workers, including Gilbert (1890), Currey et al. (1985) and more recent Oviatt et al. (1992), Oviatt (1997) and Godsey et al. (2005a). A detailed map of the major lake levels was completed by Currey et al. (1984) and published by the Utah Geological and Mineral Survey. Lake Bonneville which is the ancestor of today`s Great Salt Lake, was located in the eastern Salt Lake Basin, and during periods of maximum lake level (18.000 years B.P.) the lake extended all the way to central and northern Utah, Idaho and to Nevada (Fig.2.7) (Gilbert, 1890; Currey et al., 1984). The maximum extent of the lake was approximately 51.3 km^2 with a maximum depth of 372 m (Gilbert, 1890; Currey et al., 1984; Patrickson et al., 2010) making this the largest Pleistocene lake in the Salt Lake Basin (Chan and Milligan, 1994; Lemons et al., 1996; Godsey et al., 2005b).
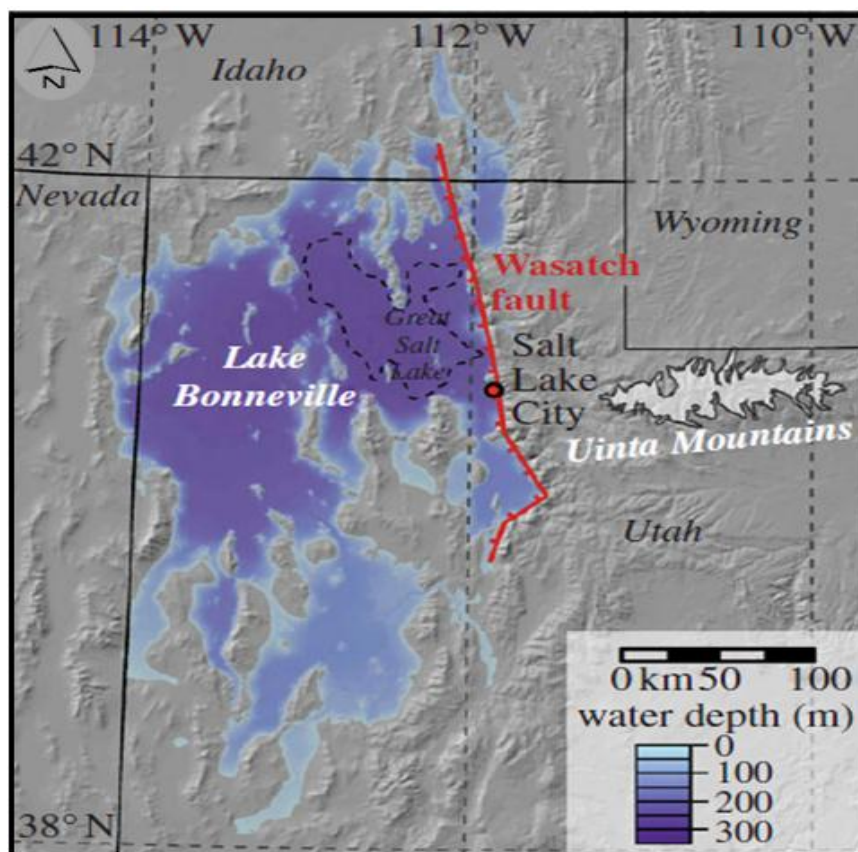
Figure 2.7: *Extent and depth of the Lake Bonneville and the area of the Salt Lake Basin (black, dotted line). Red line represent the different segments along the Wasatch Fault, red circle show location of the Salt Lake City, map from (Hampel et al., 2010).*

The lake has been endorheic (hydrologically closed) for much of its history, making it extremely sensitive to climate changes (Sack, 1999;Patrickson et al., 2010). Lake Bonneville was likely a result of a colder and wetter regional climate during the Last Glacial Maximum (LGM) (Jewell, 2010), and climate models estimates a paleoprecipitation value up to 33% higher than the modern (Mears, 1981; Lemons et al., 1996; Lemons, 1997; Link et al., 1999). The difference in temperature and precipitation pattern are assumed to have been caused by a split in the jet stream by the Laurentide ice sheet during the LGM, which had a large effect on the atmospheric circulation (Kutzbach et al., 1993; Thompson et al., 1993; Schofield et al., 2004; Jewell, 2007; Jewell, 2010).From 30.000-12.000 years B.P. the transgressive/regressive cycle created four mappable shorelines which are detailed summarized by Oviatt et al. (1992). The cycles fluctuated as a response to changes in precipitation, evaporation, stream inflow and water discharge (Currey et al., 1984; Milligan and Lemons, 1998).
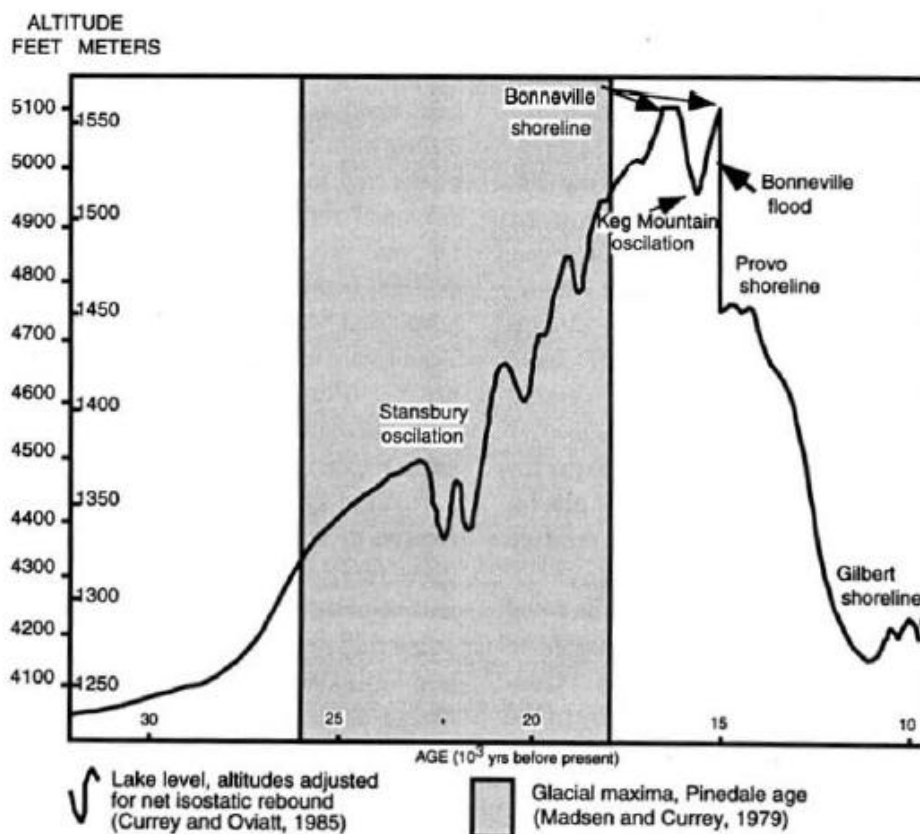
Figure 2.8: *Hydrography of Lake Bonneville with the four mappable shorelines, and time of glacial maximum during the Pinedale age Glaciation (grey area). Elevations of the lake levels are adjusted for isotactic rebound and faulting and correlated with marine isotope stage 2, from (Milligan and Lemons 1998).*

The first transgression 23.000-20.000 years B.P. produced the first shoreline at 1372 m asl called the Stansbury with an approximately surface lake area of 24.08 km^2 (Gilbert, 1890; Currey et al., 1984). The lake level continued to rise, reaching the highest level at approximately 18.000 years B.P., producing the Bonneville shoreline, at 1552 m asl (Fig.2.8) (Currey et al., 1984; Oviatt et al., 1992) which was the maximum level achieved. After the Bonneville flood, at approximately 17.500 years B.P., the lake level fell rapidly 110 m and stabilized at 1445 m asl around 14.500-13.500 years B.P. forming the Provo level (Currey et al., 1984; Godsey et al., 2005b). The Provo level was stable for 2500 years (Jewell, 2007) although it actually represents a series of multiple shorelines formed rather than the single shoreline original proposed by Gilbert (1890). In the original mapping of the shorelines Gilbert (1890) described the Provo deposits as larger than the Bonneville shoreline, although by Provo time the area of Bonneville Lake had decreased by a third (Currey et al., 1984; Sack, 1999). Based on sediment volumes of the Bonneville and Provo component in the American Fork Delta, Gilbert (1890) calculated a duration time for the Provo level and Bonneville level. According to Gilbert (1890) the Provo level was estimated to have existed five times longer than the Bonneville level. Furthermore Pack (1939) estimated a duration time of approximately 2000-3000 years longer for the Provo level compared to Bonneville shoreline. This suggestion has been accepted by several workers, including Ives (1950) and Crittenden (1963).

Warmer and drier climate lead to a rapid drop after the Provo level (DuRoss et al., 2012). Around 11.000-10.000 years B.P., the lake level fell to 1293 m asl (Fig.2.8), marking the lowest mappable shoreline with a surface area of approximately 17 km^2. There was a further, rapid lake level drop over the next 2000 years of approximately 175 m, resulting in the historic low and modern level (Currey et al., 1984; Oviatt et al., 1992). This final regression marked the end of Lake Bonneville cycle and the establishment of the modern Great Salt Lake (Currey et al., 1984; Oviatt et al., 1992; Godsey et al., 2005b; Godsey et al., 2011), indicating dramatic regional climatic changes (Spencer et al., 1984; Godsey et al., 2011). Isotactic rebound, followed by removal of the water has complicated the story in the center of the basin where some of the shorelines are 60-70 m higher (Bills et al., 1994; Hampel et al., 2010; Karow and Hampel, 2010), this does not affect the study area.

2.5 Lake Bonneville deposits and depositional features in the basin

Previous works (Gilbert, 1890; Chan and Milligan, 1994; Jones and Marsell, 1955; Schofield et al., 2004; Godsey et al., 2005a; Godsey et al., 2005b) have identified a number of depositional features along the Salt Lake Basin, including fan deltas and spits. Further, different shoreline positions resulted from Lake Bonneville fluctuations and are prominent landscape elements along the basin (Case, 1990). Each of the shorelines represent a time when the lake level was constant at this elevation long enough to deposits significant amounts of sand and gravel causing the shorelines to advance into the lake.

The term fan delta was originally used by Mcpherson et al. (1987) and Postma and Roep (1985) to describe a gravel rich alluvial fan entering a standing body of water. Several fan deltas have been observed along the Salt Lake Basin both at Bonneville and Provo levels (Fig.2.9) (Jones and Marsell, 1955; Chan and Milligan, 1994). According to Blair and McPherson (1994a) three conditions are needed for fan deltas to form: steep topographic gradients, sediments for fan accumulation and high water discharge for the transport of sediments. During Lake Bonneville times, these conditions resulted in prominent fan deltas, mainly preserved at the regressive phase of the Provo level. Fan delta deposits lower than the Provo level are observed, but are largely destroyed by erosion or human activity (Jones and Marsell, 1955).
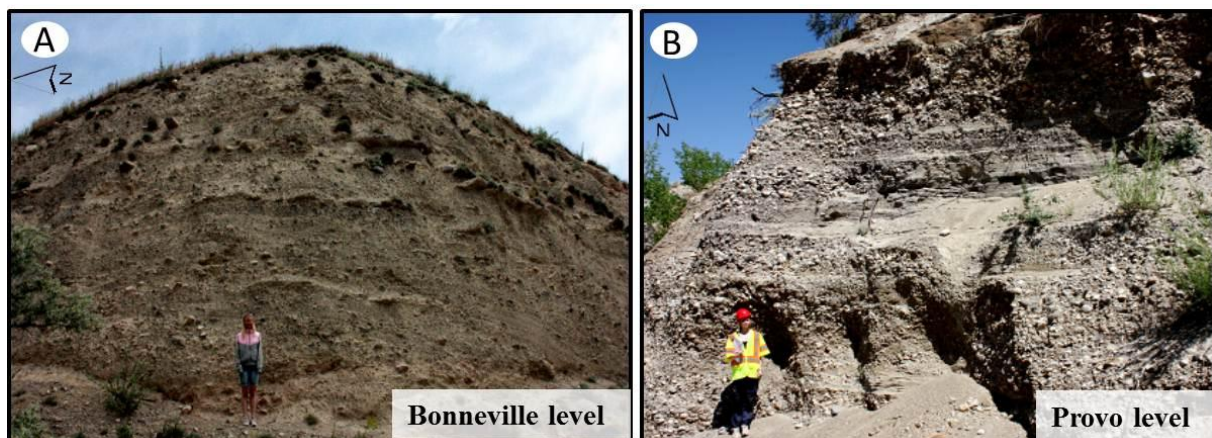
Figure 2.9: *A) Fan deposits at Bonneville level, City Creek Canyon; B) Fan deposits at Provo level, Big Cottonwood Canyon. Cf.Fig.2.2 for locations.*

The term spit has been defined by Evans (1942) as a ridge of sediments attached to land at one end and terminating into open water at the other end, and is characterized by transport of

sediments by longshore currents (Jewell, 2007). Spit formation in the Salt Lake City segment is most prominent in the Traverse Mountains at Point of Mountain (cf.Fig.2.2 for location), consisting of alternating layers of gravel and coarse sand with steeply dipping forests. The spit makes the boundary between the Salt Lake City segment and the more southern Provo segment (Jones and Marsell, 1955; Machette et al., 1991) and is suggested to have been formed by wave action towards the south, which carried sand and gravel to be deposited in front of the Traverse Mountains as a spit (Fig.2.10.A and B) (Schofield et al., 2004; Jewell, 2007). The deposit aggraded and prograded towards the south and the spit system has been suggested to extend approximately 200 m from the Traverse Mountains westward into the Salt Lake Basin (Schofield et al., 2004). Smaller spits have also been identified at the mouths of Big Cottonwood and Little Cottonwood Canyons in a southwesterly direction from the Mount Olympus (cf.Fig.2.2 for location) (Jones and Marsell, 1955). These, were first described by Gilbert (1890) as deltas building out of the mouth of the two canyons at Provo level, but have subsequently been re-interpreted. The spits have similar southward prograding orientation to the Point of Mountain spit system (Jones and Marsell, 1955).
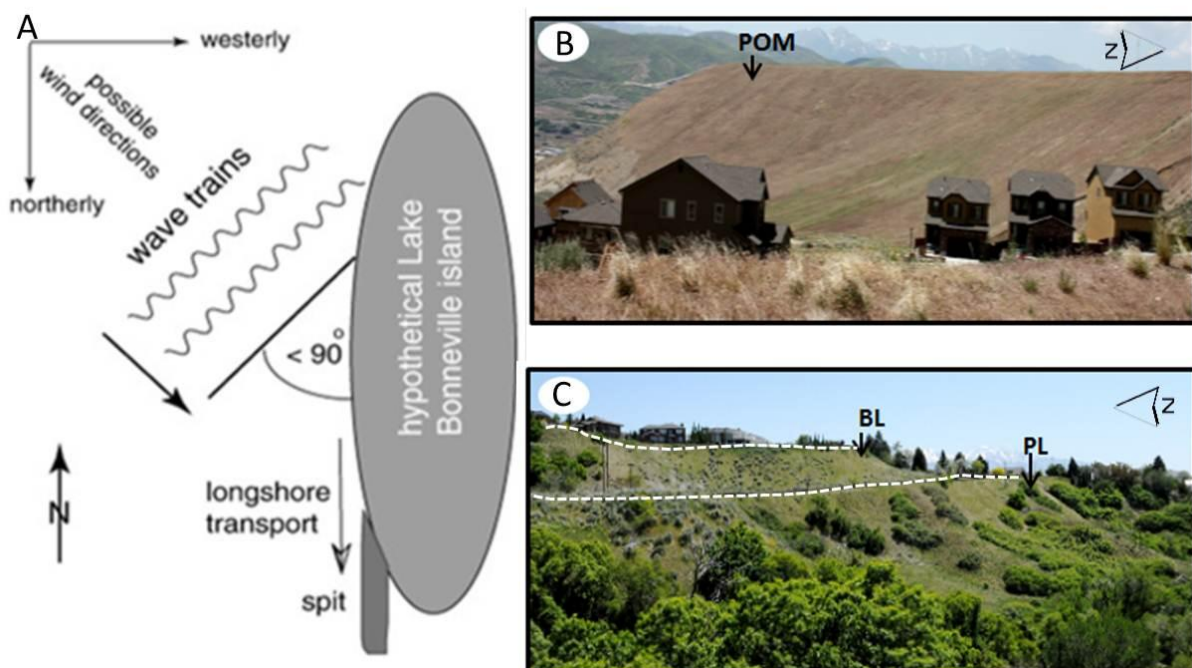
Figure 2.10: *A) Idealized wind and wave direction in Lake Bonneville times along the segment. Longshore transport of sediments from the north resulted in spit formation in the south, from (Schofield et al., 2004); B) Morphology of Point of Mountain spit (POM) located in the southern segment boundary; C) Different shoreline elevations in City Creek Canyon, BL (Bonneville level), PL (Provo level). Cf. Fig.2.2 for map of locations.*

2.6 Catchment area vs. fan area relations

Factors such as tectonic relief and slope, climate, vegetation, catchment lithology and area, together with human and geological factors, all influence the amount of sediment discharged from the catchment area (Fig.2.11) (Bull, 1977; Milliman and Syvitski, 1992; Lemons et al., 1996; Whipple and Trayler, 1996; Vezzoli, 2004; Densmore et al., 2007; Syvitski and Milliman, 2007). Some of the basic principles of analyzing sediment discharge, yields and depositional volumes for a given catchment area are summarized in this section.
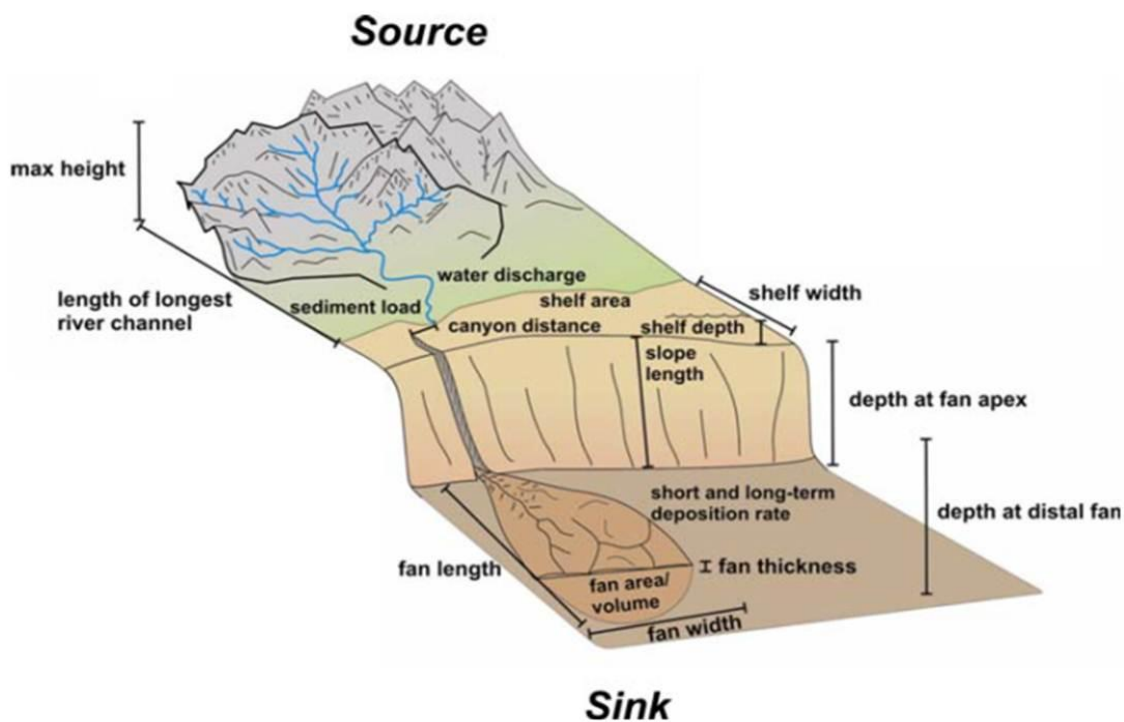
Figure 2.11: *Different parameters controlling sediment discharge from the catchment area towards the basin within a source-sink system, from (Martinsen et al., 2011).*

The correlation between catchment area and fan area is well recognized in the literature by several workers including Bull (1962), Hooke (1968) and Lecce (1991). Bull (1962) was the first to recognize that when the drainage basin area increase the fan area also increases, expressed with the following equation;

$$A_{f=} cA_d^{\ n} \qquad\qquad (2.1)$$

where A_f is the fan basin, A_d the drainage basin, *n* is the exponent coefficient (n=0.88), *c* the empirical coefficient reflecting the lithology of the drainage area (c=1.3 for shale-poor area with ≤70 % shales, c=2.4 for shale-rich area, with ≥70 % shales) (Bull, 1962; Hooke, 1968; Bull, 1972).

It follows that the catchment-fan relation also depends upon the underlying catchment lithology. The primary role of catchment lithology in controlling size of alluvial fans (A_f) was first described by Bull (1964) but later modified to the following equation by Hooke and Rohrer (1977):

$$A_f{}^{1/n} = \sum C_i A_{di} \qquad\qquad (2.2)$$

where A_{di} is the area of the drainage basin consisting of lithology i, and C_i is the coefficient of the relative erodibility of this lithology. According to Hooke and Rohrer (1977) a higher Ci value indicates a higher erodibility rate of lithology i, and a greater sediment contribution to the fan volume, while a low Ci value indicates a lower contribution of sediments. According to Vezzoli (2004) slower erosion of resistant catchment lithology results in higher relief and increasing erosion rate with time, whereas erosion associated with weaker rocks results in low-relief and decrease in erosion rate with time.

The sediment discharges varies with time and are highly affected by tectonic and climatic changes (Leeder, 1997). External factors such as climate and tectonics are closely linked; however tends to operates over different timescales (Harvey, 2002). Climatic changes (humidity and aridity) affect the alluvial fan deposits on a timescales of 10^2-10^4 years, whereas tectonic activity tends to operate on timescales with 10^4 years and more (Harvey et al., 2005). Studies of tectonic activity and the control of sedimentation in rift basins have been disentangled by a succession of workers (Gawthorpe and Hurst, 1993; Allen and Densmore, 2000; Gawthorpe and Leeder, 2000; Cowie et al., 2006; Viseras et al., 2003; Allen et al., 2013). According to Whipple and Trayler (1996) and Allen et al. (2013) sediment discharge tends to increase as the tectonic uplift rate in the area increases. Furthermore, higher rates of tectonic uplift are associated with steeper river profiles, higher erosion rates and greater sediment transport, along with more accommodation space for the deposition of sediments. Climate, affects the sediment production by different rate of bedrock weathering, along with changes in water and sediment discharge and fluctuations in lake levels creating or destroying accommodation space.

The Salt Lake City segment consists of catchments with varying areas and bedrock lithologies, and with a prominent climatic and tectonic history, making this study area a perfect testing ground for some of these principles.

3 Methods

3.1 Introduction

Two weeks of field-work in five of the seven major catchments located in the Salt Lake City segment and their associated fan areas were undertaken. Additionally, calculations of sediments volumes, digital mapping (DEM lidar data) and use of software programs (ArcGis, RiverTools, and Petrel) for extracting catchment characteristics and for fan mapping were done. ArcGis is a geographical information system with intergrated applications such as ArcMap, ArcCatalog and ArcToolbox, and is normally a tool applied for creating and using maps, compiling and analyze geographic information and mapped data. RiverTools is a GIS application normally used for extracting hydrologic data and drainage network flows for large DEM (digital elevation model) data. Petrel is a reservoir modeling software.

A 2 m lidar derived DEM dataset was uploaded to RiverTools software for extracting drainage flow and channel profiles (Appendix A for details). ArcGis software was applied for extracting lithological information from the geological map, and to define the catchment areas within the segment. Petrel was used for fan mapping, including fan area and length. Furthermore Sedlog, which is a software program used for creating graphic sedimentary logs, was used for redrawing logged sections undertaken in the field. Summary of the applied software and definition of estimated parameters are listed in Table 3.1.

Tabel 3.1: Defining geological parameters and applied software

Geological parameters	Description	Applied software
Drainage basin area, (Ad)	Total catchment area which discharge sediments to the fan deltas, (km^2)	RiverTools
Basin length, (L)	Straight-line from the mouth of the canyon to the beginning of the main stream in the drainage basin, (km)	RiverTools
Basin relief, (H)	Vertical distance between the highest elevation of the basin and the fan top, (km).	RiverTools
Catchment lithology	Bedrock lithology in the drainage basin area	ArcGis
Sediment volumes	Sediment (km^3) deposited in the basin during the last 30.000 yrs.	Geometrical exercise
Sediment flux (Qs)	Amount of sediment discharge from the catchments $(km^3/yrs.)$ during Lake Bonneville times	The BQART model
Fan mapping	Fan area (km^2) and length (km)	Petrel
Sedimentary logs	Redrawing of logged sections from the field-work	Sedlog, Corel Draw

The method applied for sediment volumes calculations is a geometrical exercise, using the mapped fan areas combined with an estimate of the lower bounding surface of the fan to define the thickness of the different deltaic packages. Given that there are uncertainties in some of the parameters used in these calculations, a high, mid and low estimate was made of the parameters and combined to give a range of volumes (described in section 3.4).

Estimations of sediment supply can be approached in several ways. Sediment yield measures sediment per unit area per unit time, whereas sediment discharge measures sediment load per unit area (Milliman and Meade, 1983; Milliman and Syvitski, 1992). For estimating the latter a model for predicting global sediment flux (the BQART model introduced by Syvitski & Milliman 2007) was applied (described in section 3.5). This was done to get an understanding of the amount of sediments discharged from the associated catchment areas and to compare with volumes of sediment observed in the basin. Calculations of the sediment volumes and estimations of sediment flux are attached in Appendix B and C respectively.

3.2 Field-methods

Two weeks of field work were undertaken in summer 2012. Much of the area is covered by the present day Salt Lake City, however there are number of good stream sections within the city's parks. Clast analysis, clast counting and facies analysis were undertaken with specific focus on features such as lithology, grain size, texture, and color. 33 clast-analyses were carried out where 11 of the analyzed sections were logged. Additionally a conglomeratic fan in the City Creek Canyon catchment (near Ensign Peak, No.1 in Fig.3.1 for location) was logged and analyzed for extracting dominant clasts lithology in the conglomeratic bedrock. The sink deposits were mainly examined at Bonneville and Provo level, because deposits of the Stansbury level are generally poorly preserved and destroyed by human activity. The logs were plotted by hand on a millimeter paper with scale of 1:50 and later redrawn digitally into Sedlog (See Appendix A for logged sections).

3.2.1   Clast counting and clast analysis

Outcrops in the fan deposits downstream of five of the seven major catchments cutting across the Wasatch Mountains in the SLC segment were analyzed (Fig.3.1 for locations). In addition studies of the Point of Mountain spit (POM 1-3 in Fig.3.1) and the area north of the spit (Draper area) were also undertaken (POM 4-5 in Fig.3.1). The five latter localities were

studied to account for a possible sediment transport by longshore drift along the basin. For each analysis a $100{\times}100$ cm^2 area was marked out and occurrence of the various lithologies were counted. Mean and max clast size were also estimated. Pie-charts of the lithologies in the logged sections were made, along with pie-charts of the average clast lithologies deposited in the different sink areas. Detail information about the $100{\times}100$ cm^2 clast-analysis of the sink deposited, coordinates and logged sections are attached in Appendix A (p.97-111). Locations of the clast-analysis within the Salt Lake Basin are displayed in Fig.3.1 (cf.Fig.2.2 for a complete map of the study area).
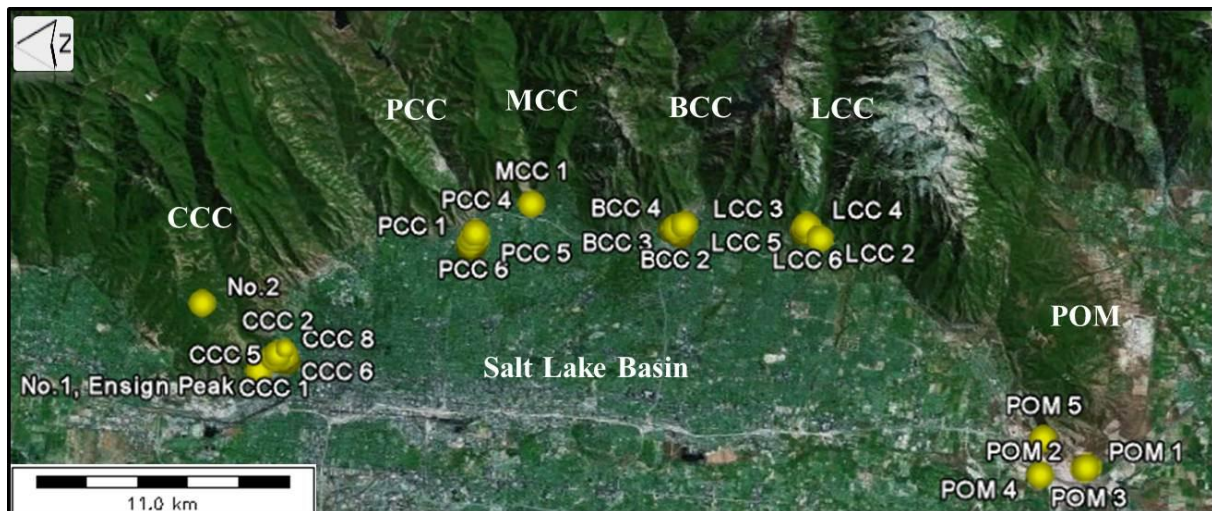
Figure 3.1: *Localities of the sink-analysis within the Salt Lake Basin. CCC1-8 (City Creek Canyon, including Ensign Peak); PCC 1-7 (Parleys Canyon); MCC 1 (Mill Creek Canyon); BCC 1-5 (Big Cottonwood Canyon); LCC 1-6 (Little Cottonwood Canyon); POM 1-5 (Point of Mountain area). Base image from Google Earth. Cf.Fig.2.2 for overview map of study area and Appendix A for coordinates.*

3.2.2   Facies Associations

Facies analysis was not a main focus during the field-work; however to provide an understanding of the depositional environment and processes the deposits were divided into three main facies associations based on different characteristics features. The three facies associations include fan delta deposits, glacial deposits, and wave-dominated deposits. These are presented in the following chapter (section 4.1) in addition to a map of the log localities and a representative logged section for each of the three facies association.

3.3 Digital mapping

3.3.1 Catchment characteristics

In order to calculate sediment volumes and discharge, estimations of catchment characteristics are required. Parameters, such as the drainage flow and channel profiles (basin length and relief) were extracted using a 2 m lidar DEM dataset uploaded to RiverTools software. The drainage flows outline the different catchment areas, and a catchment map (based on the drainage flows extracted from RiverTools software) was imported into ArcGis software for defining the specific drainage catchment areas (Fig.3.2.A). Since the catchment areas have not change considerably since the late Pleistocene, the modern drainage catchments are used in this present study. Geological map of the study area by Hintze et al. (2000) was uploaded to ArcGis and intersected with the extracted catchment areas map (Fig.3.2.B, cf.Fig2.5). ArcGis was then used to extract the geological formations present in each of the catchments (cf. Table 2.1). Based on the bedrock and the geological formations extracted from ArcGis the catchment bedrock was catagorized into seven main lithology groups including: quartzite, limestone, sandstone, conglomerate, volcanic rocks, monzo-granite and shale (Fig.3.2.C).
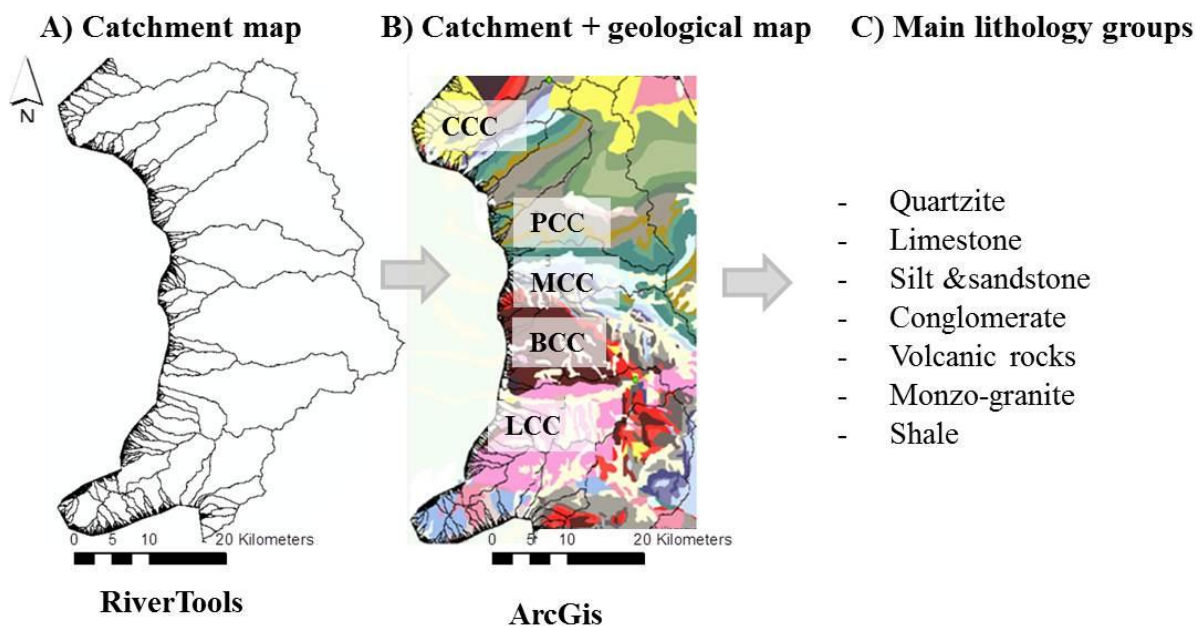
Figure 3.2: *A) Map illustrating the different catchment areas defined from drainage flows using RiverTools software; B) Catchment map intersected with a geological map of the study area by Hintze et al. (2000) for extracting the different geological formations using ArcGis software; Catchments include CCC (City Creek Canyon); PCC (Parleys Canyon); MCC (Mill Creek Canyon); BCC (Big Cottonwood Canyon); LCC (Little Cottonwood Canyon); C) The seven classified lithology groups based on the geological formations extracted from the geological map in ArcGis software.*

Basin shape measures the elongation of the drainage basin area. For a given area the R_f number increases when the basin elongation decreases. Elongation shape of the drainage basin areas was calculated with the following equation:

$$R_f = A_d / L^2 \qquad\qquad (3.1)$$

where Ad is the drainage basin area and L is the basin length (cf. Table 3.1). Results are presented in the following chapter.

3.3.2 Fan mapping

The fan deltas of the seven catchments were mapped using 2 m DEM dataset uploaded to the Petrel reservoir modelling software. Polygons were created for each of the seven fan deltas based on the terrain of the detailed DEM data and contour intervals (Fig.3.3), and fan areas and lengths were extracted. Additionally, using Bull (1962) model (eq. 2.1), the predicted fan areas from the associated catchments in the segment were estimated. From eq.2.1, c=1.3 for shale-poor area with $\leq$70% shales, whereas c=2.4 for shale-rich area, with $\geq$70 % shales. Since all catchments comprises $\geq$70 % shales, c =1.3 were applied in the equation. This gives a predicted model with a positive trend line of the catchment-fan area relation. Results are presented in following chapter (section 4.9).
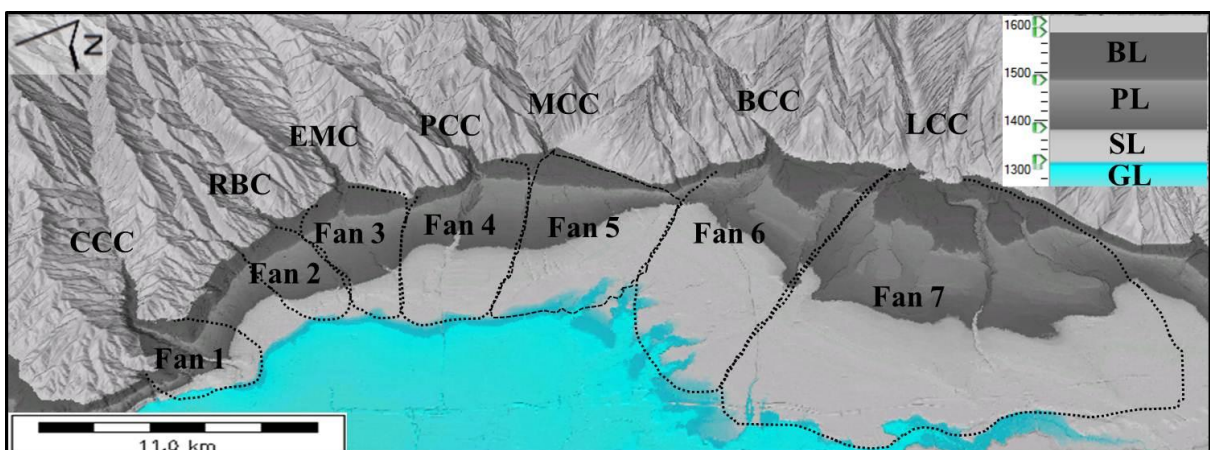
Figure 3.3: *2 m DEM data illustrating the mapped fan delta areas from the seven associated catchments within the Salt Lake City segment. CCC-City Creek Canyon (fan1), RBC- Red Butte Canyon (fan 2), EMC- Emigration Canyon (fan 3), PPC- Parleys Canyon (fan 4), MCC- Mill Creek Canyon (fan 5), BCC- Big Cottonwood Canyon (fan 6), LCC- Little Cottonwood Canyon (fan 7), BL (Bonneville level, 1552 m asl), PL (Provo level, 1445 m asl), SL (Stansbury level, 1372 m asl), GL (Gilbert level, 1290 m asl).*

3.4 Sediment volume calculations

Fan volumes deposited in front of the seven major catchments in the Salt Lake Basin were calculated. The method used was a geometrical exercise which, was applied to calculate the volumes deposited in each individual fan delta lobe associated with the two major shorelines levels (Bonneville and Provo levels), in addition to a total volume of sediments deposits in the basin. The largest uncertainty with this approach was the estimations of the pre-existing lake floor morphology which forms the basal surface of the fans. To address this, a range of surfaces were used. The simplest approach was to project the top of the Stansbury shoreline which lies at 1372 m asl. The top surface was defined by the mapped shoreline elevation. The difference between this surface and top of the Bonneville and Provo levels was used to define the thickness of the different deltaic packages. The subsequent thicknesses of the Bonneville and Provo package are 180 m for Bonneville delta (1552-1372 m asl.), and 73 m for Provo delta (1445-1372 m asl.) (Fig.3.4). The thickness thus reflect the water depth of the lake at the time of deposition.
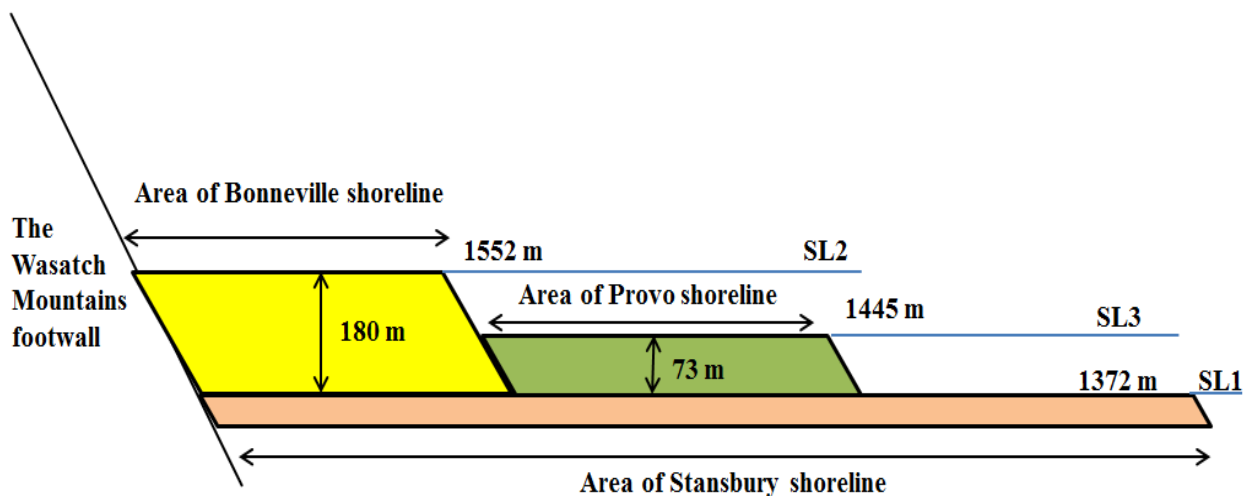
Figure 3.4: *Simplified figure illustrating the area of Stansbury, Bonneville and Provo delta and the thickness of the different deltaic packages based on top Stansbury as datum. Stansbury shorelines (SL1) at 1372 m asl. Bonneville shoreline (SL2) at 1552 m asl, Provo shoreline (SL3) at 1445 m asl. The thickness of Bonneville delta is estimated to be 180 m, and thickness of Provo delta is estimated to be 73 m.*

The top Stansbury depositional surface may have dipped basinward at between 0° and 15°, the latter being a typical dip for an alluvial fan surface. Low, mid and high case volumes were then calculated using combinations of these parameters. These are displayed graphically in Fig.3.5 as the high (red line), mid. (orange line) and min. (green line) cases. The high case of volumes (red line) represents a flat surface. The mid case of volumes (orange line) represents

a dipping surface of 7.5° from the present mouth of the canyons, while the low case of volumes has the steepest dip (green line) (Fig.3.5).
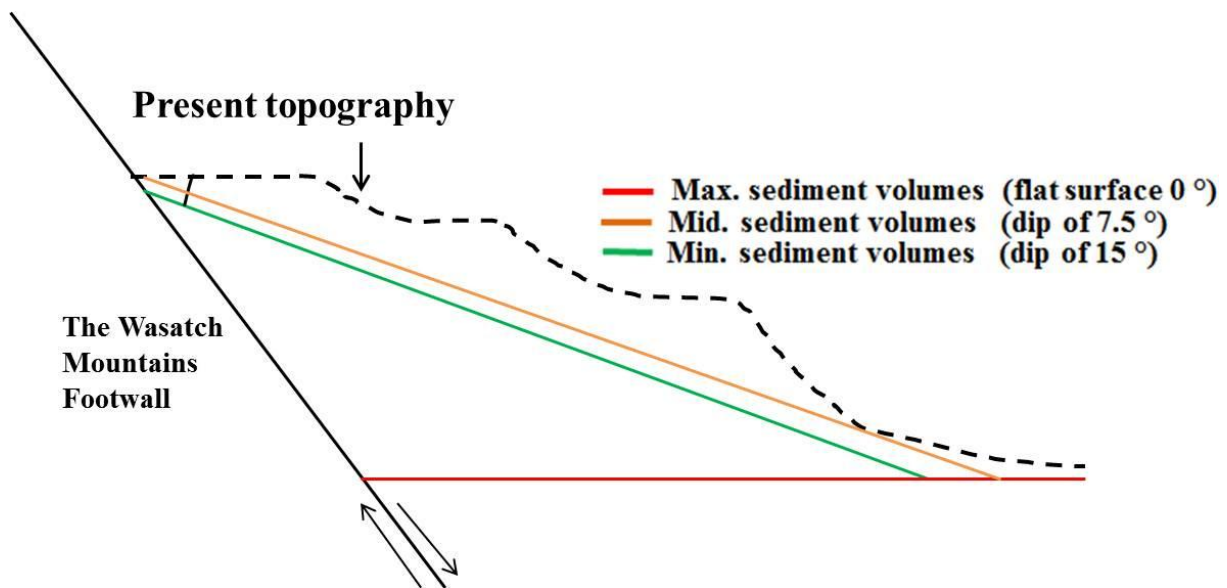
Figure 3.5: *The different ranges of possible sediment volumes based on varies assumptions. Red line maximum sediment volumes based on an assumption of a flat lake floor; Orange line mid sediment volumes based on a dipping surface of 7.5°; Green line minimum sediment volumes based on an assumption of 15° dipping surface.*

The surface area of the two shorelines (Bonneville and Provo levels) and the surface areas of the corresponding fan deltas were extracted using Petrel software (described in fan mapping, section 3.3.2). The relevant area was then multiplied by the relevant thickness accounting for different dip of the basal surface (as described above). See Appendix B for details of the calculations, p.112.

3.4.1 Sediment yield rate calculations

By dividing the calculated sediment volumes with the representative catchment area, (combined with the time constrains for sediment deposition) sediment yield rates were estimated. Time interval of sediment deposition (Lake Bonneville times) is approximately 30.000 years, which presents the time constrain for the yield rates. Results are presented in the following chapter (section 4.10.3, Table 4.8).

3.5 Sediment flux estimations, the BQART model

Sediment flux (discharge) to the basin is influenced by tectonic and geomorphic conditions (relief and catchment area), geology (lithology and glacial cover), geography (runoff and temperature) and human activity. For predicting global sediment flux based on these parameters, Syvitski and Milliman (2007) introduced the BQART model. For catchment systems having a temperature higher than $\geq 2°C$ the sediment flux is expressed with the following equation:

$$Q_s = wBQ^{0,31}A^{0,5}RT \qquad\qquad (3.2)$$

where Q_s is in (10^6t/yr.), $w = 0.0006$ for units of 10^6 t/yr., Q water discharge is in km^3/ yr., B accounts for the important geological and human factors (glacial erosion, lithology reservoir trapping and soil erosion), R is the basin maximum relief in km, A the drainage basin area and T is the average temperature in °C (Syvitski and Milliman, 2007).

Furthermore Syvitski and Milliman (2007) observed a relationship between drainage area (A) and water discharge (Q), expressed with the following equation:

$$Q = 0,075A^{0,8} \qquad\qquad (3.3)$$

where (Q) is in m^3/s and A in km^2.

Sediment fluxes (Q_s) from the BQART model is given in 10^6 tons, but converted to km^3 for comparison with the results of the calculated sediment volumes (method described previous section). Making this conversion from weight to volume the porosity for the uppermost layer and sediment density has to be considered. In these calculations a porosity of 30% has been applied, along with a sediment density of 2700 kg/m^3. Results are presented in the following chapter (section 4.10.4, Table 4.9). See Appendix C for calculations, p.113-114.

3.5.1 Defining the B factor

The B factor could affect the sediment discharge up to an order of magnitude (Syvitski and Milliman, 2007). To improve the BQART model ability to estimate discharge, some factors need to be determined:

$$B = I \times L \times (1 - T_E) \times E_h \qquad\qquad (3.4)$$

where *I* is the glacial erosion factor, *L* is the lithology factor, T_E is the sediment trapping factor, whereas E_h is the human-influenced soil erosion factor. These two latter factors will not be considered in the calculations; however differences in glacial erosion (*I*) and lithology factor (*L*) within the segment are well established and accounted for in these calculations.

Glacial erosion factor *(I):* Vezzoli (2004) observed a positive relation between glacial erosion and sediment production. Based on those observations Syvitski and Milliman (2007) expressed in the following algorithm for glacier erosion factor (*I*):

$$I= (1+0.09A_g) \tag{3.5}$$

where A_g is the percentage area from the total catchment area covered by glacier (Syvitski and Milliman, 2007). The glacial erosion factor (*I*) from eq.3.5 can range from 1 (0% glacial cover) to 10 (100% glacial cover).

Glacial erosion factor (*I*) needs to be considered during the time interval of full-glaciation (30-12.000 years B.P.) for Little Cottonwood Canyon, Big Cottonwood Canyon and Mill Creek Canyon. A well-documented record of full catchment glaciation is established for the Little Cottonwood Canyon during Lake Bonneville times, giving a glacial erosion (*I*) of 10.0 (A_g=100 %). However, only upper parts of Mill Creek Canyon and Big Cottonwood Canyon catchments were covered by ice in the glacial period. According to Lemons and Chan (1999) Big Cottonwood Canyon catchment had a glacial cover (A*g*) of 25 % of the total catchment area, whereas the Mill Creek Canyon has established to have a thinner ice and lower glacial cover compared to the Big Cottonwood Canyon. Based on Atwood (1909) mapped extent of the Pleistocene glaciers in the SLC segment (cf. Fig.2.6) a glacial cover (A*g*) of 15% is applied for the Mill Creek Canyon catchment in eq.3.5. The above *Ag* values give a glacial erosion factor (*I*) of 2.35 and 3.25 for Mill Creek Canyon and Big Cottonwood Canyon respectively (Table 3.4).

Lithology factor *(L):* Based on the hardness of the catchment bedrock (*L*=0.5 less erodible and *L*=3 most erodible), six lithology classes were defined by Syvitski and Milliman (2007) with different lithology factor (*L*):

1) Hard high-grade metamorphic and acid plutonic rocks (*L*=0.5)
2) Mixed, mainly hard lithology (*L*=0.75)
3) Volcanic rocks and carbonate outcrops (*L*=1)

4) Mixed, mainly soft lithology *(L=1.5)*

5) Sedimentary rocks and alluvial deposits (*L*=2)

6) Weak material, crushed rocks or loess (*L*=3)

Based on the lithology classes presented by Syvitski and Milliman (2007) the catchments are categorized into three different classes. City Creek Canyon, Red Butte Canyon, Emigration Canyon, Parleys Canyon and Mill Creek Canyon are associated with sedimentary rocks (*L*=2, class 5), Big Cottonwood Canyon is associated with a mix of lithologies dominated by resistant quartzite (*L* =0.75, class 2), whereas the Little Cottonwood Canyon is associated with volcanic rocks, dominated by quartz monzo-granite (*L*=1, class 3) (Table 3.4).

From eq.3.4 a total *B* factor (*L* × *I*) applied for the glaciated catchments in the glaciated period is 4.7 for the Mill Creek Canyon, 2.4 for the Big Cottonwood Canyon and 10.0 for the Little Cottonwood Canyon. Based on Kaufman (2003) findings a mean annual temperature of 1.1°C is applied in eq.3.2 for the glacial period (30-12.000 years B.P.), 6.6°C for the 12-6000 years B.P. period and a temperature of 10.9°C during the last 6000 years B.P. (Table 3.4).

Table 3.4: Parameters applied for the sediment flux (Qs) estimations, the BQART model

	City Creek Canyon	Red Butte Canyon	Emigration Canyon	Parleys Canyon	Mill Creek Canyon	Big Cottonwood Canyon	Little Cottonwood Canyon
Catchment area (km^2)	45.5	22	47.6	134.3	56.4	130.5	70.9
Max. relief (km)	1.2	1.1	0.9	0.8	1.3	1.4	1.6
Litholgy factor (*L*)	2.00	2.00	2.00	2.00	2.00	0.75	1.00
Glacial erosion factor (*I*)	0	0	0	0	2.35	3.25	10
Water discharge, (*Q*) (km^3/yr.)	0.05	0.02	0.05	0.11	0.06	0.11	0.07
Temperature °C (30-12.000 years B.P.)	1.1	1.1	1.1	1.1	1.1	1.1	1.1
Temperature °C (12-6000 years B.P.)	6.6	6.6	6.6	6.6	6.6	6.6	6.6
Temperature °C (6000-present)	10.9	10.9	10.9	10.9	10.9	10.9	10.9

3.5.2 Uncertainties related to the BQART model

Uncertainty with sediment flux estimations from the BQART model in this study is mainly associated with defining the *B* factor for the catchments including classification of lithology factor (*L*) and the glacial erosion factor (*I*). Catchments dominated by sedimentary rocks are categorized into class 5 with a lithology factor (*L*=2), however different types of sedimentary rocks are observed within the catchments which have dissimilar erodibility rates. Sandstone, which tends to contain relatively high quartz fraction, will be more resistant compared to limestone, shale and siltstone. Limestone (predominantly comprising the Mill Creek Canyon catchment) is highly susceptible to chemical weathering and could be transported as dissolved load, whereas shale (comprising parts of the Parleys Canyon catchment) is more readily eroded.

Results from the BQART model will be affected by the glacial erosion (*I*) factor expressed in the following equation: *I=(1+0.09A$_g$)*. A higher degree of glacial cover (*A$_g$*) gives an increased glacial erosion factor (*I*), which tends to produce larger sediment volumes transported towards the fan deltas.

Warmer temperature and wetter climate are, according to Syvitski and Milliman (2007), associated with higher sediment production, water discharge (*Q*) and sediment flux (*Qs*). Uncertainties are also associated with temperature (*T*) *°C* values applied in the BQART model calculations, especially the full-glacial period temperatures have large error bars ($1.1\pm2.5°C$). Error bars for the 12.000-6000 years interval is $6.6\pm1.9°C$ and $10.9\pm1.3°C$ for last 6000 years. Together these will give uncertainties in the BQART model.

4   Results

4.1 Facies Associations, description and interpretation

Three main facies associations have been interpreted based on field-data from the depositional basin and are described in Table 4.1. Localities and logged sections showing the typical appearance for each representative facies associations are displayed in Fig.4.1 (cf.Fig.2.2 for a complete map of the study area). Deposits from facies association A is the most abundant in the basin. This facies association is interpreted to be fan delta deposits, with sediments both from subaerial and subaqueous components of the fan (Fig.4.2). Facies association B (glacial deposits, Fig.4.3) and facies association C (wave-dominated deposits, Fig.4.4) are observed at particular locations in the segment (Fig.4.1). 11 sections of the 33 studied outcrops (cf.Fig.3.1 for localities) have been logged. Facies association A, fan delta deposits comprises 94 % of the logged section and facies association B, glacial deposits and facies association C, wave-dominated deposits both comprises 3 % of the logged sections (Appendix A for logs, p.97-111).
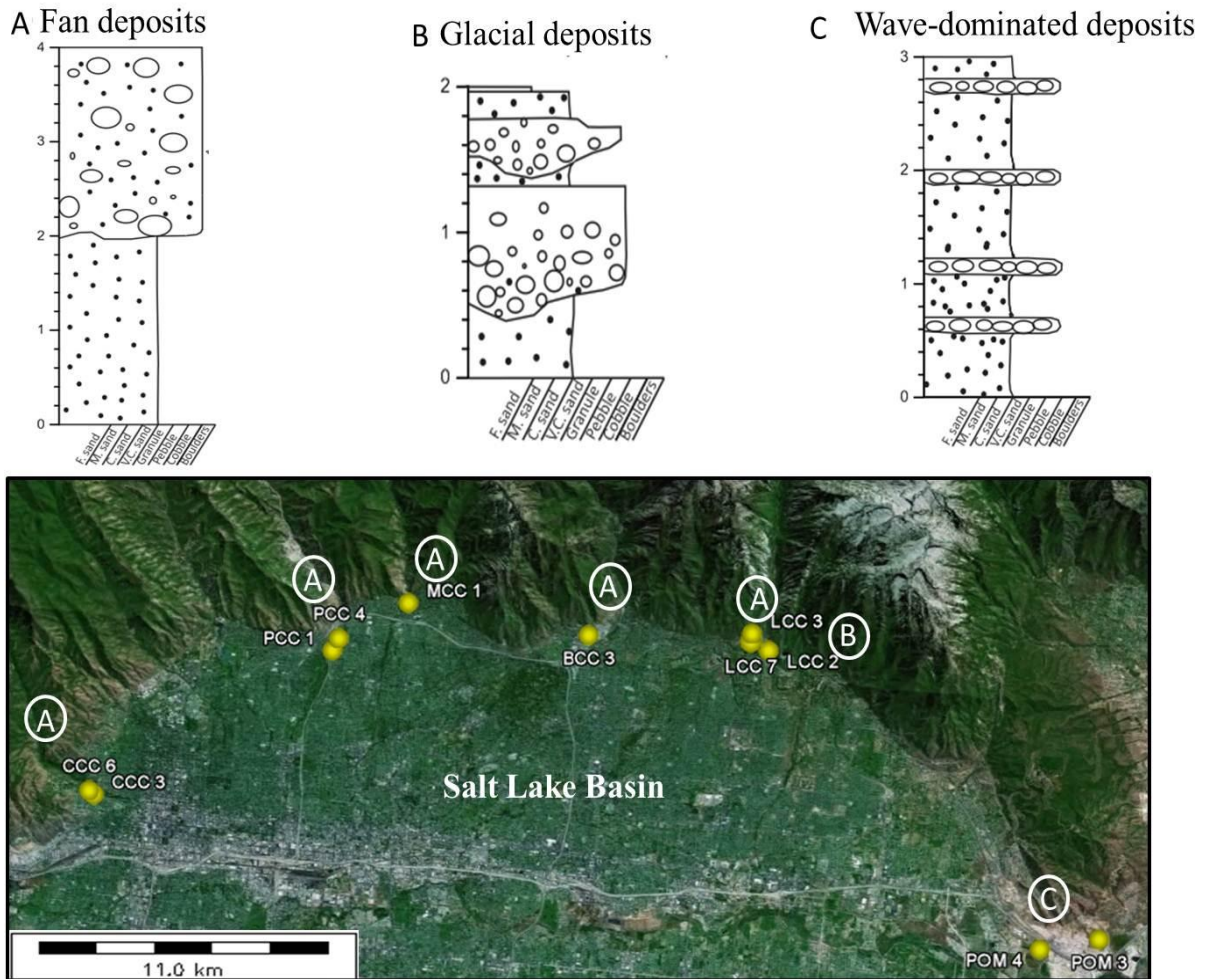
Figure 4.1: *Location of logged sections and a representative log from the three interpreted facies associations within the basin. Facies association A (fan delta deposits) is characterized by matrix-supported conglomerate, with poorly sorted and subangular-subrounded clasts; localities CCC 3, CCC 6, PCC 1, PCC 4, MCC 1, BCC 3, LCC 3, LCC 7, POM 4. Facies association B (glacial deposits) is characterized by larger cobbles and boulders within a finer-grained matrix, location LCC 2. Facies association C (wave-dominated deposits) is characterized by well sorted and rounded granules, interbedded with thinner layers of pebbles and clast-supported matrix, location POM 3. See Appendix A (p.97-111) for logs and coordinates. Table 4.1 for detail description.*

Table 4.1: Facies assocoation, description and interpreation

Facies Association	Description	Interpretation	Observed in
A: Fan delta deposits	**1)** The deposits are conglomeratic and comprise clasts from coarse sand to cobbles and boulders size. The deposits may exhibit a weak fabric but are predominantly massive and chaotic. Clasts are mostly subangular to subrounded and poorly sorted, and poorly graded. The deposits are mainly matrix-supported consisting of a mixture of mud and very fine sand to very coarse sand. The clasts sizes ranges from a few cm up to 45 cm. Dipping beds (approximately 15°) within some of the deposits are observed (Fig.4.2.A). Thickness of the deposits ranges from 1,5-11 m. **2)** The deposits consist of well-sorted and subrounded sand and gravel, with a clast-supported framework. The beds often show horizontally to sub-horizontally stratified layers with occasional sand units present. Thickness of the deposits ranges from 0,5-3 m (Fig.4.2.B)	**1)** The thick, chaotic mixture of poorly sorted clasts without any significant internal layering indicate deposition after debris-flows when the slope or strenght of the flow is reduced. The dipping beds are interpreted to be delta foresets formed when sediment deposition progrades basinwards, making up the subaqueous component of the fan delta. **2)** The clast-supported, well rounded and deposits with distinct imbrication, indicating deposits from stream-flow processes in the mid to lower parts of the fan delta, making up the subaerial component of the fan delta.	**CCC 1-8, PCC 1-7, MCC 1, BCC 1-4, LCC 1,3,4,5,6,7 POM 4-5** (Fig.4.1 for location)
B: Glacial deposits	The deposits are coarse-grained, diamict, normally with clasts ranging from gravel to boulders size within a finer-grained silty-sandy matrix. The deposits are normally relatively unconsolidated with lithology consisting mainly of monzo-granite from the Little Cottonwood stock, additionally to limestone and sandstone clasts. Thickness of the deposits ranges from 0,5-2 m (Fig.4.3)	The unconsolidated, poorly sorted deposits with large boulders in a finer-grained matrix are interpreted to be till deposit of glacial origin. The large cobbles and boulders size clasts within the fine-grained material indicate glacial erosion of sediments and deposition during times of high meltwater discharge to transport large clasts of boulder size.	**BCC 5 and LCC 2** (Fig.4.1 for location)
C: Wave-dominated deposits	The deposits are well sorted and rounded, clast-supported fine-medium gravel, inter-bedded with layers of subrounded, clast-supported very coarse gravel. No evidence of fluvial input. Clast-sizes are relative small ranging from 0,1-5 cm, showing a distinct orientation.Thickness of the deposits ranges from 2-6 m (Fig.4.4)	The deposits show no evidence of fluvial input, and the small, well-sorted and well-rounded clasts along with a clast-supported framework suggest sediment redistribution by longshore drift. These deposits have been interpreted to be a part of a large spit system, formed from longshore currents generated in the Pleistocene Lake Bonneville.	**POM 1-3** (Fig.4.1 for location)
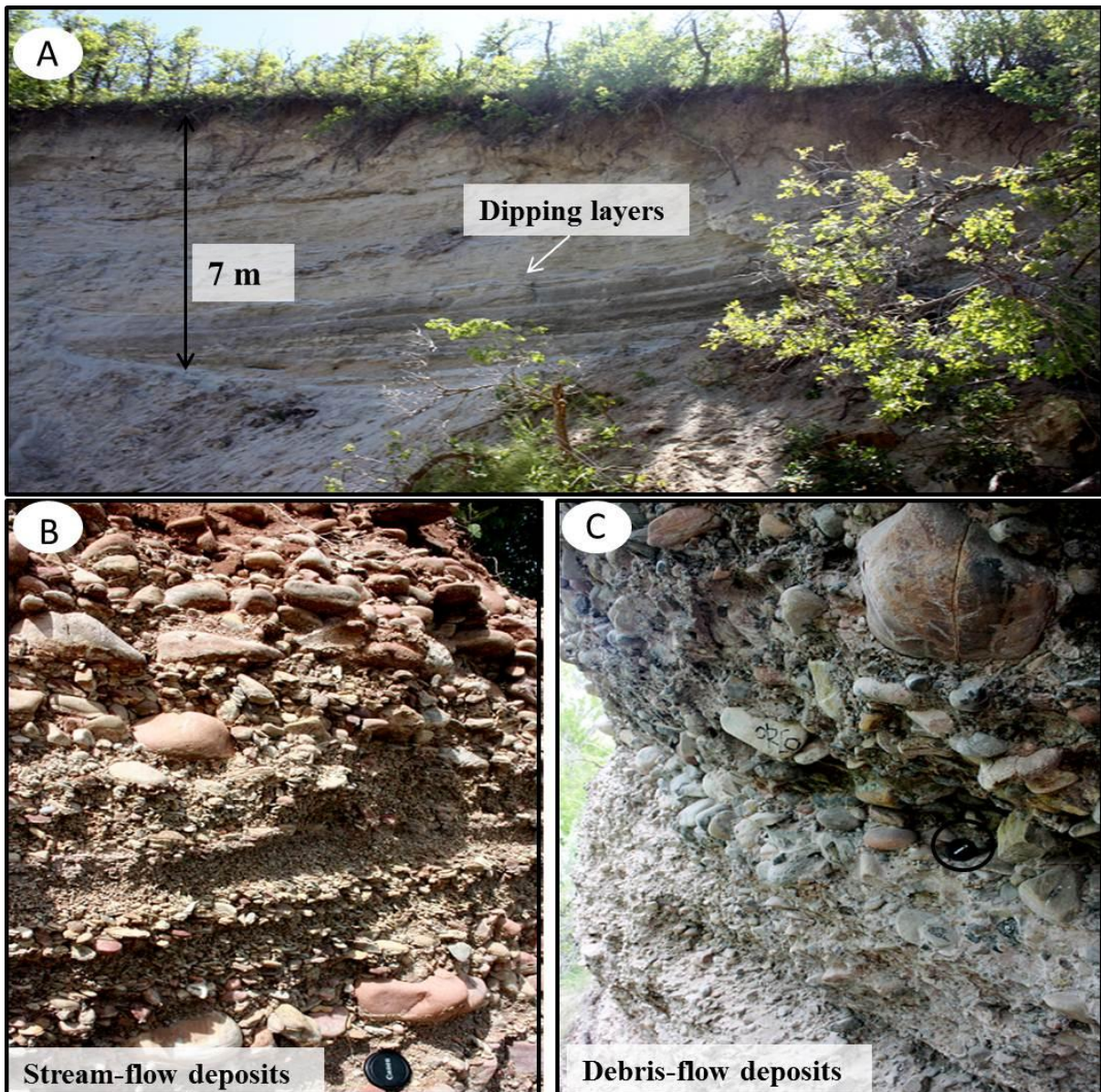
Figure 4.2: *Facies association A (fan delta deposits); A) Fine-grained fan delta with distinct dipping layers interpreted to be delta forests, thickness of the deposits is 11 m, location LCC7 (Appendix A for log p.108); B) Clast-supported framework with good rounded clasts interpreted to be stream-flow deposits, thickness of the deposits is 3 m location PCC 4 (Fig.4.1 for locations and Appendix A for logs,p.102); B) Conglomeratic and poorly sorted clasts interpreted to be debris-flow deposits, thickness of the deposits is 6 m, location CCC6 (Fig.4.1 for locations and Appendix A for logs, p.100).*
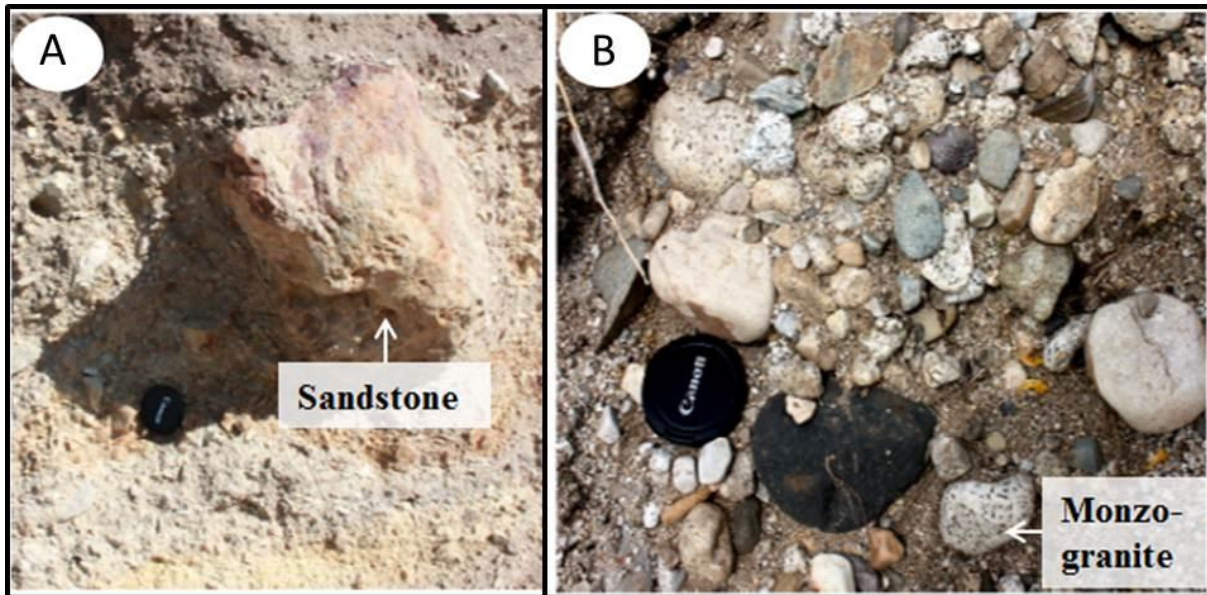
Figure 4.3: *Facies association B (glacial deposits); A) Large boulder size sandstone clast (45 cm) within a fine-grained matrix interpreted to be of glacial origin; B) Diamict deposits, mainly poorly sorted monzogranite clasts, thickness of the deposits is 2 m, location LCC 2 (Fig.4.1 for location and Appendix A for log, p.107).*
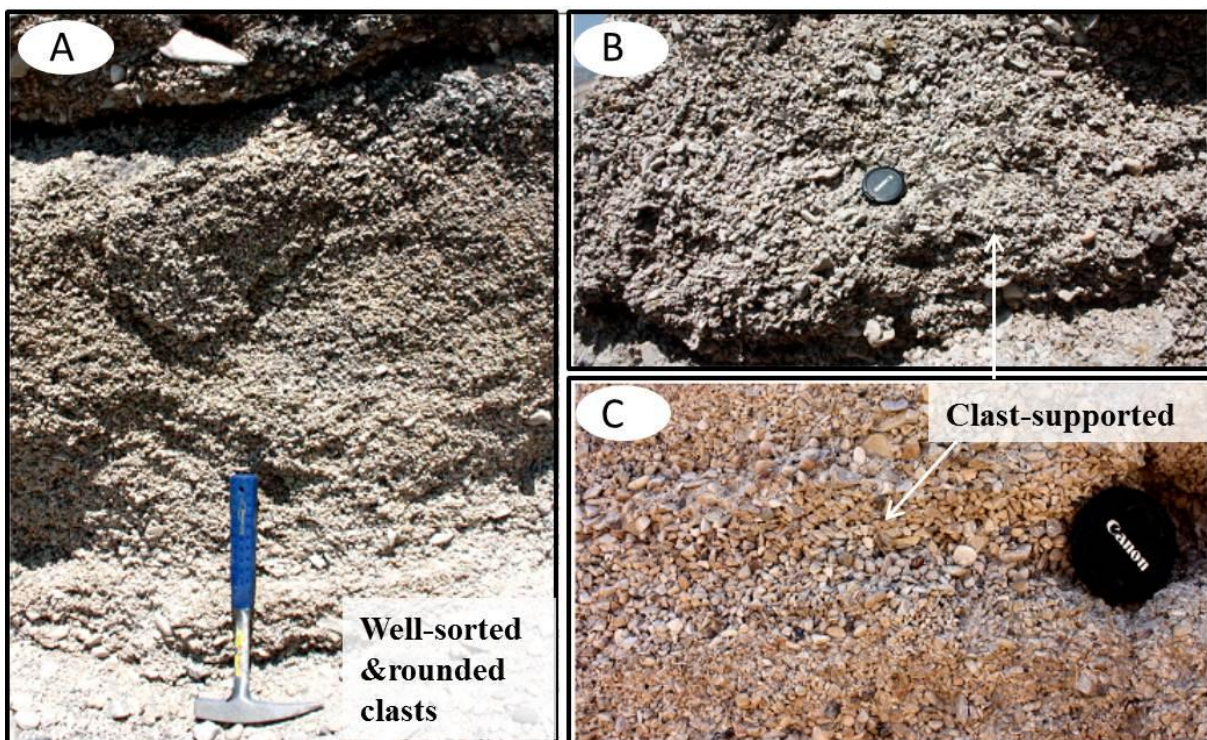
Figure 4.4: *Facies association C (wave-dominated deposits); A) B) and C) Well-sorted and rounded clasts with clast-supported framework and no fluvial input, interpreted to be a part of a larger spit system. Thickness of the deposits is 3 m, location POM 3. (Fig.4.1 for location and Appendix A for log, p.111).*

4.2 Drainage system analysis

4.2.1 Catchment characteristics

To provide a better understanding of the factors controlling sediment discharge from the catchments and sediment deposited in the basin, the complete sedimentary system needs to be analyzed. In this section estimations of different catchment characteristics are presented (Table 4.2). The following sections will, based on field-data, focus on source-sink analysis of the five major drainage systems from the north-south. Finally, the source-sink analysis for the large spit system at Point of Mountain marking the southern boundary of the SLC segment is presented.

Table 4.2: Catchment characteristics and lithology within the Salt Lake City segment [a] from Cook, 1984

	City Creek Canyon	Red Butte Canyon	Emigration Canyon	Parleys Canyon	Mill Creek Canyon	Big Cottonwood Canyon	Little Cottonwood Canyon
Catchment area (km^2)	45.5	22.0	47.6	134.3	56.4	130.5	70.9
Basin length, (L) (km)	16,2	8,5	14,7	22,0	15.8	20.0	17.0
Max. elevation, (km)	2.7	2.6	2.5	2.5	3.0	3.3	3.4
Stream gradient, [a]	0.06	0.13	0.04	0.04	0.07	0.05	0.09
Basin shape, (Rf)	0.16	0.29	0.21	0.27	0.22	0.32	0.24
Present annual precipitaion (cm) [a]	80	76.2	72.6	78.2	96.2	112.3	125.7
Dominant catchment lithologies	Conglomerate, limestone	Shale, limestone	Shale, limestone	Limestone, shale silt&sst.	Limestone	Quartzite	Igneous rocks
Pleistocene glacial cover	No	No	No	No	15 %	25 %	100 %

Fig.4.5 summarizes the shape and drainage network in the seven major catchments in the Salt Lake City segment. Further the main groups of catchment lithologies (quartzite, limestone, sandstone, conglomerate, volcanic rocks, monzo-granite and shale) are presented. Basin shape (R_f) (cf.Table 4.2) affects and control the sediment transport to the fan area together with factors such as basin slope, relief and stream feeder, and have a major impact on the sedimentary processes on the fan system (Blair and McPherson, 1994b). City Creek Canyon,

Emigration Canyon, and Mill Creek Canyon have a low R_f value indicating high elongated catchment shape, whereas Red Butte Canyon, Parleys Canyon, Big Cottonwood Canyon and Little Cottonwood Canyon have a larger R_f value and thereby a lower elongation shape. The drainage network in the segment is mainly dendritic. The drainage network and pattern are influenced by the catchment area, climate (vegetation and run-off) and tectonic, together with catchment lithology and the orientation and presence of basement structures and weakness zones (Cook et al., 1984).
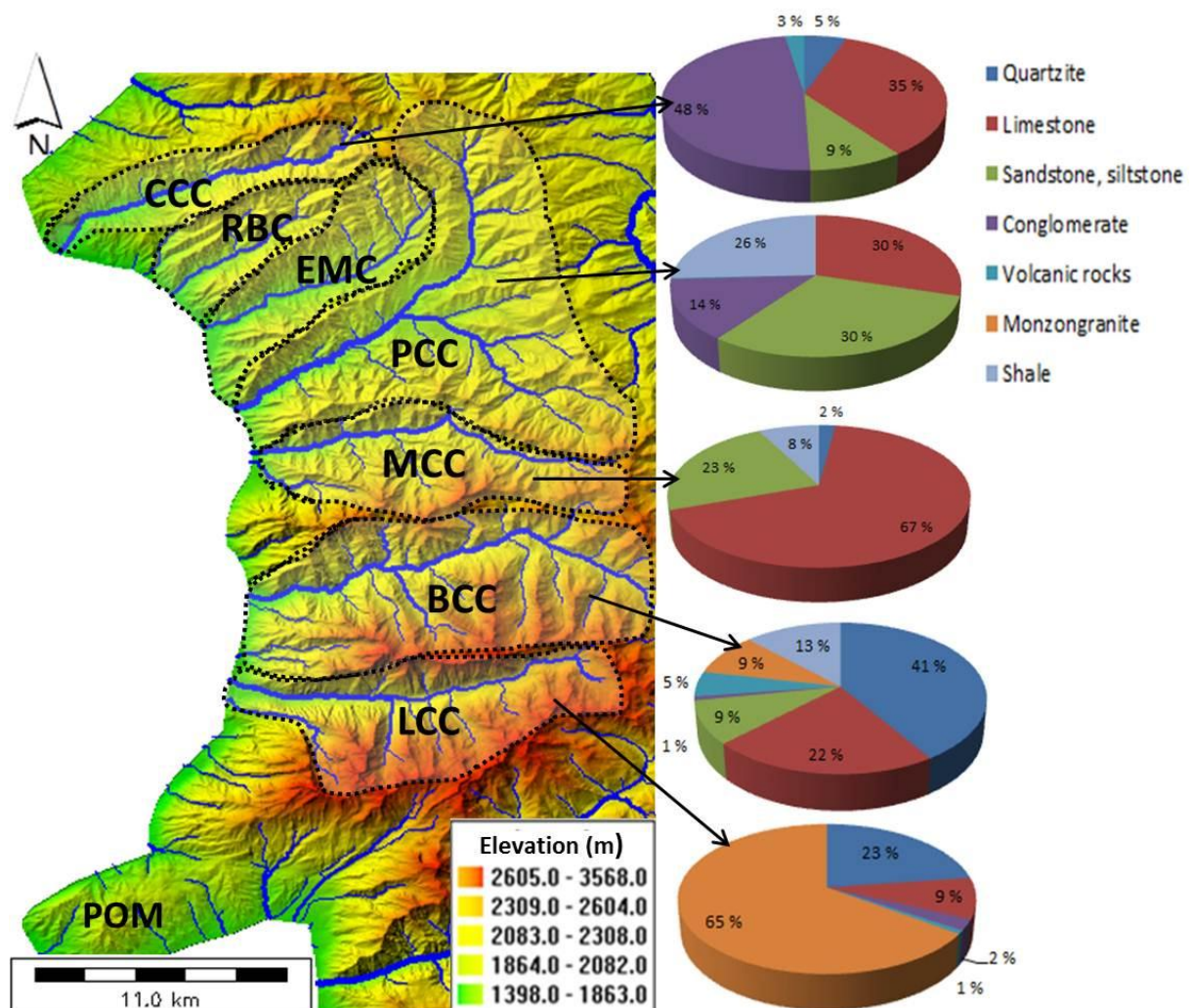
Figure 4.5: *Shaded relief of the Salt Lake City (SLC) segment illustrating the different catchment shapes (black, dotted line), drainage network and bedrock lithologies. The catchments lithologies are divided into seven main groups based on the geological formations extracted from ArcGis (cf. Fig.2.5). Color label represents the different elevations (m), from lowest elevation (green) to the highest elevation (red). The major catchments are CCC (City Creek Canyon), RBC (Red Butte Canyon), EMC (Emigration Canyon), PCC (Parleys Canyon), MCC (Mill Creek Canyon), BCC (Big Cottonwood Canyon, LCC (Little Cottonwood Canyon), POM (Point of Mountain spit, located in the Traverse Mountains).*

4.3 Source to sink analysis of the City Creek Canyon drainage system
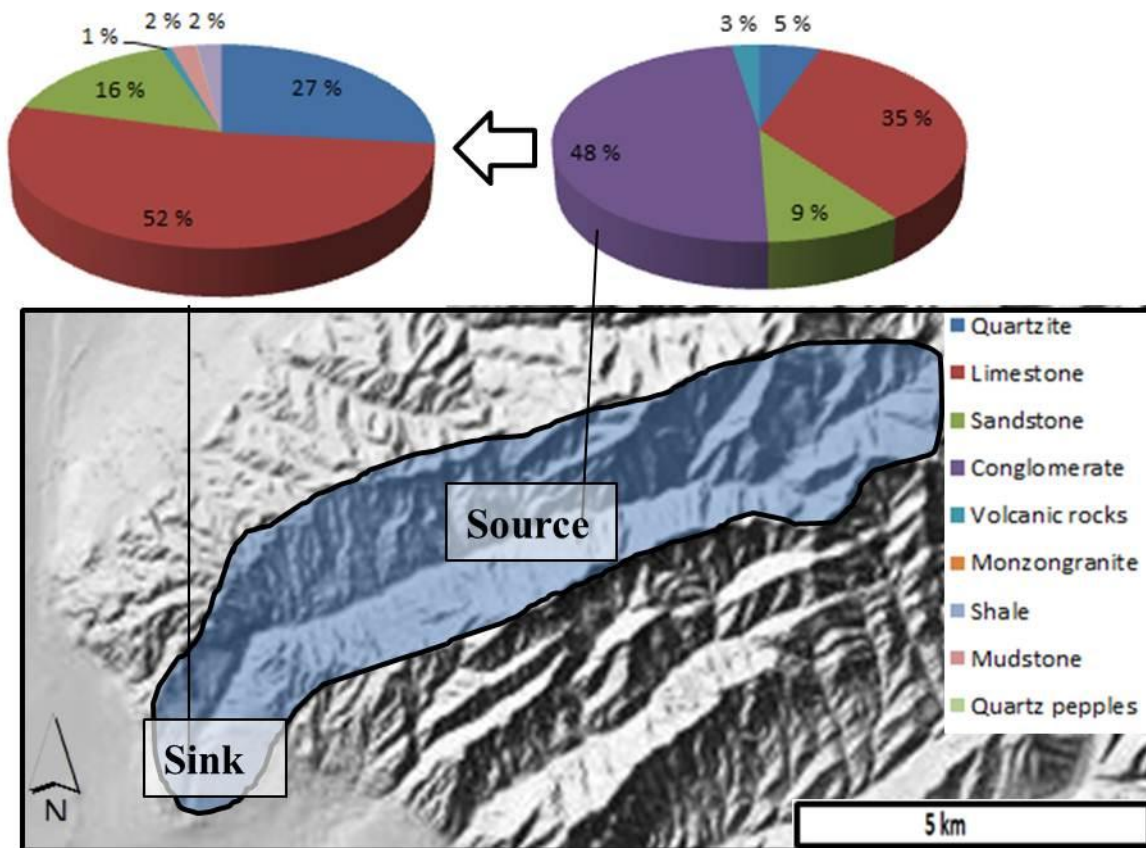
Figure 4.6: *Catchment lithology and clast lithology in the City Creek Canyon (pie-charts). Terrain data extracted from 1.25 m lidar earth data (http://stage.mapserv.utah.gov/raster/).*

4.3.1 Catchment area

City Creek Canyon is located in the Salt Lake Salient, and is the northernmost catchment in the SLC segment (cf.Fig.2.2). The extracted lithologies in the catchment consist of 48% conglomerate, 35 % limestone, 9 % sandstone, 5 % quartzite and 3 % tuff and porhyr (Fig.4.6). The geological formations in the catchment are mainly conglomerate of Wasatch Fm. (Fig.4.7.B) together with limestone of Morgan, Round Valley, Great Blue, Humbug and Deseret Fms. (Fig.4.7.A). The canyon consists of two types of conglomerate (informally named No.1 and No.2). Further examination of the clasts present in the conglomerate type No.1 was accomplished in a Cenozoic fan in the located near Ensign Peak (Appendix A for log and location, Fig.A.2, p.97). The Cenozoic fan is characterized by well-cemented, massive deposits, subrounded clasts and poorly sorting, indicating sediment transport by debris-flow. Clast-analysis in the ancient conglomeratic fan indicates that the dominant lithologies are mainly limestone, along with pink quartzite clasts. The limestone clasts are subrounded and are normally the largest clasts found in the area, with the largest clast

measured up to 46 cm. Further up in the canyon conglomerate No.2 is present (Fig.4.7.B, cf.Fig.3.1 for location) consisting of pebble and cobble conglomerate and sandstone with subangular-subrounded clasts of limestone and both pink and white quartzite clasts. Conglomerate No.2 (the Wasatch Fm.) is the thickest deposits at the Salt Lake Salient ranging up to over 500 m (Hintze, 2005).
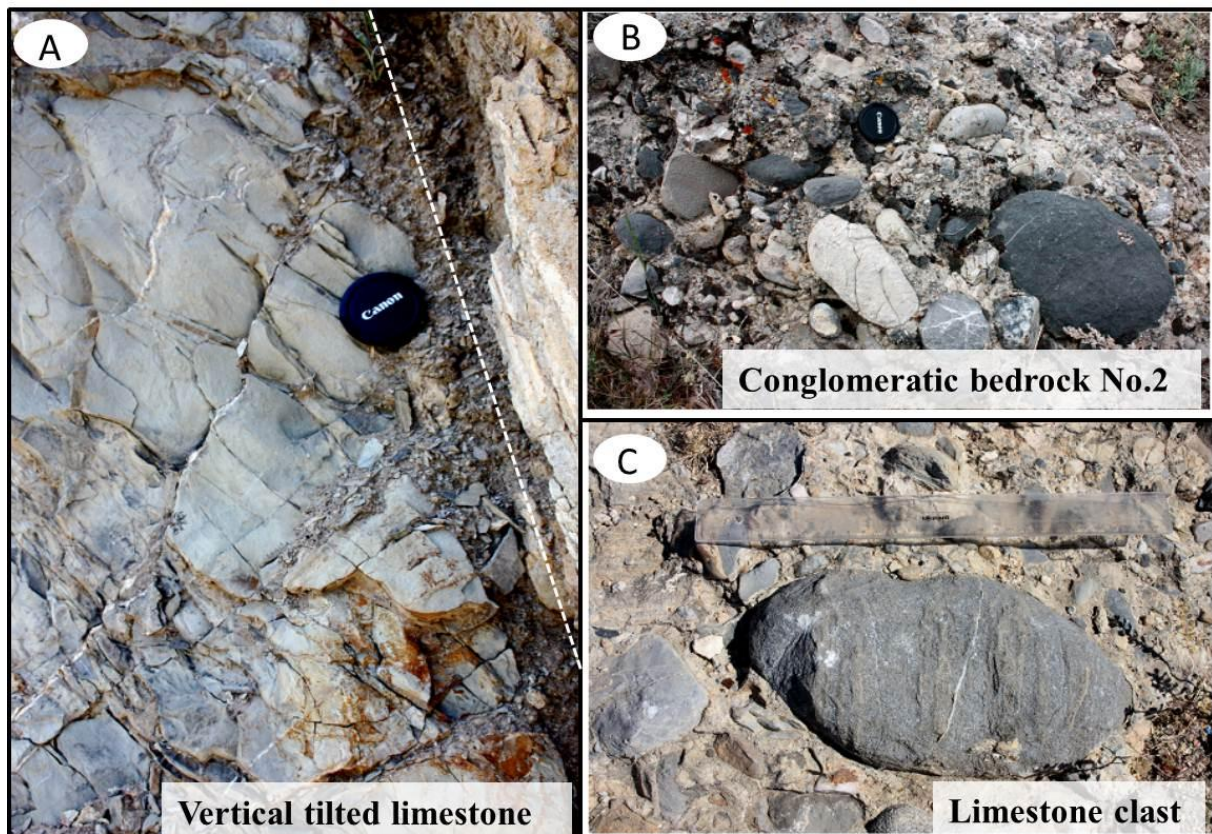
Figure 4.7: *A) Vertical tilted bedrock consisting of limestone; (B) Conglomeratic bedrock (No.2), poorly sorted and dominated by limestone and quartzite clasts; C) Close-up view large limestone clast deposited in the conglomeratic bedrock No.2 (cf.Fig.3.1 for location, 40°49'8.73"N,111°51'23.89"W).*

4.3.2 Associated sink deposits, fan 1

Eight outcrops in the sink deposits in City Creek Canyon (CCC) were studied. See Fig.3.1 for locations and Appendix A for logged sections (Fig.A.3 and Fig.A.4, p.99-100). The studied deposits include sediments from both Provo and Bonneville level, and are predominantly of facies association A, fan delta deposits. The Provo deposits are generally more massive and thicker than sediments at the Bonneville level. The studied outcrops at Provo level are typically up to 3-6 m thick, compared to about 1-3 m at Bonneville level. Few sedimentary structures were identified in the deposits.

The clasts at the Bonneville level are subangular-subrounded, poorly sorted and matrix-dominated, they include the largest clast seen in the area (40 cm). The deposits are generally unconsolidated and considerably affected by Holocene faulting, shown by fault-line scarps cutting the sediment (Fig.4.8.A) with a height of approximately 4-6 m. Calcite veins cutting through some of the deposits are a characteristic for several of the outcrops, mainly in association with the surface-faulted sediments (Fig.4.8.C). The dominant lithologies for the sediments at the Bonneville level are subrounded limestone clast (Fig.4.8.B), and pink quartzite clasts. A few conglomerate clasts are observed in the outcrop area.
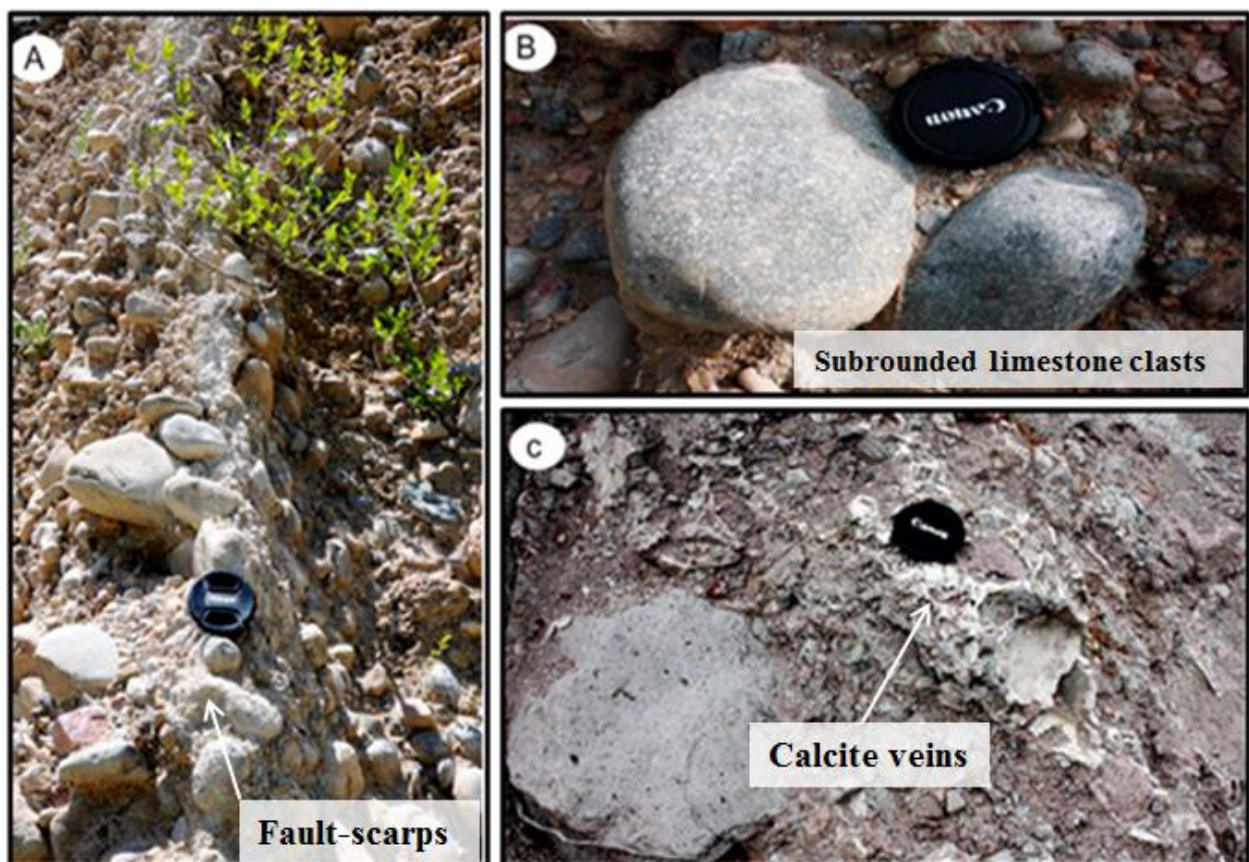
Figure 4.8: *A) Deposits affected by surface-Holocene faulting making prominent fault scarps in the sediments, location CCC 7; B) Large, subrounded, limestone clasts in a sandy matrix, location CCC 2; C) Calcite veins cutting the deposits, location CCC 3, Bonneville level (for CCC 3 cf. Fig.3.1 for location and Appendix A for log, p.99).*

The Provo deposits found in City Creek Canyon are characterized by poorly sorted, subangular-subrounded clasts, consisting of silt, sand, gravel, pebbles, cobbles and boulders. Some horizontal bedding and imbrication were observed, but the deposits generally have a chaotic structure and are carbonate cemented. The lithologies are dominated by big subrounded limestone clasts, together with white quartzite and sandstone clasts.

## 4.4 Source to sink analysis of the Parleys Canyon drainage system
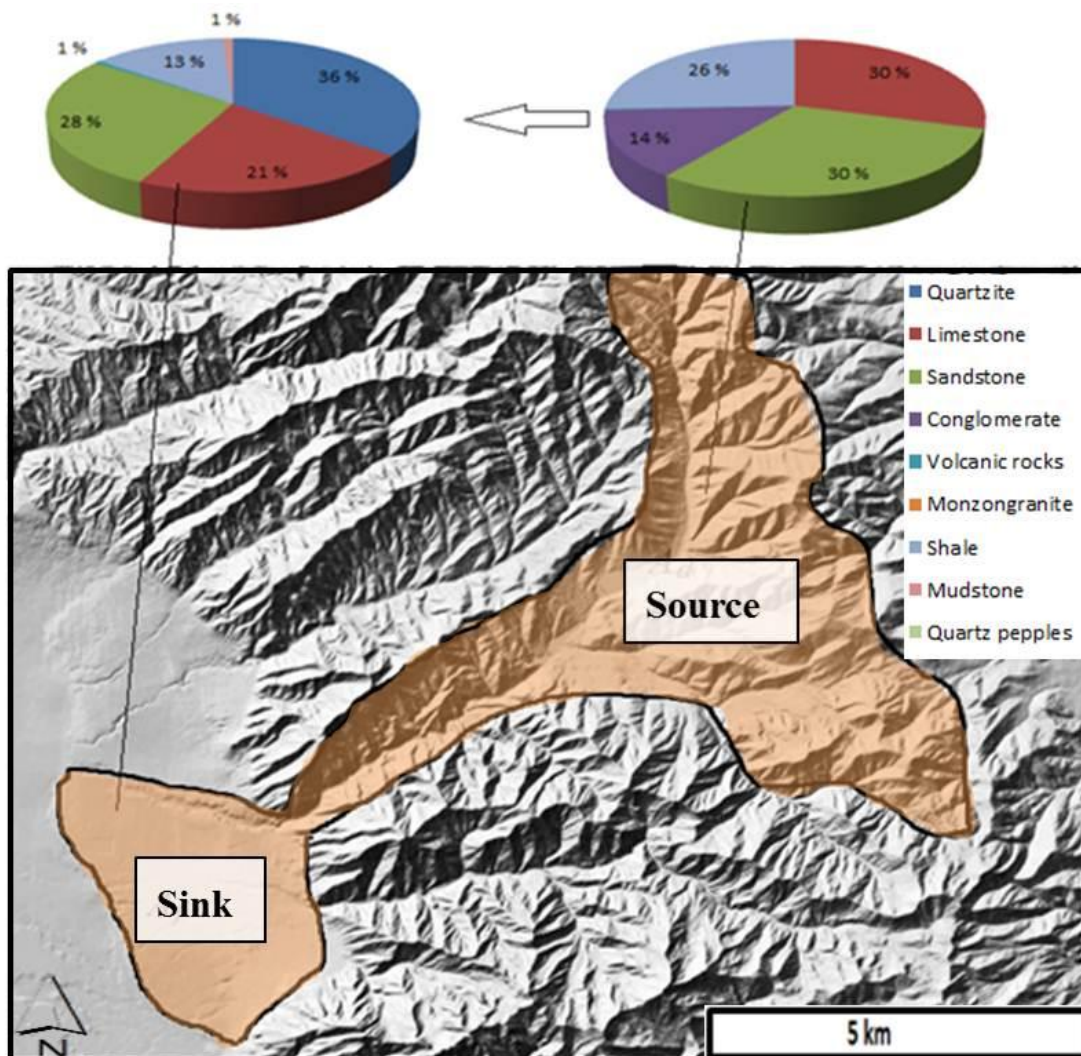
Figure 4.9: *Catchment lithology and clast lithology in the Parleys Canyon (pie-charts). Terrain data extracted from 1.25 m lidar earth data (http://stage.mapserv.utah.gov/raster/).*

4.4.1 Catchment area

Parleys Canyon catchment is covered with little to moderate vegetation with some forestation. The canyon is associated with a Sevier aged syncline and associated faulting making the rocks in the center of the canyon younger than the rocks at the edges. The lithologies in the canyon were deposited in Jurassic to Triassic time (245 Ma to 145 Ma). The Parleys Canyon catchment comprises the finest-grained bedrock in the segment, and the extracted lithologies consist of 30 % limestone, 25 % conglomerate, 30 % sandstone & silt, and 15 % shale (Fig.4.9). The geological formations in the catchment are mainly the Twin Creek Limestone, Preuss Sandstone and fine-grained red-silty sandstone and shale from Ankareh Fm. (Fig. 4.10).
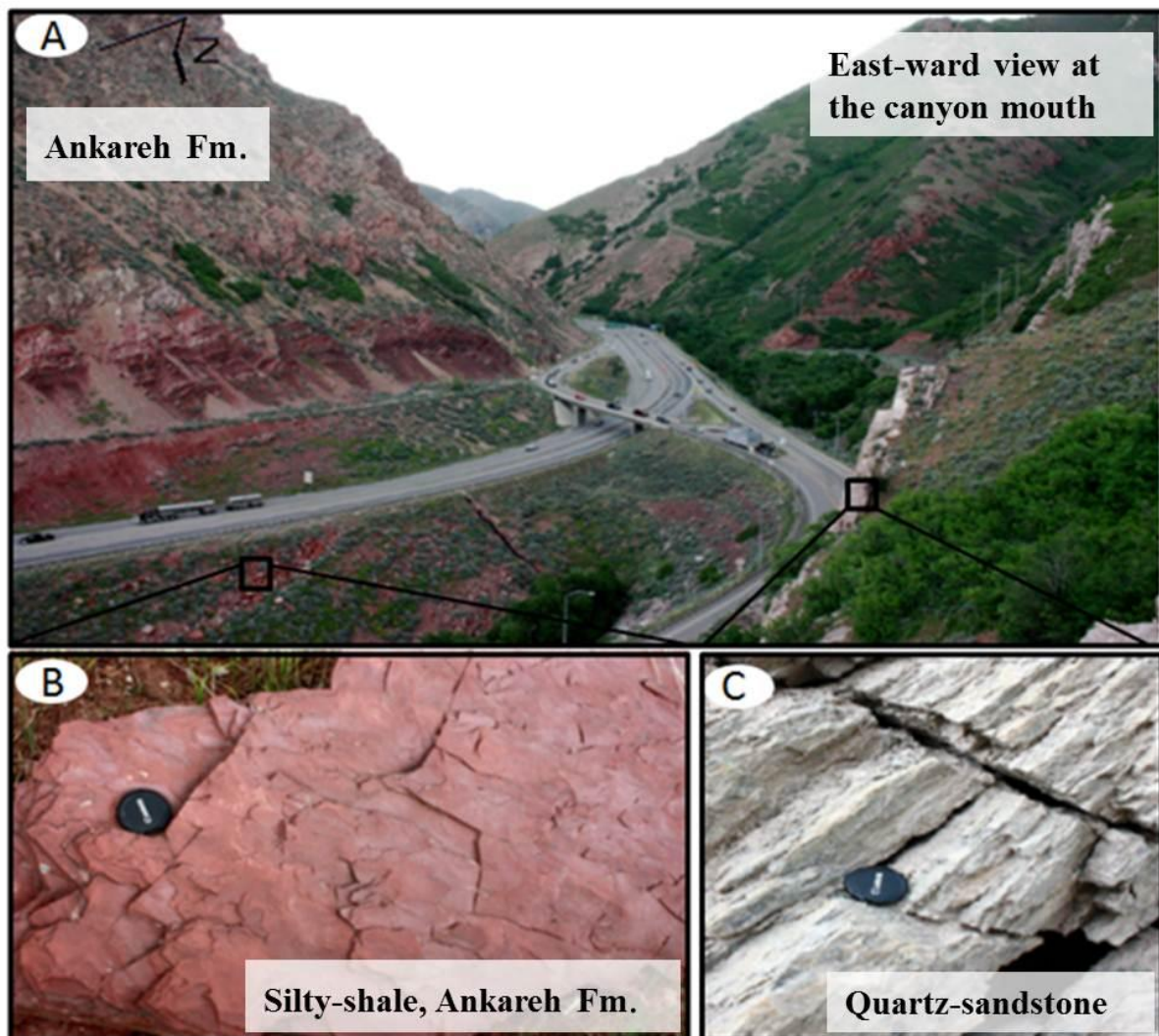
Figure 4.10: *A) Eastward view into mouth of the Parleys Canyon catchment, contact between the Ankareh Fm. and light-colored quartz sandstone; B) Close-up view of the red-silty sandstone and shale, the Ankareh Fm.; C) Close-up view of the quartz sandstone.*

4.4.2 Associated sink deposits, fan 4

Seven outcrops of the sediments that were eroded of Parleys Canyon (PCC) were studied. See Fig.3.1 for locations and Appendix A for logged sections (Fig.A.6 and Fig.A.7, p.102). The fan delta deposits, facies association A, in front of the Parleys Canyon have a distinctive reddish-brown color compared to the other localities (Fig.4.11). Clasts in the fan delta deposits are subrounded, poorly sorted and generally matrix-supported consisting of gravel, cobbles and boulders (Fig.4.11.B), often with fine-sand and reddish silt deposited in the upper part (Fig.4.11.A). Thin layers of clast-supported deposits showing horizontal layering and bedding are present. However, the deposits are generally massive with a chaotic structure,

indicating sediment transport processes dominated mainly by debris-flow and stream-flow (Fig.4.11.A). A 45 cm white quartzite clast at Provo level is the biggest clast measured, while the mean grain size of the clasts in the canyon is approximately 5-10 cm. The dominant lithologies in the studied outcrops are red sandstone, quartzite and limestone (Fig. 4.11.B). Red mudclasts are frequently observed (Fig.4.11.C).
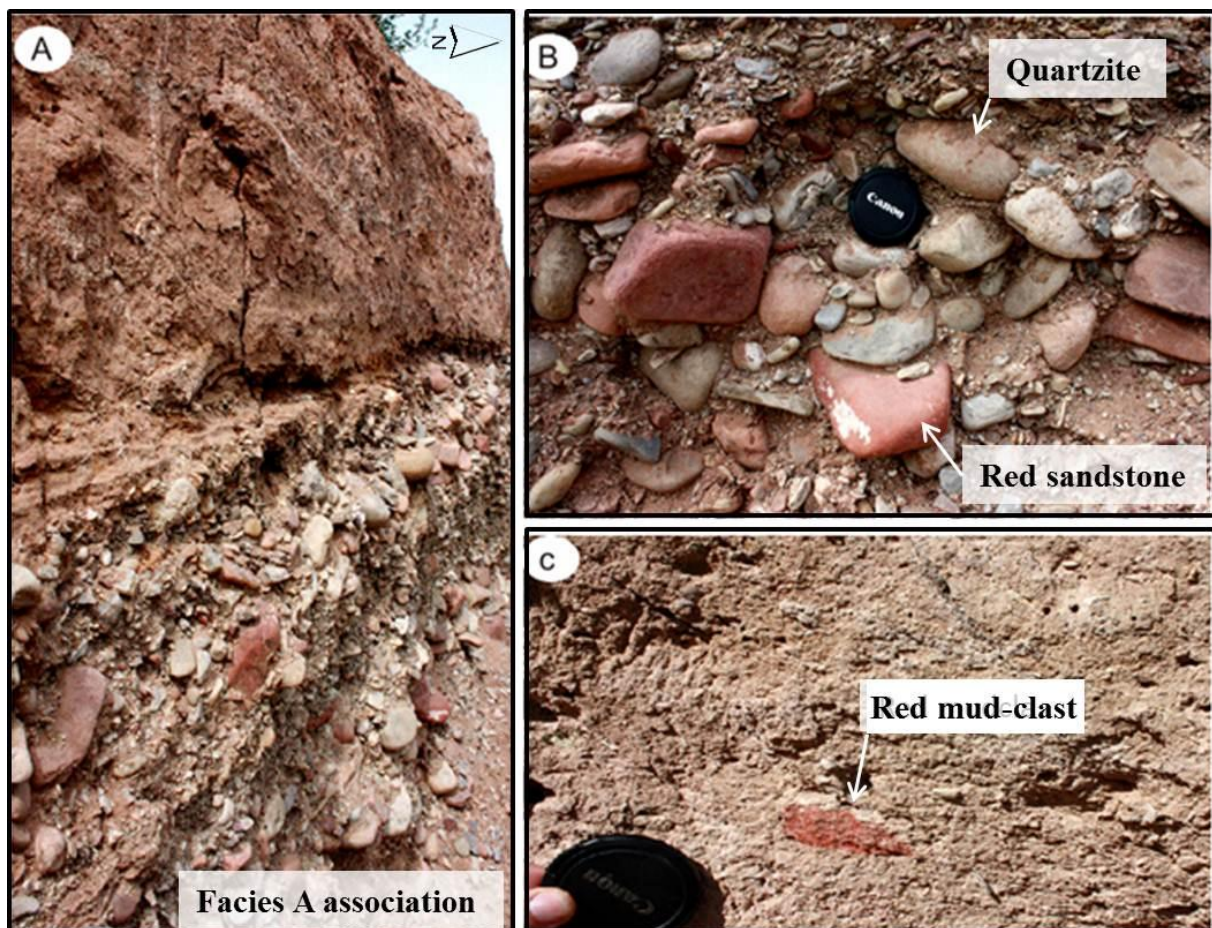
Figure 4.11: *A) Reddish, subrounded-subangular, matrix-supported deposits consisting of gravel, cobbles and boulder sized clasts with finer material in the upper part, location PCC 5; B) Typical frame-work of the clasts, dominated by red sandstone and quartzite, location PCC 1 (Appendix A for log, p.102; C) Red mudclasts frequently observed, location PCC 5 (cf. Fig.3.1 for locations).*

The deposit at the Bonneville level generally consists of matrix-supported dominated conglomerates with a medium-coarse sand matrix and subrounded and poorly sorted clasts (2-4 cm). Massive beds are most common; however some flow orientation is present, especially in lower to middle parts. The biggest clast in the area was a red sandstone which was 30 cm. Deposited at the Provo level contrast with the Bonneville deposited in terms of texture and grain size. Subrounded clasts are present within a silt-fine grained sandy matrix, showing

medium-good sorting. The mean grain size is approximately 3-4 cm, while the biggest clast measured is 8 cm consisting of pink quartzite.

4.5 Source to sink analysis of the Mill Creek Canyon drainage system
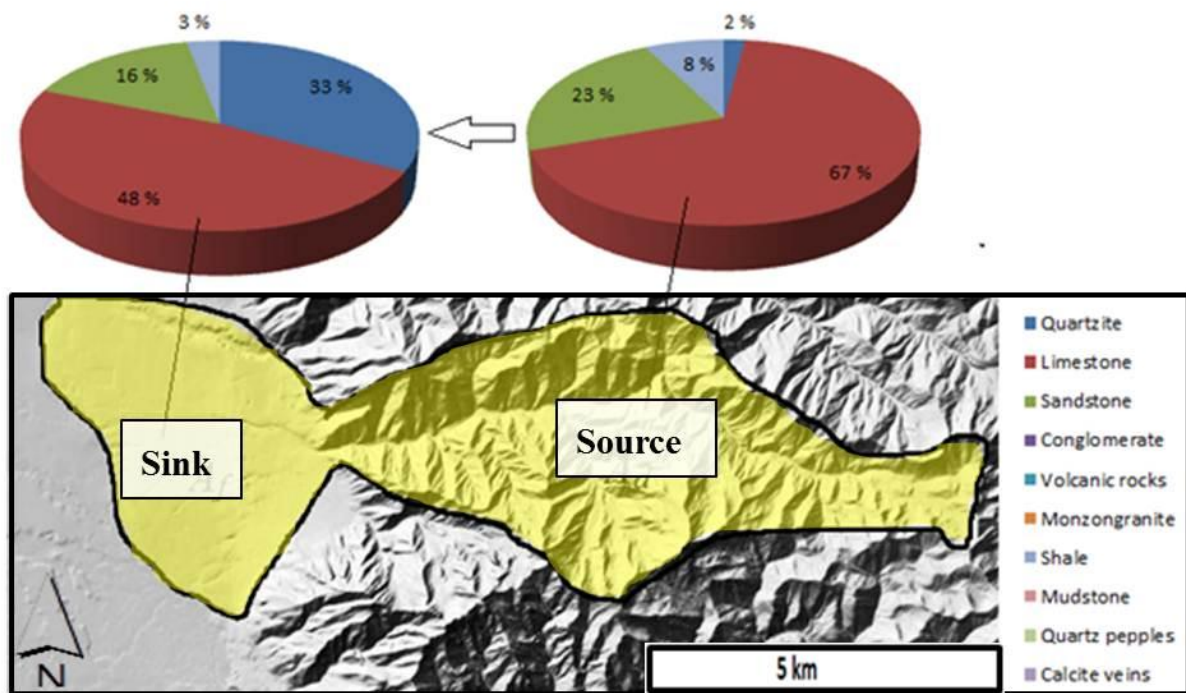
Figure 4.12: *Catchment lithology and clast lithology in the Mill Creek Canyon (pie-charts). Terrain data extracted from 1.25 m lidar earth data (http://stage.mapserv.utah.gov/raster/).*

4.5.1 Catchment area

The lower parts of Mill Creek Canyon catchment differs from the upper parts. The lowest part is dominated by a V-shaped morphology, with steep flanks consisting of the Weber Quartzite (Fig.4.13.A). Further up in the canyon the landscape changes from a V-shaped form to a U-shaped morphology, as a result of partial Pleistocene glacial cover in this region (approximately 15% of the catchment area). The extracted lithologies in the catchment consist of 67% limestone, 23% sandstone & siltstone, 8% shale and 2% quartzite (Fig.4.12). The sediment sources are mainly in limestone from the Park City (Fig.4.13.C) and Thaynes Fms., in addition sandstone from the Weber Sandstone Fm. (Fig.4.13.B) and the Nugget Sandstone Fm. are present.
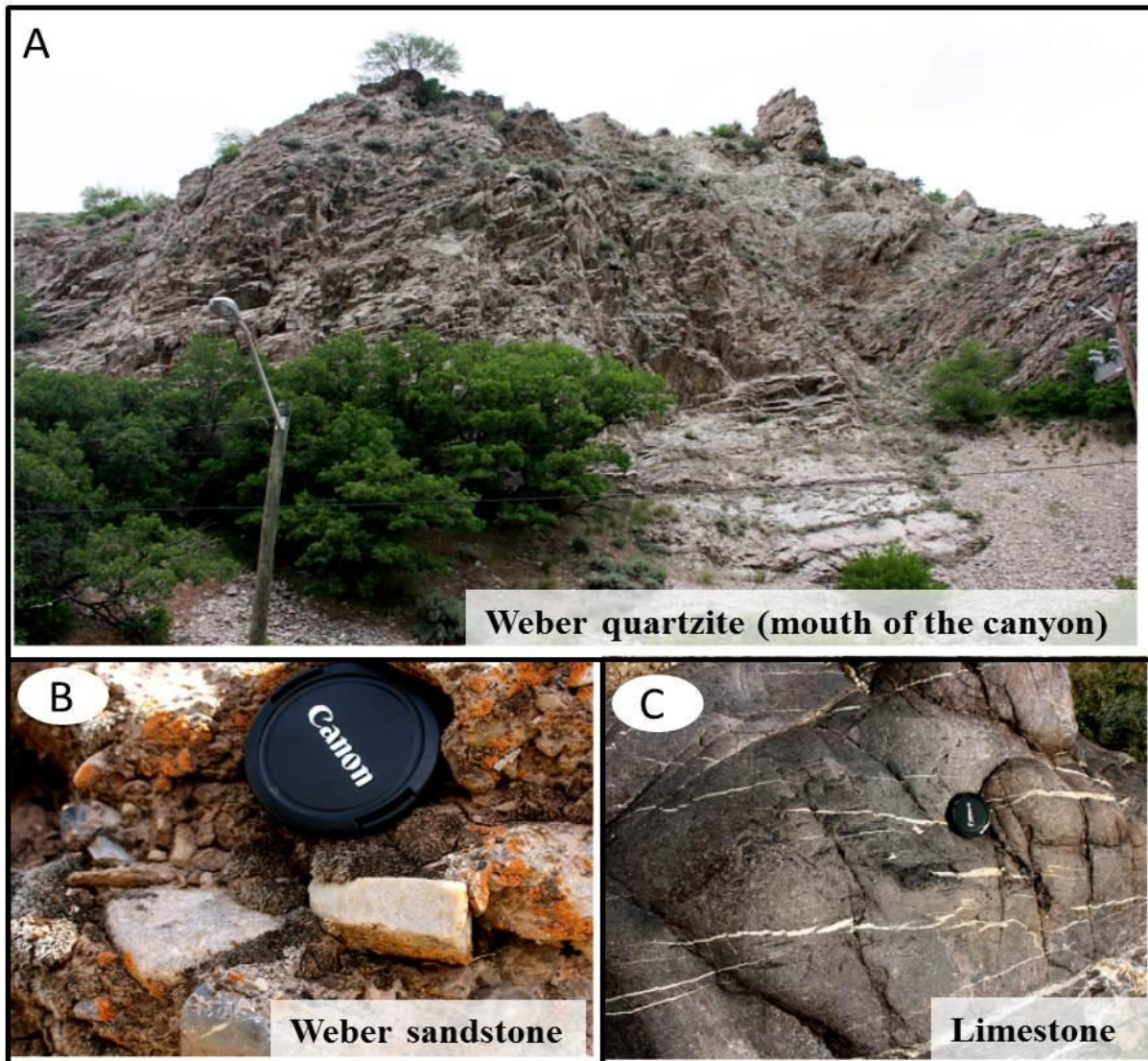
Figure 4.13: *A) Weber Quartzite Fm. observed in mouth of the canyon; B) Close-up view of the Weber Sandstone Fm. consisting of white quartzite and calcareous sandstone; C) Close-up view of the limestone observed in the catchment area.*

4.5.2 Associated sink deposits, fan 5

There is a lack of well exposed and preserved outcrops in the Mill Creek Canyon (MCC) sink area. One outcrop of Lake Bonneville deposited was examined. See Fig.3.1 for location and Appendix A for logged section (Fig.A.9, p.104). This outcrop consists of a clast-supported, subrounded carbonate cemented upper layer with some horizontal orientation. The lower layer is more chaotic, poorly sorted and unconsolidated (Fig.4.14.A).The deposit is interpreted to be of facies association A, fan delta deposits. The mean grain size in the upper part is 5-7 cm, while the largest measured clast is 12 cm consisting of limestone. The biggest clast measured in the lower part is a 20 cm white quartzite clast, and the mean grain size of the clasts is 10

cm. In general dominant clast lithologies in the outcrop are limestone and white quartzite. Limestone clasts, from the upper part of the outcrop, are frequently observed with distinct fossils, including brachiopods and crinoids (Fig.4.14.B) from the Park City Fm.
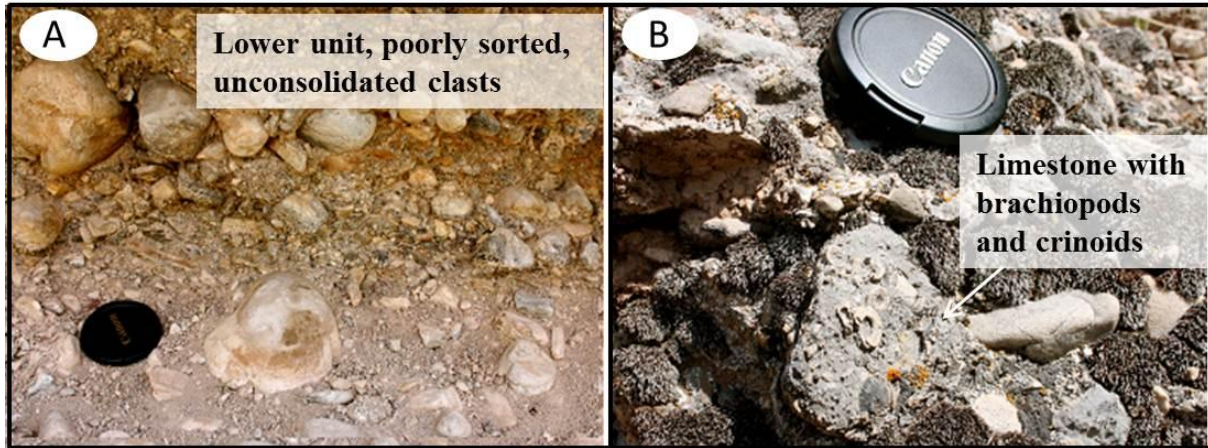
Figure 4.14, *A) Lower unit of the fan delta deposits, poorly sorted clasts and unconsolidated deposits, location MCC 1; B) Limestone from the Park City Fm. observed with crinoids and brachipods (*cf. *Fig.3.1 for location and Appendix A for log, p.104).*

4.6 Source to sink analysis of the Big Cottonwood Canyon drainage system
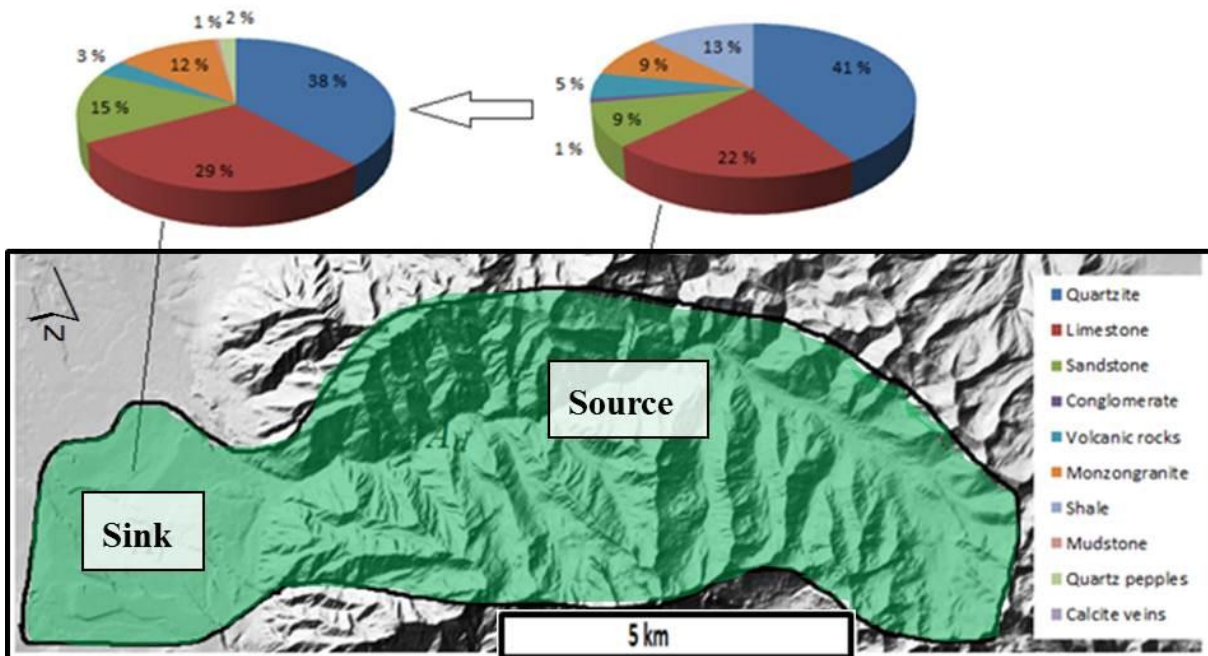
Figure 4.15: *Catchment lithology and clast lithology in the Big Cottonwood Canyon (pie-charts). Terrain data extracted from 1.25 m lidar earth data (http://stage.mapserv.utah.gov/raster/).*

4.6.1 Catchment area

Big Cottonwood Canyon is located 19 km south-southeast of the Salt Lake City and south of the Mill Creek Canyon, within the Mount Olympus Mountains (cf.Fig.2.2). The catchment is characterize by a relative U-shaped valley with steep, treeless peaks (Fig.4.16.B) (James, 1979) in the upper part and more steep sided V-shaped valley in the lower part. The extracted lithologies in the catchment consists of 41% quartzite, 22% limestone, 13 % shale, 9 % monzo-granite, 9 % sandstone and siltstone and 5 % volcanic rocks (Fig.4.15). The upper parts of the canyon consist of softer lithology than the lower parts. Dominant geological formations in the catchment are highly metamorphosed quartz schist from the Little Willow Fm. overlain by reddish-brown quartzite, interbedded with shale and siltstone of the Big Cottonwood Fm. (Fig.4.16.A).
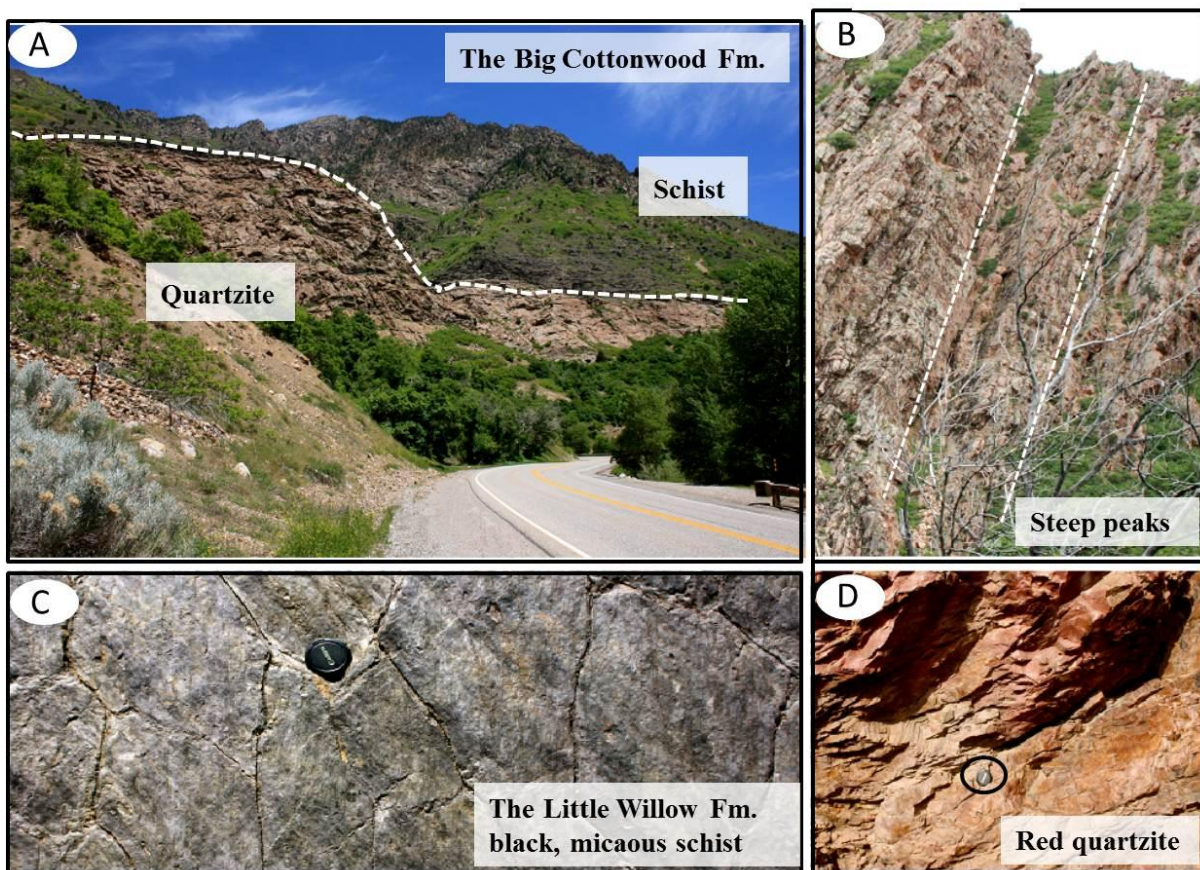
Figure 4.16: A*) Reddish-brown quartzite, interbedded with shale and siltstone of the Big Cottonwood Fm; B) Morphology of the uplifted and tilted peaks in the canyon; C) Close-up view of low-grade micaous schist with mud cracks; D) Close-up view of fractured and weathered quartzite of the Big Cottonwood Fm.*

4.6.2 Associated sink deposits, fan 6

Five outcrops from the fan delta associated with in the Big Cottonwood Canyon (BCC) were studied. See Fig.3.1 for locations and Appendix A for logged section (Fig.A.11, p.105). Overall coarse-grained, poorly sorted; subrounded sediments are observed. The deposits are dominated by facies association A, fan delta deposits, however facies association B, glacial deposits is observed. The sediments from the fan delta deposits (Fig.4.17.A) are characterized by matrix-dominated deposits, with grain size ranging from gravel to boulders size, with bed thickness ranging from 1-5 m. At Bonneville level the deposits are generally chaotic with grain sizes ranging from pebbles to boulders, and often deposited with finer-grained material such as sand and silt at the top. The dominant clast lithologies present in the outcrops are decomposed monzo-granite (Fig.4.17.B) and relative large limestone and quartzite clasts (ranging from 5-25 cm). Some evidence for current ripples is observed in the deposits. Additionally observations of a several black schist and red mudclast were done (Fig.4.17.C and Fig.4.17.D respectively).
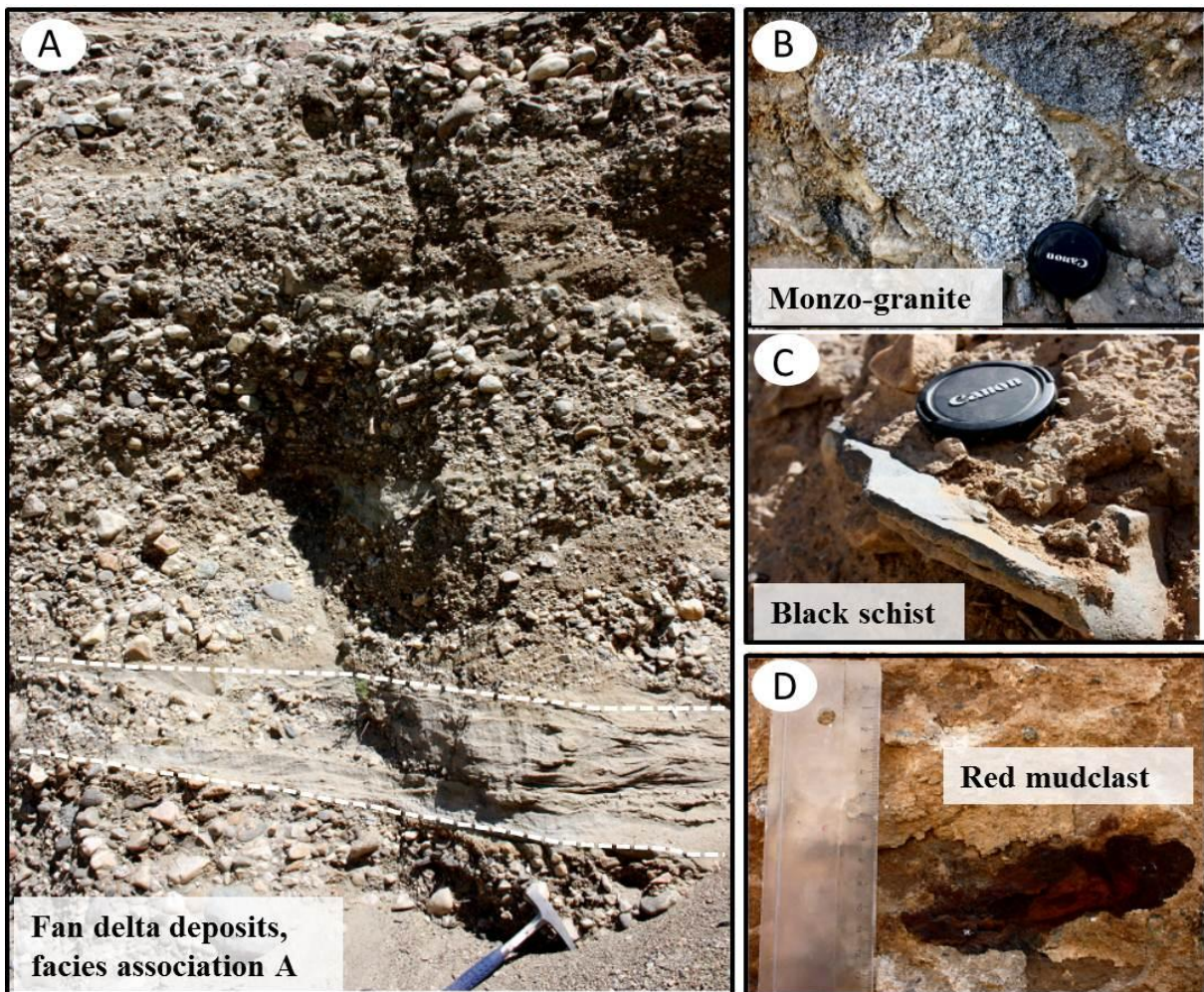
Figure 4.17: *A) Facies association A, fan delta deposits, with poorly sorted clasts and interbedded layers of sand, location BCC 3 (Fig.3.1 for location and Appendix A for log, p.105); B) Close-up view of decomposed monzogranite clasts; C) Close-up view black micaous schist observed in the fan deposits; D) Close-up view of red mudclast.*

Facies association B (glacial deposits) observed at Provo level (location BCC 5, cf.Fig.3.1) consists of clasts ranging up to boulder size within a relative fine-grained sandy matrix. The clasts contain a lot of mica, which most likely originated from the black low-grade micaous schist observed in the catchment area. The biggest clast in the Big Cottonwood Canyon fan area is observed at this locality (40 cm sandstone). The mean grain size is approximately 8-10 cm. Limestone and quartzite dominates the clast lithology in the studied outcrops.

4.7 Source to sink analysis of the Little Cottonwood Canyon drainage system
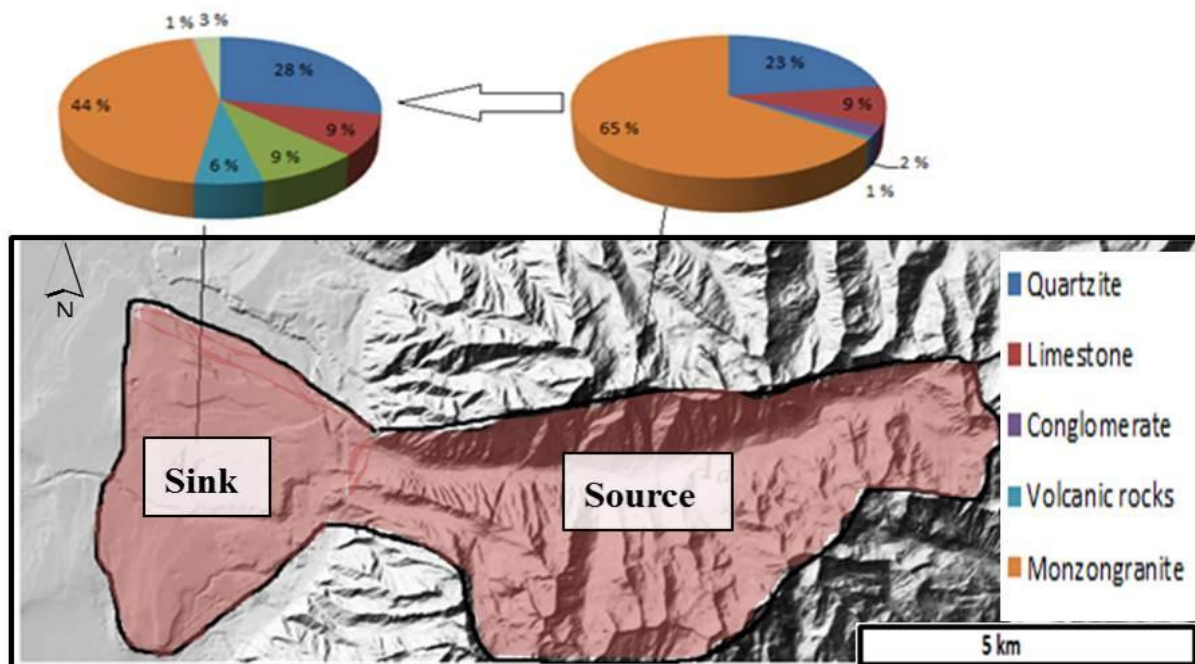
Figure 4.18: *Catchment lithology and clast lithology in the Little Cottonwood Canyon (pie-charts). Terrain data extracted from 1.25 m lidar earth data (http://stage.mapserv.utah.gov/raster/).*

4.7.1 Catchment area

Little Cottonwood Canyon is located 20 km south-southeast of the Salt Lake City (Madsen and Currey, 1979). The vegetation in the canyon mainly consisted of arboreal species such as oak, box elder, aspen, while the floor of the canyon upstream from an altitude of 2280 m consists mainly of a mix of valley-bottom forest such as quaking aspen, spruce elderberry and oak, and the downstream side by maple (Madsen and Currey, 1979). Little Cottonwood Canyon was heavily glaciated during Pleistocene time resulting in a steep U-shaped valley (Richmond, 1964; Atwood, 1909). Additionally, several smaller glacial tributaries are associated with the glacier system in the canyon (Atwood, 1909). Final Pleistocene de-glaciation in the upper and middle part of the canyon ended about 13.000 years B.P., although pollen ratio in the area suggesting temperatures below average until 8.000 years B.P. (Madsen and Currey, 1979; Lemons et al., 1996).

The topography of the catchment is established to be asymmetrical where the western peaks (Twin Peaks) are higher than those on the eastern side (Lone Peak). The topography in Twin Peaks ranges from approximately 3200- 3400 m, whereas the Lone Peaks maximum elevation

is approximately 3200 m. The asymmetry is partly a result of uplift of the range along the normal faults, and partly caused by the resistant rocks of the Little Cottonwood Stock which underlay the western peaks. The lithology of catchment is relatively homogenous compared to the other catchments in the segment. The extracted catchment lithologies consists of 65% quartz monzo-granite, 23 % quartzite 9 % limestone, 2 % conglomerate, 1% volcanic rocks (Fig.4.18).The dominant geological formations are mainly Little Cottonwood Stock (intrusion of monzo-granite) (Fig.4.19.C), granodiorite from the Alta stock, and white, quartz-sandstone in addition to Cambrian-age light-dark colored limestone (Fig.4.19.B).
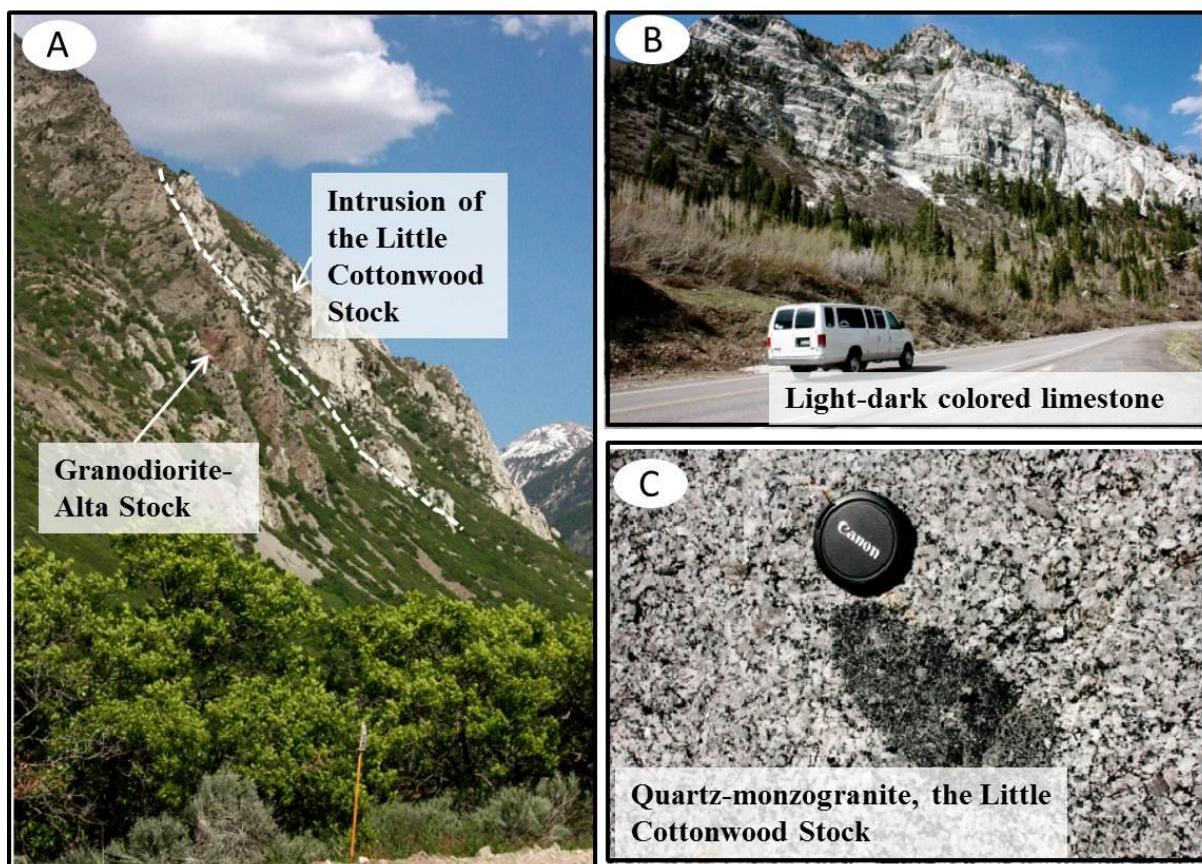
Figure 4.19: *A) Intrusion of monzo-granite, the Little Cottonwood Stock, steep resistant peaks makes the appearance of the catchment; B) Bedrock of Cambrian-age light-dark colored limestone; C) Close-up view of the monzo-granite intrusion, the Little Cottonwood Stock.*

4.7.2 Associated sink deposits, fan 7

Seven outcrops of the deposits basinward of the Little Cottonwood Canyon (LCC) were studied. See Fig.3.1 for locations and Appendix A for logged section (Fig.A.13-15 p.107-108). The sink deposits included facies association A, fan delta deposits and facies association B, glacial deposits. Generally finer-grained deposits are observed compared to the previously

studied sink deposits. The fan delta deposits are characteristic by poor sorting, subrounded clasts consisting of granules, pebbles, cobbles and boulders within a sandy matrix, and with a thickness ranging from 0.5-4 m. The clast lithology consists predominantly of monzo-granite, together with a high percentage of quartzite clasts.
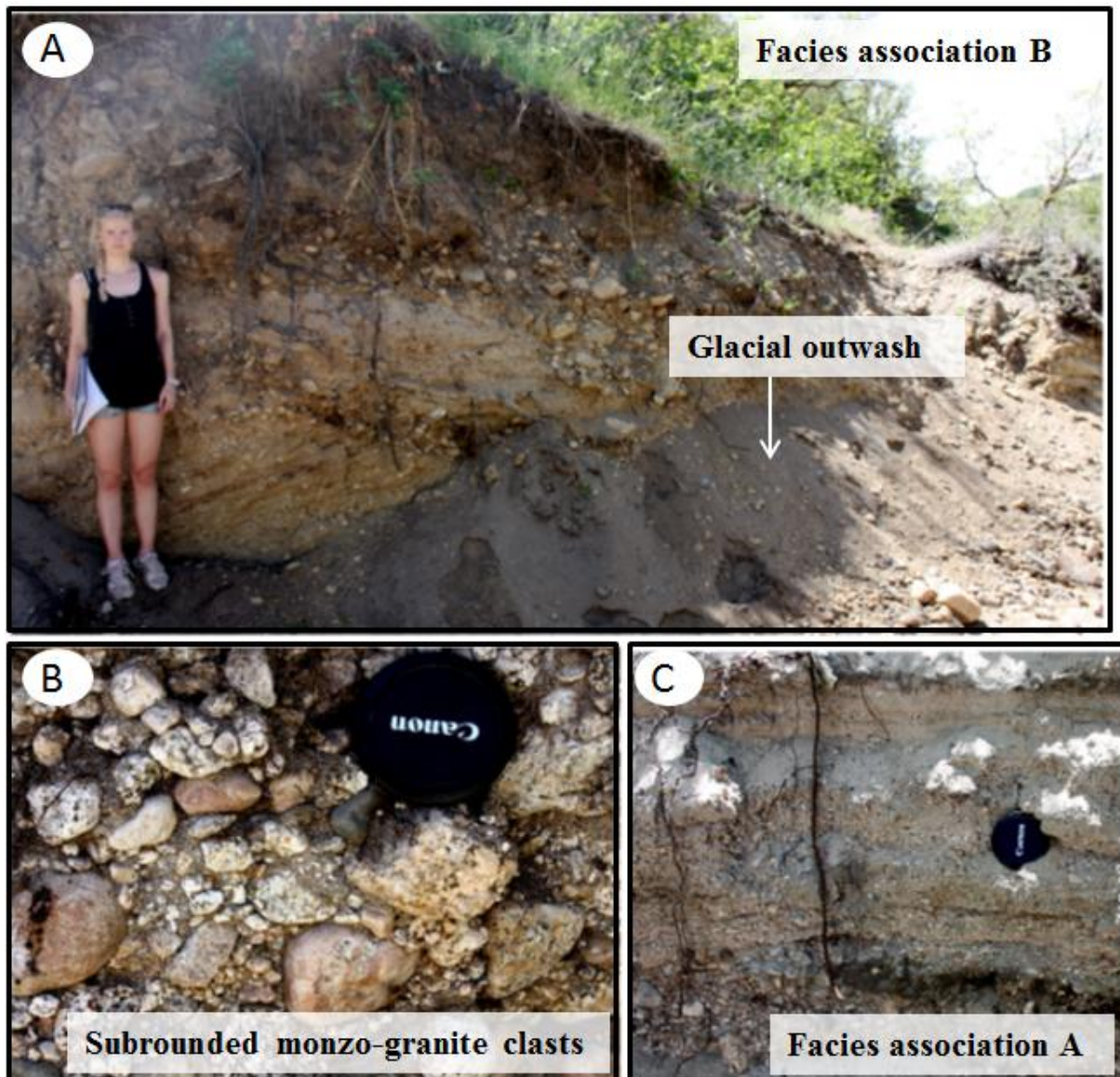
Figure 4.20: *A) Facies association B, glacial deposits with clasts ranging from coarse sand-boulder size, location LCC 2 (log Appendix A, Fig.A.13, p.107, cf.Fig.4.1 for location); B) Subrounded monzo-granite clasts with pebbles, cobbles and boulders grain size in a crushed sandy matrix, location LCC 1 (cf.Fig.3.1 for location); C) Parts of facies association A, with medium-coarse sand matrix interpreted to be stream-flow deposits, location LCC 3 (log Appendix A, Fig.A.14, p.107, cf.Fig.4.1 for location).*

Grain size from the glacial deposits of facies association B ranges from coarse sand to boulder size, within a fine-grained sandy matrix (Fig.4.20.A). The clasts show medium-good rounding, and the largest clast observed is a 45 cm sandstone clast. Monzo-granite clasts are

the dominant lithology in the outcrop. Overall the monzo-granite clasts are more rounded and larger compared to the other clasts (Fig.4.20.B). The stream-deposits of facies association A generally show a distinct stream orientation, with clasts varying from fine sand-boulder size.

4.8 Source to sink analysis of the Point of Mountain spit system
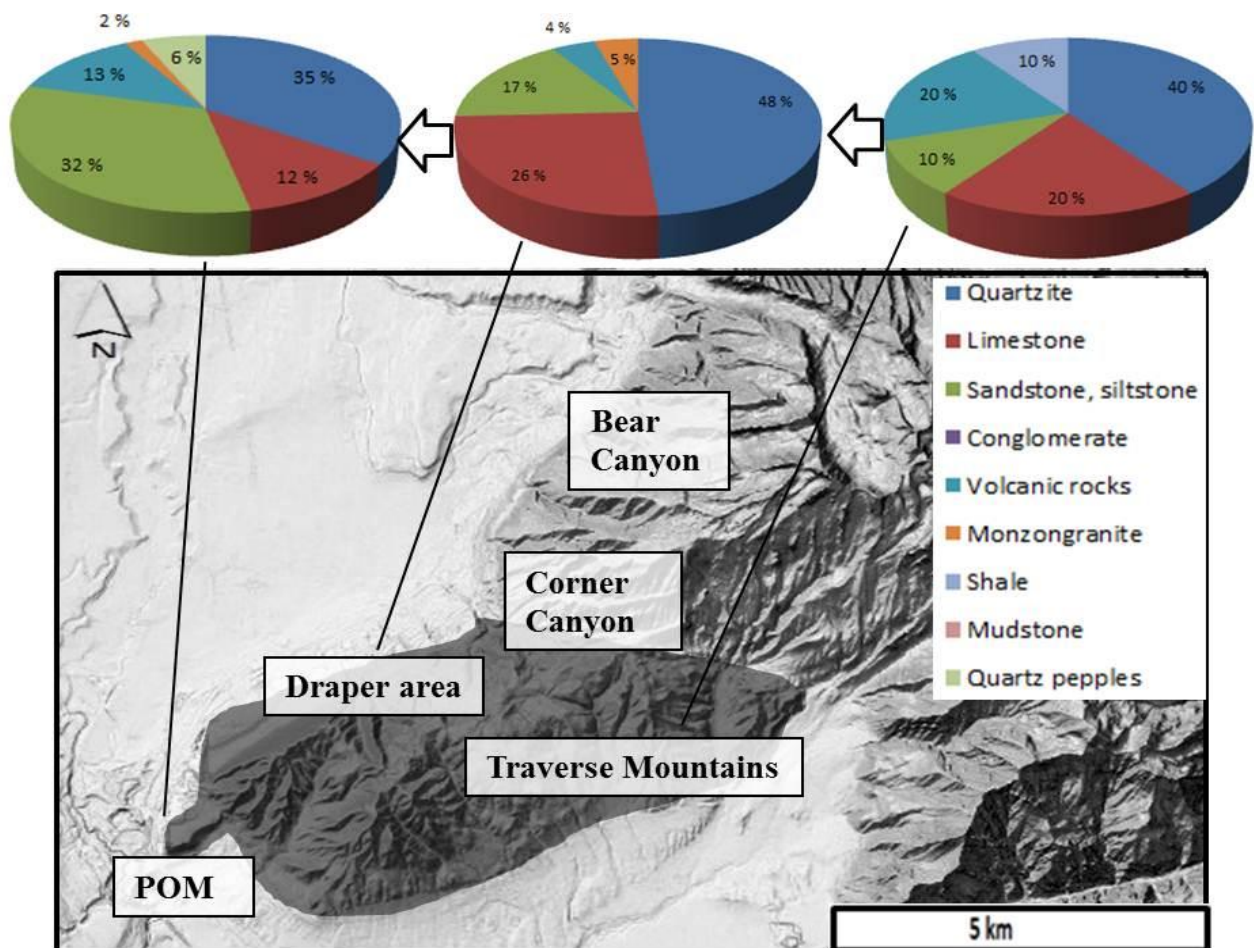
Figure 4.21: *Catchment lithologies in the Traverse Mountains and clast lithologies of Draper area and the Point of Mountain (POM) spit system (pie-charts).Terrain data extracted from 1.25 m lidar earth data (http://stage.mapserv.utah.gov/raster/).*

4.8.1 Catchment area, the Traverse Mountains

The Traverse Mountains area includes the Point of Mountain area which is located in the southeast of Salt Lake City and marks the southern boundary in the segment (cf.Fig.2.2 for overview map) (Schofield et al., 2004; Jewell, 2007). Draper area is located between the Little Cottonwood Canyon and Point of Mountain spit (Fig.4.21). Corner Canyon (Fig.4.21) intersects the Wasatch Mountains and Traverse Mountains and is the largest drainage

catchment in the area (Schofield et al., 2004). The extracted lithologies in the Traverse Mountains are 40 % quartzite, 20 % limestone, 20 % volcanic rocks, 10 % shale and 10 % sand and siltstone (Fig.4.21). According to Personius and Scott (1992) and Schofield et al. (2004) four bedrock units have been identified in the Point of Mountain area. Quartz monzo-granite from the Little Cottonwood Formation and low-high grade Archean-Proterozoic metamorphosed rocks from the Big Cottonwood Fm. are observed north of Corner Canyon. South of Corner Canyon the bedrock consists of Oligocene volcanic flows, tuff and breccia consisting of andesite, latite and quartz latite, together with the Oquirrh Fm. consisting of sandstone and limestone. The Big Cottonwood Fm. (quartzite and shale) decreases from 80% at Bear Canyon to 50 % at Corner Canyon, in contrast with the Little Cottonwood quartz monzo-granite, which increases from 20 % at Bear Canyon up to >40 % at Corner Canyon. Further south from the Corner Canyon, the quartz monzo-granite decreases and disappears (Schofield et al., 2004).

4.8.2 Associated sink deposits

Five outcrops of sink deposits of the Traverse Mountains were studied; three of which were located at the Point of Mountain spit (POM 1-3) and two outcrops located in Draper area (POM 4-5, at Provo and Bonneville level respectively). See Fig.3.1 for locations and Appendix A for logged sections (Fig.A.17 and Fig.A.18, p.110-111). The outcrops in Draper area are interpreted to be of facies association A, fan delta deposits (Appendix A, Fig.A.17, p.110 for log). The deposit generally shows poor sorting and subangular-subrounded clasts dominated by quartzite and limestone clasts, with a matrix consisting of fine-coarse grained sand. The biggest observed clast at the Provo level is measured to be 50 cm, whereas the largest measured clast at the Bonneville level is approximately 5 cm. The deposit is characterized by thick extremley poorly sorted clast consisting of sand, gravel, pebbles, cobbles and boulders within a matrix of fine-coarse sand. The clasts are subangular-subrounded and a general chaotic texture is common. However some bedding and flow orientation are present in middle parts of the fan.

The spit deposits at Point of Mountain are dominated by clast-supported alternating layers of coarse sand, gravel and pebbles with well-sorted and rounded clasts. The deposits are interpreted to be facies association C, wave-dominated deposits (Fig.4.22.A, Appendix A, Fig.A.18, p.111 for log). Dominant lithologies in the spit deposits are quartzite, together with

sandstone and limestone clasts. The biggest clast measured at the spit is 15 cm; while the mean grain size is approximately 2-3 cm. Monzo-granite clasts from the Little Cottonwood Stock and numerous of other igneous rocks were observed in the spit deposits (Fig.4.22.C).
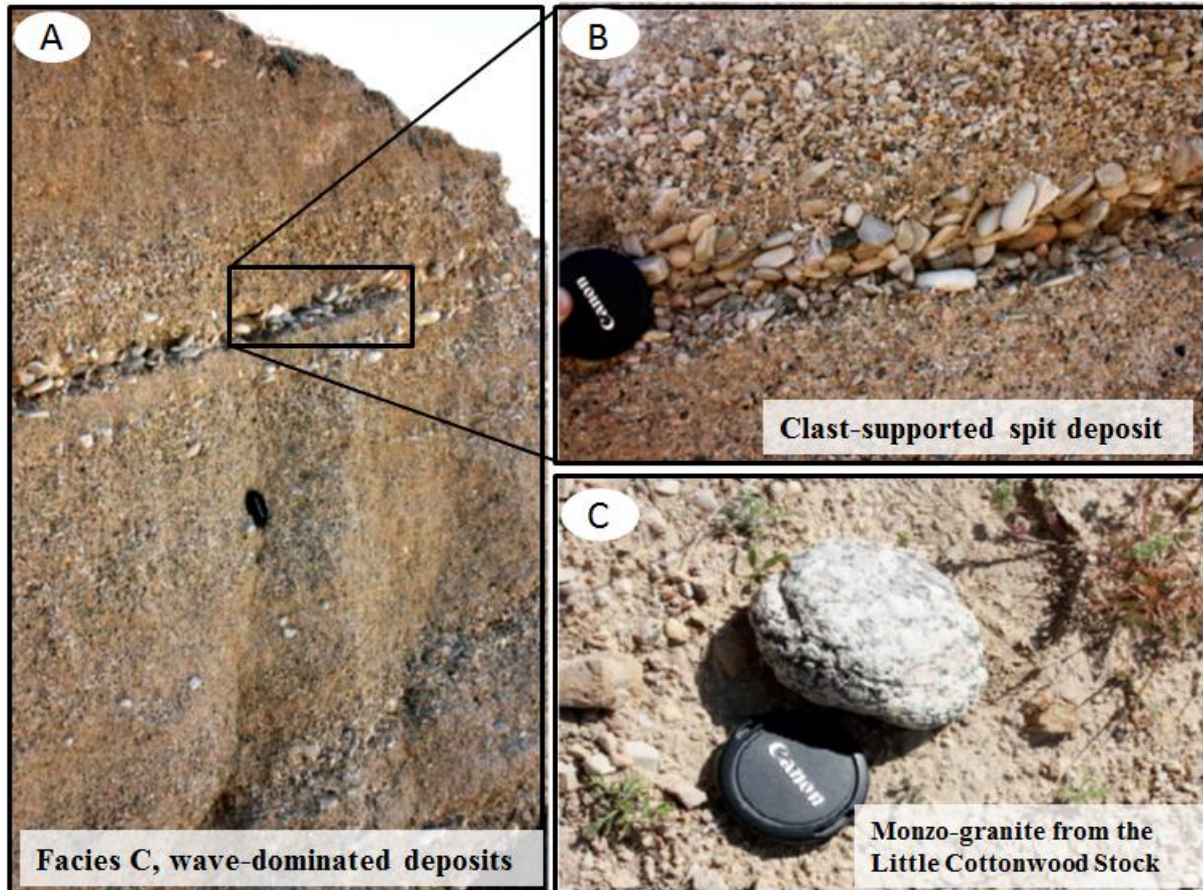
Figure 4.22: *A) Facies association C (wave-dominated deposits) location POM 3 (cf. Fig.4.1 for location and Appendix A for log, p.111); B) Close-up view of the clast-supported alternating layers of pebbles and gravel sized clasts; C) Monzo-granite clasts Little Cottonwood Stock intrusion observed in the spit deposits.*

4.9 Fan mapping

The estimated size of the catchments contributing to fan delta deposits within the basin, varies from 45.5 to 134.3 km^2, while the mapped associated fan area ranges from 5.0 to 85.4 km^2 (Table 4.3).

Table 4.3: Associated fan area and length for the different catchments and estimated fan area according to Bull`s (1962) equation (eq.2.1)

	CCC Fan 1	RBC Fan 2	EMC Fan 3	PCC Fan 4	MCC Fan 5	BCC Fan 6	LCC Fan 7
Catchment area (km^2)	45.5	29.1	47.6	134.3	56.4	130.5	70.9
Fan length (km)	3.7	4.3	6.6	7.3	8.3	9.1	9.6
Fan area (km^2)	5.0	8.7	13.0	16.0	26.8	53.4	85.4
Fan area (km^2) Bull 1962	37.4	19.6	38.9	96.9	45.2	94.6	55.2

There is a significant increase in fan area towards the south. This is not obviously related to the size of the catchment area. The same trend is observed in fan length, which also increases towards the south (Table 4.3). Fig. 4.23 illustrates the ratioes of the catchment/ fan area within the SLC segment, indicating a significant lower ratio for the Little Cottonwood Canyon drainage system (LCC, fan 7).
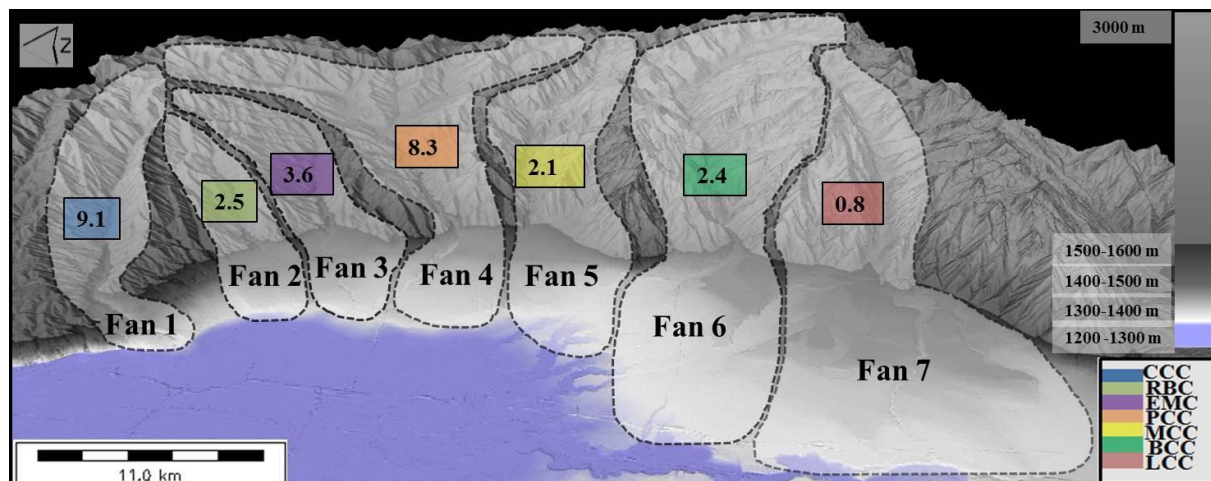
Figure 4.23: *Catchment/fan ratio within the Salt Lake City segment. Grey area demonstrates the approximately morphology of the catchment and fans. CCC (City Creek Canyon, fan 1), RBC (Red Butte Canyon, fan 2), EMC (Emigration Canyon, fan 3), PCC (Parleys Canyon, fan 4), MCC (Mill Creek Canyon, fan 5), BCC (Big Cottonwood Canyon, fan 6), LCC (Little Cottonwood Canyon, fan 7).*

Fan vs. catchment area are displayed graphically in Fig.4.24, the plot shows a very poor correlation between fan size and catchment area. Bull (1962) observed an increase in fan area along with increase in catchment area (cf.eq.2.1, chapter 2.6, p.23). The black trend line on

the plot is based on Bull`s (1962) proposed relationship between catchment and fan area The plot suggest that the majority of the fans are smaller than would be anticipated by Bull`s model with the exception of Little Cottonwood Canyon which is larger. These observations suggest that parameters other than catchment area are controlling fan size. This will be discussed further in the following chapter.
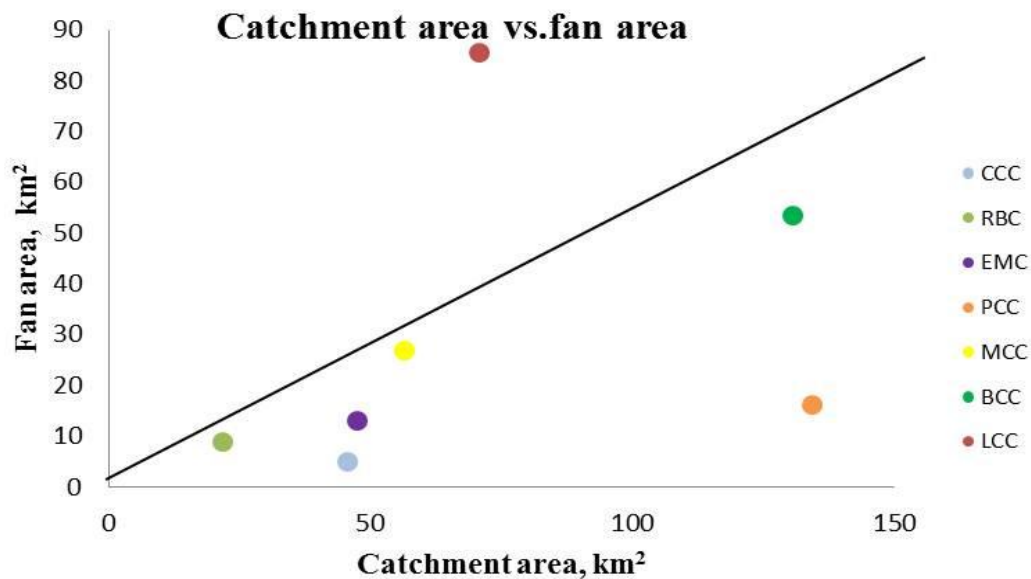
Figure 4.24: *Fan vs. catchment area in the Salt Lake City segment, and Bull`s (1962) proposed relationship for the segment (black trend line, eq.2.1, p.23). CCC (City Creek Canyon), RBC (Red Butte Canyon), EMC (Emigration Canyon), PCC (Parleys Canyon), MCC (Mill Creek Canyon), BCC (Big Cottonwood Canyon), LCC (Little Cottonwood Canyon).*

4.10 Sediment budget within the Salt Lake Basin

Calculations have been made of the total sediments volumes within the basin and the volumes delivered to individual fan deltas and fan delta lobes from the catchment area (using the method described in section 3.4). Additionally, sediment yields (fan volume/catchment area) have been estimated. The results of these analyses are presented below.

4.10.1 Total sediment volume within the basin

Table 4.4 shows the estimates for the total volume of sediments deposited in the Salt Lake Basin during Lake Bonneville times. The total volume (based on the mid case volume) of basin sediments is estimated to be approximately 17 km^3 with a maximum and minimum volume ranging from approximately 18 km^3 to 16 km^3. The surface area of the Bonneville fan system was measured to be 61.8 km^2 while the surface area of the Provo shoreline was measured to be 91.3 km^2 (Appendix B, p.112). While the Provo delta area is larger the total volume is slightly less because the deltaic package is thinner (cf.Fig.3.4).

Table 4.4: Total sediment volumes within the Salt Lake Basin

	Bonneville shoreline	Provo shoreline	Total sediment volumes
Max. Sediment volumes (km^3)	11.1	6.7	17.8
Mid. sediment volumes (km^3)	10.5	6.3	16.8
Min. sediment volumes (km^3)	9.8	5.9	15.7

4.10.2 Sediment volumes deposited in individual fan delta lobes

In addition to the total volume of sediments in the basin, volumes of sediments in the different fan delta lobes during both Bonneville and Provo shoreline were calculated (Table 4.5 and Table 4.6 respectively). Generally both shorelines are associated with the same increasing trend of fan volumes from north to south, with significantly higher fan volumes in Big Cottonwood Canyon fan delta lobe (lobe 6) and Little Cottonwood Canyon fan delta lobe (lobe 7).

Table 4.5: Sediment volumes deposited in individual fan delta lobes: Bonneville shoreline

	CCC Lobe 1	RBC Lobe 2	EMC Lobe 3	PCC Lobe 4	MCC Lobe 5	BCC Lobe 6	LCC Lobe 7
Max.sediment volumes (km^3)	0.5	0.3	0.8	0.5	1.2	2.1	3.8
Mid.sediment volumes (km^3)	0.4	0.3	0.7	0.5	1.2	2.0	3.6
Min.sediment volumes (km^3)	0.4	0.3	0.7	0.4	1.1	1.9	3.3

Table 4.6: Sediment volumes deposited in individual fan delta lobes: Provo shoreline

	CCC Lobe 1	RBC Lobe 2	EMC Lobe 3	PCC Lobe 4	MCC Lobe 5	BCC Lobe 6	LCC Lobe 7
Max.sediment volumes (km^3)	0.1	0.3	0.4	0.6	0.7	1.1	2.7
Mid.sediment volumes (km^3)	0.1	0.3	0.4	0.6	0.6	1.0	2.5
Min.sediment volumes (km^3)	0.1	0.3	0.3	0.6	0.6	0.9	2.3

Lobe 1 CCC (City Creek Canyon), lobe 2 RBC (Red Butte Canyon), lobe 3 EMC (Emigration Canyon), lobe 4 PCC (Parleys Canyon), lobe 5 MCC (Mill Creek Canyon), lobe 6 BCC (Big Cottonwood Canyon), lobe 7 LCC (Little Cottonwood Canyon).

4.10.3 Total sediment volumes deposited in the individual fan deltas

Based on volumes of the two fan delta lobes (Table 4.5 and Table 4.6) the total individual fan delta volumes (fans 1-7) deposited in front of each catchment are presented, along with the estimated sediment yields from the associated catchment areas (Table 4.7 and Table 4.8 respectively). The trend of increased fan volumes from the north to the south is indicated (Table 4.7). Additionally, generally highest sediment yields are found for the the catchments located in the south (Table 4.8). Little Cottonwood Canyon catchment located furthest to the south show almost an order of magnitude higher sediment yield compared to other catchments within the segment.

Table 4.7: Sediment volumes in the individual fan deltas CCC (City Creek Canyon, fan 1), RCC (Red Butte Canyon, fan 2), EMC (Emigration Canyon, fan 3), PCC (Parleys Canyon, fan 4), MCC (Mill Creek Canyon, fan 5), BCC (Big Cottonwood Canyon, fan 6), LCC (Little Cottonwood Canyon, fan 7)

	CCC Fan 1	RBC Fan 2	EMC Fan 3	PCC Fan 4	MCC Fan 5	BCC Fan6	LCC Fan 7
Max.sediment volumes (km^3)	0.6	0.7	1.2	1.1	1.9	3.2	6.4
Mid.sediment volumes (km^3)	0.6	0.6	1.1	1.1	1.8	3.0	6.1
Min.sediment volumes (km^3)	0.5	0.6	1.0	1.0	1.7	2.8	5.7

Table 4.8: Sediment yields to the associated catchments, CCC (City Creek Canyon), RBC (Red Butte Canyon), EMC (Emigration Canyon, PCC (Parleys Canyon), MCC (Mill Creek Canyon), BCC (Big Cottonwood Canyon), LCC (Little Cottonwood Canyon)

	CCC	RBC	EMC	PCC	MCC	BCC	LCC
Max.sediment yield, km/yrs.	4.36×10^{-7}	1.00×10^{-6}	8.21×10^{-7}	2.84×10^{-7}	1.13×10^{-6}	8.24×10^{-7}	3.07×10^{-6}
Mid.sediment yield, km/yrs.	4.10×10^{-7}	9.44×10^{-7}	7.72×10^{-7}	2.67×10^{-7}	1.06×10^{-6}	7.75×10^{-7}	2.88×10^{-6}
Min.sediment yield, km/yrs.	3.85×10^{-7}	8.84×10^{-7}	7.22×10^{-7}	2.50×10^{-7}	9.92×10^{-7}	7.25×10^{-7}	2.70×10^{-6}

Fig.4.25.A graphically shows the fan volumes (1-7) in the basin based on the results from Table 4.7, while Fig.4.25.B graphically presents the sediment yields from the associated catchment areas based on the results from Table 4.8.
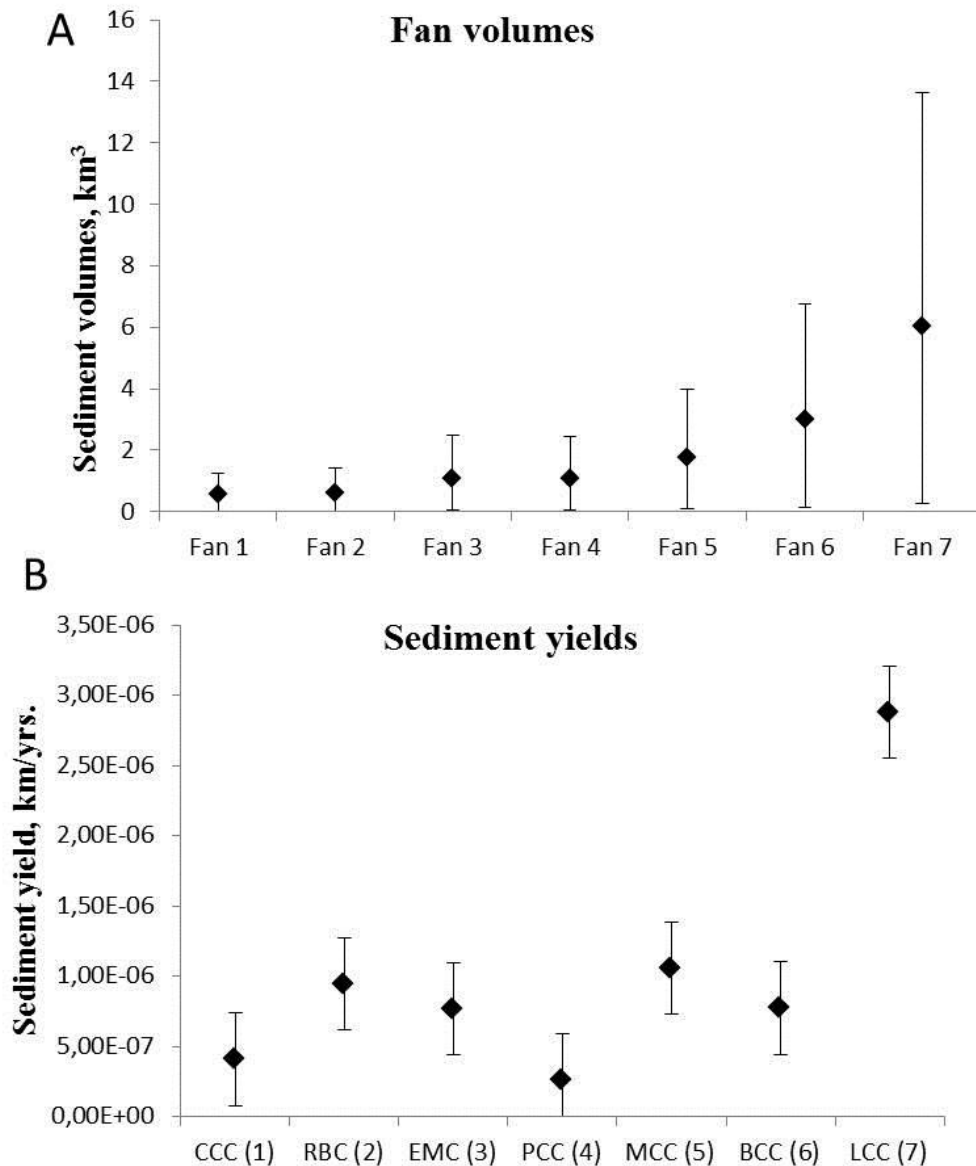
Figure 4.25: *A) Fan volumes (km³) deposited in front of each catchment (based on Bonneville and Provo fan delta lobes volumes); B) Sediment yields (km/yrs.) for each associated catchment area. Black squares in graph A represent the mid. case of fan volumes, the upper and lower error bar represent the high case and low case of fan volumes respectively. Similar error bars are applied for graph B, representing an upper and lower error bars for high sediment yields and low sediment yields respectively. CCC (City Creek Canyon), RCC (Red Butte Canyon), EMC (Emigration Canyon), PCC (Parleys Canyon), MCC (Mill Creek Canyon), BCC (Big Cottonwood Canyon), LCC (Little Cottonwood Canyon).*

4.10.4 Sediment flux (Qs) from the different catchment areas, the BQART model

To provide a better understanding of the calculated basin volumes, sediment discharge from the different catchments during Lake Bonneville times (30.000 years B.P.) were estimated using the BQART model (cf. chapter 3.5, eq.3.1). Dissimilar *B* factors were applied for the seven catchment areas along the segment, including lithology factor (*L*) and glacial erosion factor (*I*) (cf. Table 3.4). Results of the sediment flux (Qs) estimations are presented in Table 4.9 where the total amount of discharge to the basin is estimated to be approximately 5.4 km^3 during the last 30.000 years B.P. (Appendix C for detail calculations, p.113-114). The highest sediment fluxes are estimated from Mill Creek Canyon catchment area (result of erosive catchment lithology and 15 % glacial cover) and from Little Cottonwood Canyon catchment (result of 100 % glacial cover 30-12.000 years B.P.).

Table 4.9, Estimations of sediment flux (km^3/30 yrs.) using the BQART model, CCC (City Creek Canyon), RCC (Red Butte Canyon), EMC (Emigration Canyon), PCC (Parleys Canyon), MCC (Mill Creek Canyon), BCC (Big Cottonwood Canyon), LCC (Little Cottonwood Canyon).

	CCC	RBC	EMC	PCC	MCC	BCC	LCC	Total flux
Sediment flux, (Qs) km^3/30 yrs.	0.5	0.3	0.5	1.0	1.3	0.7	1.1	5.4
Lithology factor (*L*)	2	2	2	2	2	0.75	1	x
Glacial cover %	0	0	0	0	15	25	100	x

5 Discussion

5.1 Introduction

Several factors including tectonics, climate, catchment characteristics and lithology are all significant controls upon the volumes of sediment being discharged from the source to the sink (Milliman and Syvitski, 1992; Syvitski and Milliman, 2007). The fan deltas deposited in front of the seven major catchments within the Salt Lake Basin can give important insight into source-to-sink behavior because many of the key parameters are fixed while others differ, allowing the relative importance of the ones that vary to be determined. All of the catchments experienced the same regional climate conditions and were connected to a single lacustrine system that underwent significant rapid lake level changes. The catchment systems differ in terms of catchment size and shape, topographic elevation, stream gradient, catchment lithology and glacial record. Overall the fan areas are smallest in north and increase towards the south. Additionally there is general an increase in sediment yield of catchments towards the south. There is also a broad change from easily eroded catchments lithologies in the north to more resistant lithologies in the south, which intuitively would favor the opposite trend in fan size than that observed. There are number of explanations for this which are explored later in this section.

The total sediment volume deposited in the basin during Lake Bonneville time is estimated to be approximately 17 km^3 (cf. Table 4.4) with 62.5 % of the total volume deposited at Bonneville level, and 37.5 % of the total volume deposited at Provo level. Furthermore the sediment volumes deposited in each individual fan delta during Lake Bonneville times (30.000 years B.P.), ranges from 0.6 to 6.1 km^3 (cf. Table 4.7). Estimated volumes of sediment discharge (from the BQART model) range from 0.5 to 1.1 km^3 in the same time period (cf. Table 4.9).

The main aim of the project was to map and link the different catchments areas with the associated fan deltas within the Salt Lake City segment, and understand how sediment discharge and fan volumes are related to different controlling factors, with a special focus on the various bedrock lithologies in the catchments. The discussion is divided into four parts, briefly dealing with the accommodation creation in the basin; then the controls on catchment discharge and comparing the disparity in sediment discharge estimated from the BQART

model with the calculated fan volumes. Finally, some implications of source-sink studies are highlighted.

5.2 Controls on accommodation space for fan delta development

Accommodation space is created by lake level changes, subsidence in the basin and to a lesser extent uplift in the hinterland (Gawthorpe and Leeder, 2000). Changes in these parameters, coupled with changes in sediment supply, produce progradational, aggradational or retrogradational deltaic packages. Colder temperatures and higher precipitation rate (33% higher than present) are well established for the Salt Lake Basin during the onset of the ancient Lake Bonneville (Lemons et al., 1996) causing the lake level in the endorheic lake to rise. The climate during the deposition of Bonneville and Provo levels was characterized by a transition to milder and dryer temperatures, resulting in major falls in the lake level. Fluctuations in the Lake Bonneville lake level are the most important control on the stratal architecture of the fan delta systems. A sequence stratigraphic interpretation of the fan delta systems based on the well-established hydrography of Lake Bonneville (Oviatt et al., 1992; Milligan and Lemons, 1998) is proposed in Fig.5.1.

Stansbury Shoreline - TST   Maximum flooding surface
Bonneville Shoreline - HST   Sequence boundary sensu Van Wagoner et al. (1990)
Provo Shoreline - FRST   Sequence boundary sensu Hunt and Tucker (1993)
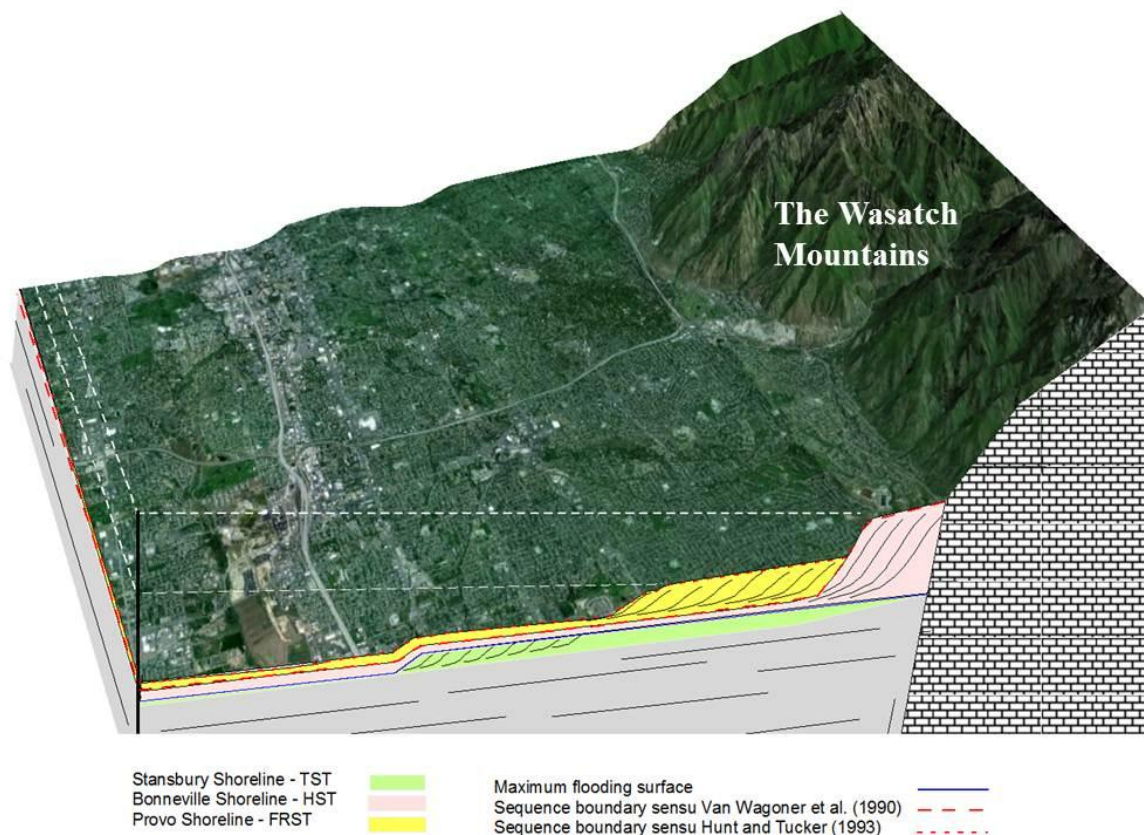
Figure 5.1: *Simplified sequence stratigraphic interpretation of the lake system in the Salt Lake Basin. The Stansbury shoreline represents the TST, seperated from the HST, Bonneville shoreline by an MFS.*

The Provo shoreline is a FRST. The position of the sequence boundary can be placed between the Bonneville and Provo fan deltas or at the present day land surface depending upon the sequence stratigraphic model followed. See text for detail, further discussion of this issue is beyond the scope of this project.

In the late Pleistocene (23-20.000 years B.P.), the lake level rose rapidly (to approximately 1372 m asl). This generated the Stansbury level shoreline which is interpreted as a transgressive system tract (TST). Further lake level rise 17.500 years B.P. resulted in the highest lake level (1552 m asl) and formed the maximum flooding surface across the basin. Subsequent progradation into the basin formed Bonneville level fan deltas which are interpreted as the highstand system tract which lasted approximately 2000-3000 years until rapid lake level fall at 14.500 years B.P. The lake level fall stabilized at 1445 m asl with subsequent deposition of Provo shoreline which is interpreted as a forced regression system tract (FRST). A series of incised valleys cut through the highstand and falling stage shorelines.

In addition to lake level rise, accommodation was also generated by subsidence along the Wasatch Fault Zone. This subsidence varied both spatial and temporally. Spatially, there is a long-term increase in fault throw from the north towards the south in the segment (from 0.2-0.4 mm/yr. to 0.6-1 mm/yr. respectively, cf. section 2.2). There is also marked short-term changes through time. During Bonneville times there were higher rate of slip (1.41 mm/yr.) than during Provo times (0.55 mm/yr., cf.Fig.2.3). A slip rate of 1.41 mm/yr. during the Bonneville times would have provided approximately 28 m (1.41 mm/yr.×2000 years duration time) of additional accommodation while 15 m (0.5 mm/yr.×3000 years duration time) was added during Provo times. Overall the space generated by subsidence is negligible compared to the hundreds of meters added and removed by the lake level fluctuations.

5.3 Possible controls on sediment discharge towards the Salt Lake Basin

5.3.1 Catchment lithology and erodibility

The fan deltas deposited in the Salt Lake Basin received sediments from catchments sourced from a variety of bedrock lithologies (cf.Fig.2.5, chapter 2.3). These lithologies have different erodibility and sediment production characteristics. Several studies have demonstrated that larger fan areas and thicknesses are associated with erodible catchment lithologies, and that lower sediment yields are found in catchments underlain by resistant lithologies. Studies by Bull (1962) and Hooke (1968) support this tendency. Bull`s (1962) work in western Fresno County, California, suggest that erodible lithologies, such as mudstone and shale, will double the fan size and thickness compared to resistant lithology, such as quartzite. In contrast work by Lecce (1991) indicates that basins underlain by resistant lithologies can produce larger fans due to the impact of the consequent gradient (Lecce, 1991).

Observations made of the fan areas in the current study indicate a poor correlation with the model of Bull (1962), but appear to be more consistent with Lecce`s (1991) finding that larger fan areas are associated with resistant catchment lithologies. Fan deltas located in southern parts of the segment (fans 6-7) are mainly sourced from catchments dominated by metamorphic and igneous rocks and are larger, while fans deposited in the north (fans 1-5) are largely sourced from catchments dominated by younger sedimentary rocks and are smaller.

Given that the thickness of the various fan systems are controlled primarily by lake level which is equal along the segment (cf.Fig.3.4), it follows that the greatest estimated volumes lie in the fans associated with catchments sourced from resistant rocks. Sediment volumes associated with the resistant catchment lithology (fans 6-7) contains approximately 63 % of the total basin volume, however the associated catchment area covers only 40 % of the total area of the drainage catchments (Fig.5.2). Little Cottonwood Canyon catchment, which predominantly consists of igneous rocks (65 %), provide the significantly highest fan volumes in the basin (fan 7).
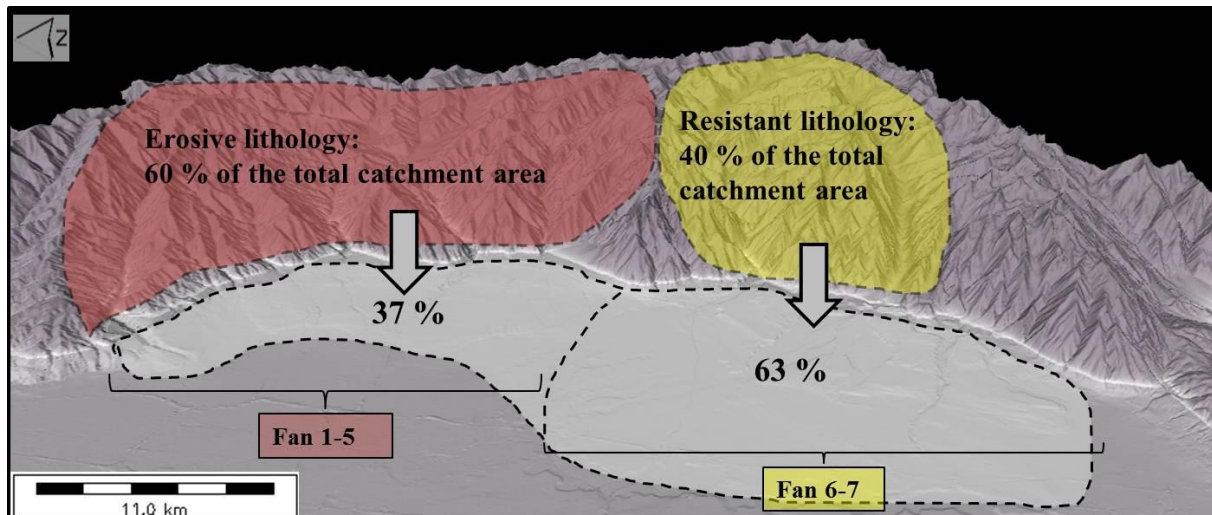
Figure 5.2: *Catchment lithology in relation to the associated fan volumes (%) deposited in the Salt Lake Basin. Catchments lithologies are divided into; Red) erosive, sedimentary rocks (60% of the total catchment area); Yellow) resistant, metamorphic & igneous rocks (40 % of the total catchment area). Fans 1-5 are associated with erosive, sedimentary bedrock lithologies and contributes with 37 % of the basin volume; Fans 6-7 are associated with resistant, metamorphic and igneous bedrock lithologies and contributes with 63 % of the basin volume.*

Fan volume calculated for the Big Cottonwood fan delta (fan 6) is almost three times higher compared to the volumes deposited in the Parleys fan delta (fan 4) which both covers approximately similar catchment area, but have relatively contrasting bedrock lithologies (cf. Table 4.7) The Parleys Canyon catchment erodes finer-grained shale, silt and sandstone, which would be expected to deliver more sediment to the associated fan compared to the Big Cottonwood Canyon fan delta which is mainly sourced from resistant, crystalline catchment lithologies, such as metamorphic quartzite (cf.Fig.4.5). Mill Creek Canyon fan delta (fan 5), which is predominantly derived from a catchment comprising limestone (67 %), has a higher sediment volume relative to other fan deltas derived from catchments dominated by other sedimentary rocks (conglomeratic bedrock in City Creek Canyon catchment, fine-grained shale, silt and sandstone in Parleys Canyon catchment).

Investigations of sediment yields (fan volume/catchment area) also suggest that more resistant bedrock lithologies deliver greater volumes of sediments to the basin than their more erodible counterparts (cf. Table 4.8). This suggests that catchment lithology is not the primary control on fan volumes in the Salt Lake Basin and that other factors are more significant. Given that many of the potential controlling parameters are constant between the catchment areas, the only remaining variable component is the degree of glacial cover and erosion during the last ice age.

5.3.2 Pleistocene Glaciation

The normal faulting along the active Wasatch Fault is associated with east-west extension resulting in a major rift basin and flexed footwalls, which have been uplifted and tilted. Greater uplift rate in the southern parts of the SLC segment (c.f. chapter 2.2) resulted in a higher topographic elevation and exhumation of more resistant catchment lithologies. These lithologies have formed steep, high-relief topography which is less readily eroded than the low-relief topography in the more erosive catchment lithologies located in the northern parts of the segment. As a consequence of colder mean temperature (1.1±2.5°C) on the highest topographic peaks, the entire Little Cottonwood Canyon catchment area and the upper parts of Mill Creek Canyon and Big Cottonwood Canyon catchments were covered by glaciers in the time period between 30.000-12.000 years B.P. (cf.Fig.2.6).

It is generally accepted that glacial erosion is more effective than river erosion (Hallet et al., 1996; Kirkbride and Mathews, 1997; Montgomery, 2002) although some authors suggest the contrary (Hebdon, 1997; Summerfield and Kirkbride, 1992). In the current study the glaciated catchments in the SLC segment are estimated to have generated the largest fan volumes in the basin, suggesting that glacial activity efficiently erodes and contributes significantly higher amounts of sediments to the fan deltas compared to fluvial erosion.

Glaciers generally have the ability to produce large volumes of sediments by plucking and scraping on the underlying bedrock (Boggs, 1995). The extent, thickness and gradient of the glacier, along with bedrock properties in the catchments, affect the ability of the ice to produce sediment and thereby the fan volumes deposited (Reading, 2009). Bedrock lithologies within the catchments associated with glaciations, are predominantly erosive limestone in Mill Creek Canyon catchment, crystalline metamorphic rocks in Big Cottonwood Canyon and igneous rocks in Little Cottonwood Canyon. Even though Mill Creek Canyon has an easier underlying substrate to erode, the glacial thickness and extent in the two catchments dominated by resistant lithologies were greater. The entire area of the Little Cottonwood Canyon catchment (70.9 km^2) was covered by ice. Further, Big Cottonwood Canyon catchment had an area of 32.6 km^2 of the total catchment (130.5 km^2) glaciated, compared to the topographically lower Mill Creek Canyon where 8.5 km^2 of the total catchment (56.4 km^2) was glaciated (Table 5.1).

Table 5.1: Relation between sediment volumes, yields and glacial cover

	CCC Fan 1	RBC Fan 2	EMC Fan 3	PCC Fan 4	MCC Fan 5	BCC Fan6	LCC Fan 7
Sediment volumes (km^3)	0.6	0.6	1.1	1.1	1.8	3.0	6.1
Sediment volumes (%)	4	4	8	8	13	21	42
Glacial cover (km^2)	0	0	0	0	8.5	32.6	70.9
Glacial cover (%)	0	0	0	0	15	25	100
Sediment yields (km/yrs.)	4.10×10^{-7}	9.44×10^{-7}	7.72×10^{-7}	2.67×10^{-7}	1.06×10^{-6}	7.75×10^{-7}	2.88×10^{-6}

Maximum ice thickness of 260 m (cf. chapter 2.4.1) has been estimated for the Little Cottonwood Canyon (Eldredge, 2010) which has twice the associated fan volumes than Big Cottonwood Canyon and 3.3 times that of Mill Creek Canyon where the catchments had a thinner ice thickness (Atwood, 1909). The fan deltas associated with the partly glaciated catchments have significant higher volumes compared to fans 1-4 which generated from the non-glaciated catchments. The area in Mill Creek Canyon catchment is approximately a 10 km^2 larger than City Creek Canyon (where both catchments are dominated by sedimentary rocks), while the fan volume is estimated to be three times larger in the Mill Creek Canyon fan delta (fan 5). Glacial erosion in the Mill Creek Canyon catchment explains the higher sediment production and deposited fan volumes compared to the City Creek Canyon fan delta (fan 1).

Fan volumes in relation to their associated catchment area and presence or absence of glaciers are illustrated in Fig.5.3. As mentioned significantly lower fan volumes are deposited from the non-glaciated catchments (fans 1-4 contributing 23 % of the total basin volume), compared with the fan deltas that were deposited in front of the catchments associated with fully or partly glaciation (fans 5-7 contributing 77 % of the total basin volume). Furthermore, the Little Cottonwood Canyon catchment (which was completely glaciated during the last glacial period and has the highest topographic elevation) contributes with approximately 42 % of the total basin volume (Table 5.1). Compared with City Creek Canyon (fan 1) which has a low elevation and the lowest calculated fan volume in the basin, as much as 10 times higher sediment volumes are estimated for the fan delta associated with the fully glaciated catchment compared to volumes deposited in front of the non-glaciated City Creek Canyon catchment.
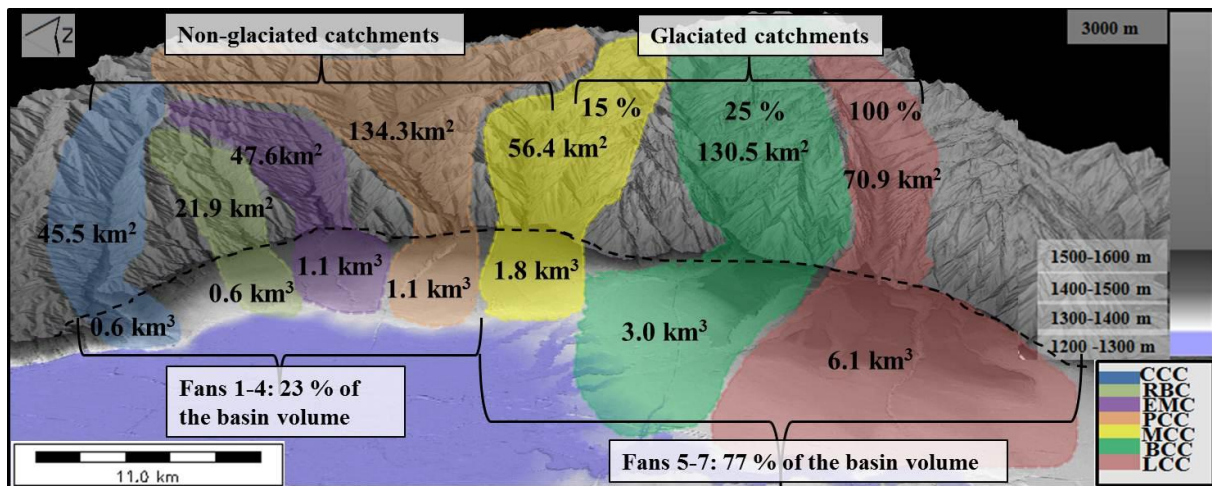
Figure 5.3: *Fan volumes in relation to their associated catchment areas and presence or absence of glaciers. Fans 1-4 (23 % of the basin volume) are associated with non-glaciated catchments; Fans 6-7 (77% of the basin volume) are associated with glaciated catchments. The glaciated catchments include Mill Creek Canyon (15 %), Big Cottonwood Canyon (25 %) and Little Cottonwood Canyon (100 %). CCC (City Creek Canyon), RBC (Red Butte Canyon), EMC (Emigration Canyon), PCC (Parleys Canyon), MCC (Mill Creek Canyon), BCC (Big Cottonwood Canyon) LCC (Little Cottonwood Canyon).*

Fig.5.4 compares the morphology of the fan deltas (fans 1-4) derived from the low-topographic, non-glaciated catchments, with the fan geometry (fans 5-7) of the high-topographic and glaciated catchments. The fan deltas deposited from the non-glaciated catchments show continuous smooth-fronted fan deltas (Fig.5.4.A). This observation may indicate constant water discharge and steady sediment supply. Further, the smooth delta fronts may indicate that the sediments have been reworked by wave-currents during Lake Bonneville times. In contrast the fan deltas deposited in front of the glaciated catchments show an irregular and lobate shape of the deltas, commonly with a southwards orientation (Fig.5.4.B). The lobate shaped fan deltas may suggest episodic release of sediments and glacial outwash associated with the deglaciation of the last ice age. Moreover, the southwards orientation of the fan delta lobes may also indicate redistribution of sediments by longshore currents with similar direction.
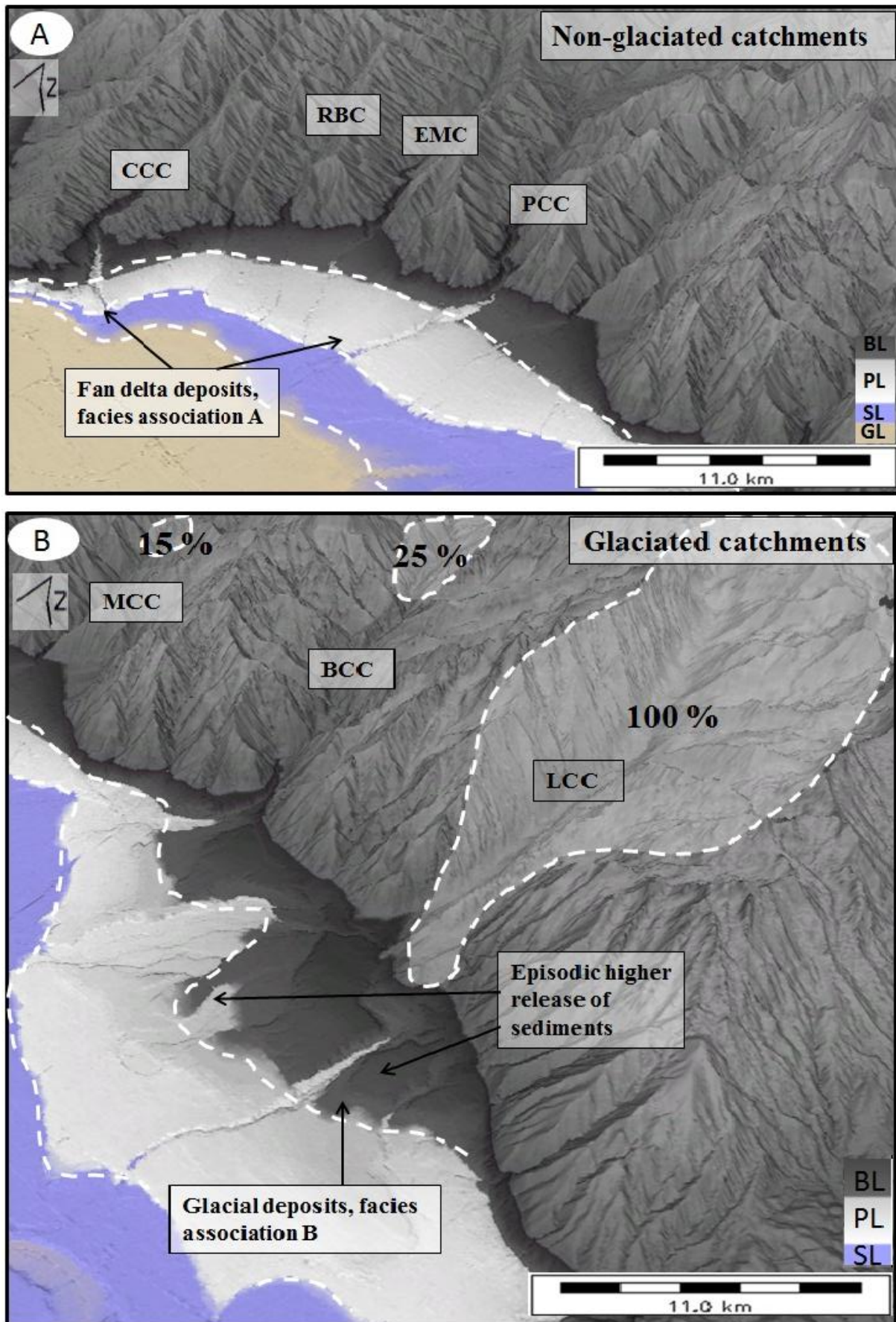
Figure 5.4*: A) 2 m DEM map illustrating the smooth and regular fan morphology (fans 1-4) of the deposits associated with the non-glaciated catchments located north in the segment. Deposit are*

dominated by facies association A (fan delta deposits); B) 2 m DEM map illustrating the irregular fan morphology (fans 5-7) associated with the glaciated catchments located south of the segment. Facies association B (glacial depoists) are observed, in addition to facies association A (fan delta deposits). CC (City Creek Canyon), RC (Red Butte Canyon), EM (Emigration Canyon), PC (Parleys Canyon), MC (Mill Creek Canyon, 15 % glacial cover), BC (Big Cottonwood Canyon, 25 % glacial cover), LC (Little Cottonwood Canyon, 100 % glacial cover). White, dotted line represents the outline of the different shoreline deposits, BL (Bonneville level), PL (Provo level), SL (Stansbury level), GL (Gilbert level).

Observations, based on the field-work, of glacial deposits (facies association B, cf.Fig.4.21.A) in the Little Cottonwood Canyon sink area (fan 7) coincides with the glaciated conditions established for the associated catchment. The fine-grain sand material observed in the Little Cottonwood fan area have large amount of boulder sized clasts within the same deposits. These large boulder sized clasts strongly indicates transportation of sediments by glaciers, whereas the fine-grained material in the fan deposits are interpreted to result from the redisposition of sand generated by glacial activity. Furthermore, Little Cottonwood Canyon has a well-defined U-shaped valley indicating a significant erosion of the bedrock by a large volume of ice. Big Cottonwood Canyon does not exhibit a consistently U-shaped valley. However, some glacial deposits (facies association B) are observed, but the associated fan delta is comprised mainly of coarse, gravelly deposits (facies association A). Similar fan delta dominated successions were observed in fan deltas 1-5, indicating sediment transportation and deposition by stream flows.

The glaciated and partially glaciated catchments with relative resistant lithology are associated with the steepest stream gradient, whereas non-glaciated catchments (dominated by erodible lithologies) have generally a gentler stream gradient (cf. Table 4.2). Catchments with a gentle stream gradient (mainly Emigration and Parleys Canyon, which both have a stream gradient of 0.04) may lead to storage of sediments in the canyon valley, also resulting to lower fan volumes in the basin. However, City Creek Canyon, which has the smallest fan area and lowest sediment volumes in the basin, shows a relative steep stream gradient (0.06). This suggests catchment lithology to may have had a greater influence for sediment discharge compared to the gradient component. The catchment consists largely of conglomeratic bedrock, which requires high energy for erosion and transport compared to limestone, shale and sandstone comprising the catchments with gentler stream gradients.

5.3.2.1 Sediment yields

The glaciated catchments are generally associated with the highest sediment yield estimations within the segment (cf. Table 4.8). According to Hallet et al. (1996) sediment yield tends to increase with increasing glacial cover, suggesting that catchments with a relative extensive glacial cover (≥30 %) generally show an average of one magnitude higher sediment yield than catchments without or with insignificant glacial cover. The results of Hallet et al. (1996) correspond to some degree for the estimated sediment yields from the catchments along the segment. Little Cottonwood Canyon, which was fully glaciated show almost an order of magnitude higher sediment yield compared with the non-glaciated catchments (cf. Table 4.8). Big Cottonwood Canyon and Mill Creek Canyon which were partially glaciated (25 % and 15 % cover respectively) show a slightly higher magnitude of sediment yields compared to some of the non-glaciated catchments, but generally relative similar yields are indicated (Table 5.1, cf. Table 4.8). These observation suggests that sediment yield is largely a result of the glacial cover in the catchment areas, and that glacial processes have significantly increased the production of sediment delivered to in the Salt Lake Basin.

Sediment yield generally tends to increase with decreasing catchment area emphasizing the importance of small, steep catchments for sediment production and transport (Milliman and Syvitski, 1992; Blum and Tornqvist, 2000). The positive inverse correltaion between the estimated sediment yields and catchment area is to some extent present within the study area, particularly for the catchments associated with glaciation. Big Cottonwood Canyon covers a significant larger catchment area (130.5 km^2) compared to the Little Cottonwood Canyon (70.9 km^2), and significant lower sediment yield is estimated for the Big Cottonwood Canyon (7.75×10^{-7} km/yrs. and 2.88×10^{-6} km/yrs. respectively, cf.Table 4.8). The non-glaciated catchments show a lower correlation between the positve invers trend of yield and corresponding catchment area. City Creek Canyon which covers the smallest catchment area (45.5 km^2) has been estimated to have relativley similar sediment yield as the Parleys Canyon which covers the largest catchment area (134.3 km^2) in the segment (Table 5.1, cf. Table 4.8).

5.3.3 Sediment routing and longshore currents along the basin

As described above, the calculated fan volumes increase from north to south within the basin. Schofield et al. (2004) emphasize a north-south longshore current transport of sediments along the Salt Lake Basin during Lake Bonneville times, with a suggested wave approach from the north-northwest (cf.Fig.2.10.A). The longshore currents direction is supported by the morphology of the Point of Mountain spit (POM in Fig.5.5). Furthermore, the presence of a bay-mouth barrier at the mouth of Corner Canyon (red circle in Fig.5.5) rather than deposition of a fan delta was used as further evidence for longshore transport by Schofield et al. (2004).
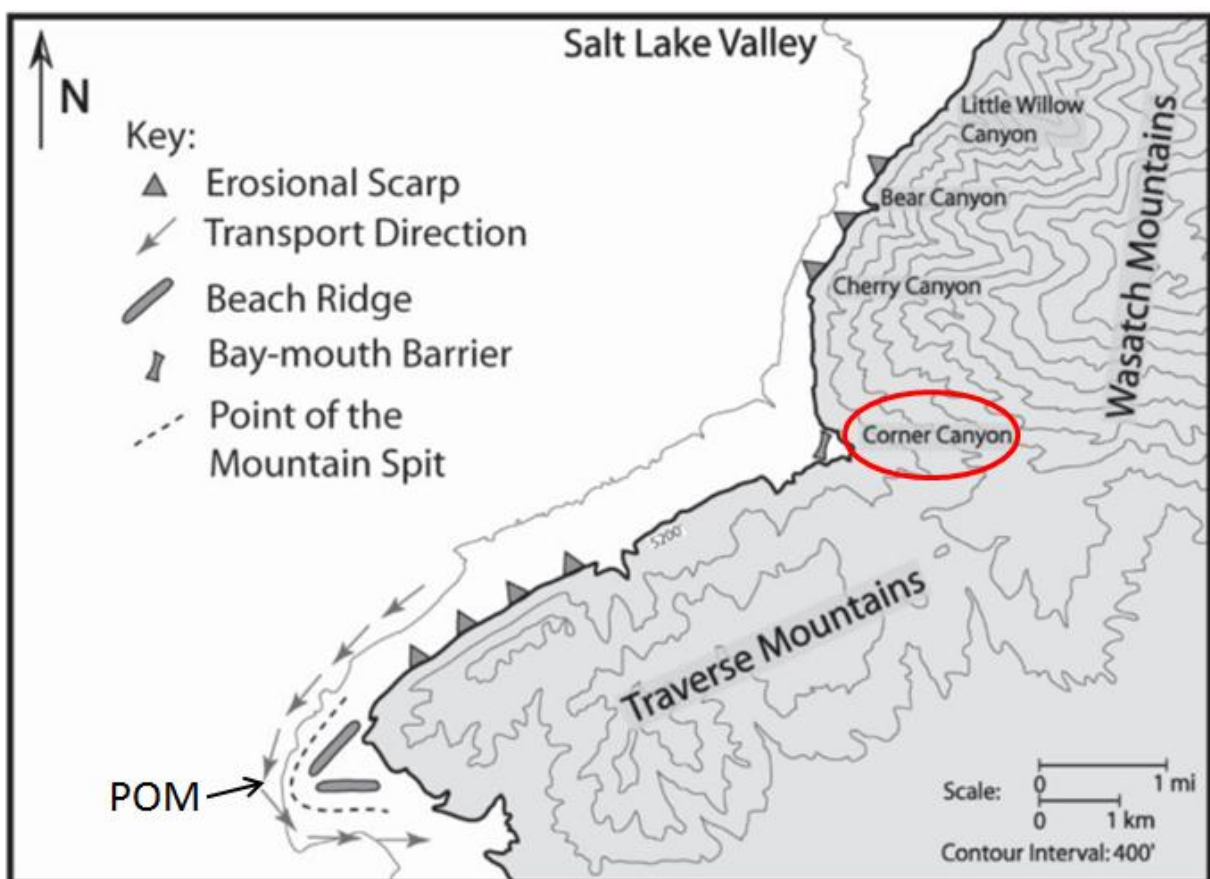
Figure 5.5: *Depositional features along the southern parts of the Salt Lake Basin suggesting deposition of a bay-mouth barrier in the mouth of the Corner Canyon (red circle), and a spit at the Point of Mountain (POM) with a wave approach from the north-northwest. Arrows indicate sediment transport direction. Map slightly modified from Schofield et al. (2004).*

North-south longshore currents may also have contributed the higher sediment volumes deposited in the southern fan deltas in the basin. This has been tested through the following approaches during the present study:

Lithological trends within the sink deposits:

- Significant higher amount of quartzite clasts are deposited in Parleys Canyon fan delta (fan 4) and Mill Creek Canyon fan delta (fan 5) compared to the amount of quartzite present in the associated catchments areas (cf.Fig.4.9 and Fig.4.12 respectively). The quartzite clast are likely to have been transported from the City Creek Canyon fan delta (fan 1) which has conglomeratic bedrock including a high amount of quartzite clasts (cf.Fig.4.6).

- Fan deltas generated from Little Cottonwood Canyon show a higher amount of sandstone compared to the catchment lithology (cf.Fig.4.18). These sandstone clasts are likely to have been transported from Big Cottonwood Canyon located further to the north where the catchment consists of approximately 9 % sandstone (cf.Fig.4.15).

- Monzo-granite clasts from the Little Cottonwood Stock were observed at the Point of Mountain spit which is located several km south from Little Cottonwood Canyon catchment where this intrusion particular appears (cf. Fig.4.22.C).

Depositional features along the basin:

- Fan mapping of the individual fan deltas and morphology of the Point of Mountain spit (cf.Fig.4.21) from the 2 m DEM dataset indicates a wave approach from the north. Furthermore the southwards orientation of the lobate shaped fan deltas observed in fans 6-7 (cf.Fig.5.4) may be a result of longshore currents reworking and redistributing sediments along the basin.

- Spit systems have been established to occur in the mouth of Big Cottonwood and Little Cottonwood Canyons with a similar southward prograding orientation as suggested for the Point of Mountain spit system (Jones and Marsell, 1955) (cf. Fig.2.10.A, chapter 2.5).

Fan volumes calculations:

- Estimations of fan areas (cf. Table 4.3) and calculations of fan volumes (cf. Table 4.7) show an increasing trend of volumes from the northern fan deltas (fans 1-4) towards the southern fan deltas (fans 5-7) along the basin.

Fig.5.6 summarizes the lithological distribution and estimated fan volumes deposited in the Salt Lake Basin, along with suggested sediment routing (transport from the source area to the depositional sink, and north-south transport by longshore currents within the sink).
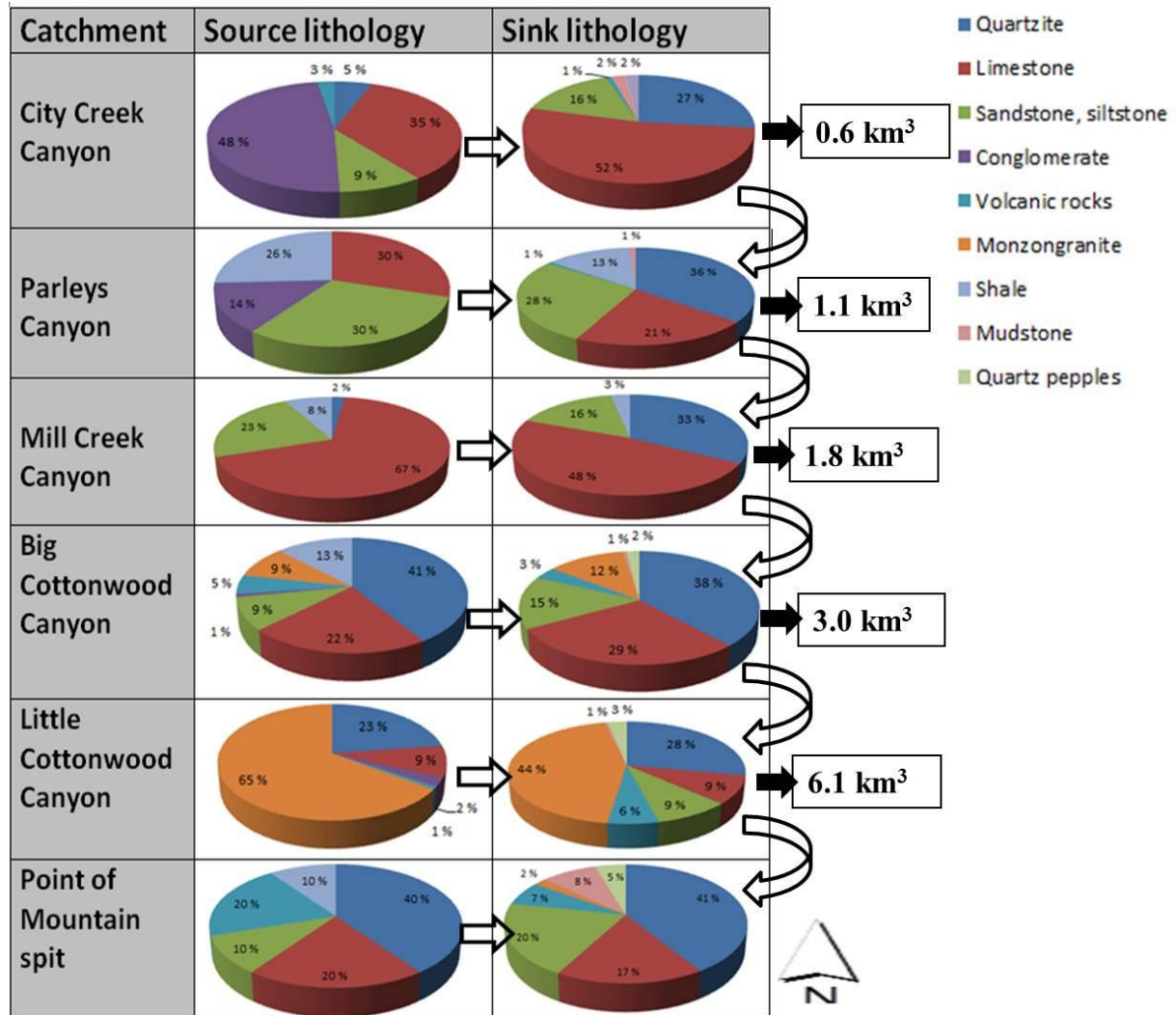
Figure 5.6: *Catchment source and sink lithologies, with the associated deposited fan volumes (km^3) within the Salt Lake Basin, which increases towards the south. Arrows to the left indicate transverse transport direction from catchment area towards the sink area. Curved arrows to the right indicate axial sediment transport by longshore currents along the basin.*

How efficient the longshore currents have been and what role they have played in the overall distribution of sediments is difficult to assess. However the lithological trends and the increasing fan volumes suggest at least some impact from north-south longshore currents. To constrain this theory further, the following section focuses on the differences in the calculated fan delta volumes and sediment discharges estimated from the BQART model.

5.4 BQART volumes and fan volumes relations

Sediment flux estimated from the BQART model provides a total volume of approximately 5.4 km^3 transported to the basin during the last 30.000 years B.P. (cf. Table 4.9). This discharge volume is significantly lower than the estimates for the total amount of volumes deposited in the seven fan deltas, which is approximately 14 km^3 during the same time period (Table 5.4, cf. Table 4.7).

For the interval 30.000-12.000 years B.P. a glacial cover (A_g) of 100 % was applied for Little Cottonwood Canyon and 25 % and 15 % for Big Cottonwood and Mill Creek Canyons respectively, resulting in a glacial erosion factor (I) of 10.0 for Little Cottonwood Cayon, 3.25 for Big Cottonwood and 2.35 for Mill Creek Canyon (cf.eq.3.5, section 3.5.1). Combining the glacial erosion factor (I) with the lithology factor (L) results in Mill Creek Canyon having a higher sediment discharge than the Big Cottonwood Canyon because of more easily eroded lithology in the former (cf.eq.3.4, section 3.5.1). Furthermore, a higher sediment discharge was estimated from the Parleys Canyon catchment (which covers approximately the same catchment area as the Big Cottonwood Canyon) as a result of a finer-grained and more readily eroded lithology. Table 5.4 compares the estimated BQART volumes with the calculated fan volumes deposited in the basin (both volumes are estimated for the time period under investigated during the last 30.000 years B.P.).

Table 5.4: Differences between the estimated BQART volumes and calculated fan volumes. Both volumes are based on the time interval of the last 30.000 years B.P.

	CCC	RBC	EMC	PCC	MCC	BCC	LCC	Total
Calcualted fan volumes (km^3)	0.6	0.6	1.1	1.1	1.8	3.0	6.1	14.2
BQART volumes (km^3)	0.5	0.3	0.5	1.1	1.4	0.7	1.1	5.4
Fan volume/ BQART volume	1.2	2.0	2.2	1.0	1.2	4.2	5.5	2.6

The largest differences between the fan volumes and the BQART volumes are found for Big Cottonwood and Little Cottonwood Canyon (marked with grey in Table 5.4), which are associated with 25 % and 100 % glacial cover respectively during the last ice age. The fan

volumes of these catchments are 4.2 and 5.5 times higher compared to the estimated volumes discharged from the catchments. The non-glaciated catchments show less disparity, but the BQART model still underestimates the amount of sediments in the order of 1.0 to 2.2 (Table 5.4). Fig.5.7 show the fan volume/ BQART volume ratio in relation to the lithology factor (*L*) and associated glacial cover (*Ag*) applied in the BQART model estimations.
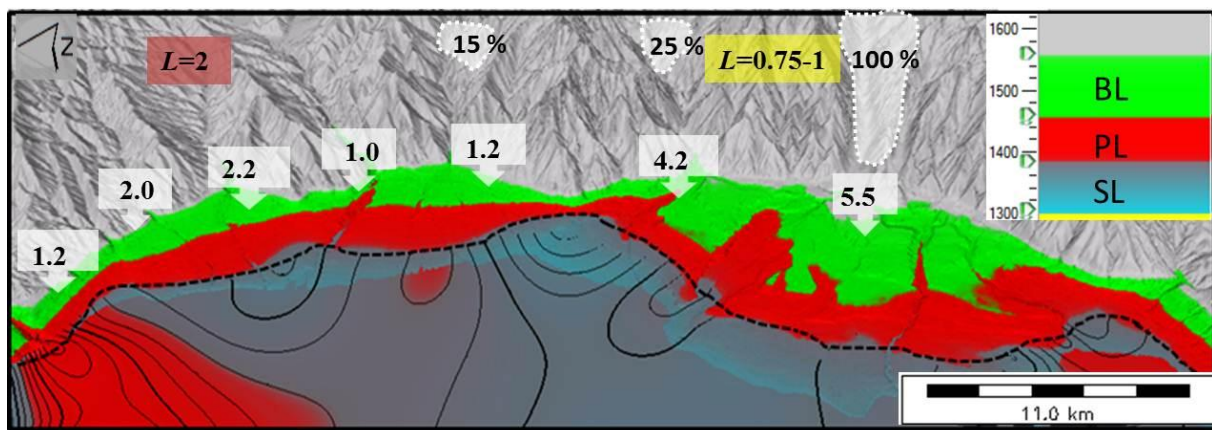
Figure 5.7: *10 m resolution DEM data illustrating the fan volume/BQART volume ratio and the relation between glacial cover (%) and lithology factor (L=2 sedimentary rocks, L=0.75-1 relative resistant igneous and metamorphic rocks). Green (Bonneville shoreline sediments BL); Red (Provo shoreline sediments PL) Black, dotted line represent the top of Stansbury shoreline (SL), approximatley 1372 meter asl.*

Fig.5.7 shows that a better correlation is observed between the estimated BQART volumes and fan volumes in the non-glaciated catchment underlain soft, erosive lithology (*L*=2), than the glaciated catchment sourced mainly in resistant lithology (*L*=0.75-1). Both calculations of fan volume and sediment discharge (from the BQART model) are associated with large uncertainties; however the trend in increasing differences in volumes from the north to south is present in both calculations (Table 5.4). Discussion related to the large disparity of sediments discharge and sediment volumes deposited in the basin can be approached in two ways.

The first approach assumes that the calculated fan volumes are directly related to the upstream catchment with no contribution from longshore drift. This assumption suggests that the BQART model highly underestimates the volumes of sediments eroded by glaciers. Even though glacial erosion is considered in the BQART model, the parameter which accounts for this in the equation may be too low. Furthermore, it may indicate that the model is less reliable in calculating sediment discharge associated with glaciated areas, particularly in

catchments underlain by relative resistant bedrock lithology, which show the greatest disparity. However the BQART model underestimated all of the sediments volumes from the catchments irrespective of whether they have been glaciated. This suggests that the assumptions in the model may require revision.

Sediment transported by longshore currents and/or sediment delivered from smaller local canyons were not considered in the BQART model. A potential north-south longshore transport system of sediments along the basin (as discussed in the previous section) would thereby be a possible factor contributing to higher differences in sediment discharge and volumes of sediment deposited for Big Cottonwood Canyon and Little Cottonwood Canyon fan deltas. A second approach would be to consider the discharge volumes from the BQART model as correct and assign the sediment volumes in the fans partly to longshore currents. As mentioned, 4.2 and 5.5 times higher volumes are present in the fans of Big Cottonwood and Little Cottonwood Canyon respectively than what can be accounted for in the BQART model (Table 5.4). This suggest, based on the assumption above, that as much as 76 % of the total fan volumes deposited in Big Cottonwood fan delta and 82 % of the total fan volumes in Little Cottonwood fan delta can be explained by sediment transport along the basin by longshore currents from north towards the south.

From several lines of evidence (e.g. calculated fan volumes, fan areas and field-data) it is reasonable to suggest that a north-south longshore transport system of sediments along the basin was instrumental in generating larger sediment volumes for the fans located in the south. This, together with glacial processes has been suggested to be the main factors controlling the sediment distribution and volumes along the Salt Lake Basin during Lake Bonneville times.

5.5 Implications of source-sink studies

Source-sink studies aim to give a complete investigation of the whole sedimentary system and to improve the understanding of complex interplays of factors controlling sediment erosion, transport and volumes of sediments deposited in the basin. The concept represents a relative new, holistic approach for studies of the depositional basin and number of source-sink studies has increased during the recent years due to modern tools and data such as digital elevation models and improved quality, quantity and availability of seismic and geomorphological data (both onshore and offshore) (Martinsen et al., 2011). Studies of the whole sedimentary system are particularly useful for the petroleum industry as a predictive tool where little data are present, or to reduce uncertainties where some data exists. Further, source-sink analysis can be used to give information to predict possible plays including reservoir, sources and seals. Several approaches of analysis have been reviewed (Martinsen et al., 2011).

One approach involves the coupling between ancient and modern sedimentary systems. In modern systems, controlling factors, such as climate and tectonic history and sediment discharge can often be interpreted more easily, compared to estimation of those factors in ancient systems which are more challenging (Martinsen et al., 2011). The potential of source-sink studies lies in dealing with these challenges, where analysis of recent and modern systems can be transferred to ancient systems to perform a higher confidence of these predictions. Recent work by Sømme et al. (2009) have applied this method, where studies of 29 modern source-sink systems have been undertaken for predicting characteristics of ancient systems with similar features. Analysis also involves the parameterization of the controls of sediment discharge and basin volume in one segment to estimating parameters of other segments within the same sedimentary system. The concept of linked segments (cf.Fig.1.1) is based on how characteristics of one segment are affected by updip segments, and influence characteristics of the downdip segments (Sømme et al., 2009). This approach can be applicable in predicting sediment distribution in the depositional basin, if characteristics of the updip segments are known.

Composition of lithology in the catchment areas influence the texture, grain size, permeability and porosity of the sediments deposited in the basin (Menacherry, 2008). Source-sink analysis in the depositional system provides information of these features and can be helpful for propose areas with good reservoir quality. E.g. catchments sourced in relative coarse-grained

granitic rocks will produce more sand in the basin compared to catchments dominated by the counterpart such as fine-grained shale. Further, sandstone, which has a high porosity and permeability, tends to produce good reservoir rocks. Knowledge about the variety and percentage of lithologies present in the catchment area can thereby be useful in predicting potential reservoir units in the depositional system.

During the last decade varies models for investigating the sediment discharge have been developed (Martinsen et al., 2011). Investigations of long-term sediment load can be approached using the BQART model introduced by Syvitski and Milliman (2007). Sediment discharge from the drainage catchments is essential in controlling sediment distribution, volumes and the stacking patterns of sandbodies in the depositional system. If parameters such as the paleodrainage area, topography, lithology and climate for a give system are established, the model can be used by the industry for estimating sediment discharge and to predict areas associated with large amounts of sediment volumes. However, the model provides a first-order control of fluvial sediment delivery and is associated with large uncertainties (some which are outlined in chapter 3.5.2). The sediment discharge also tends to be unsteady through time influenced by climate and tectonic changes (Leeder, 1997). This, together with that volumes of sediment discharged from the drainage catchments do not necessary end up in the depositional basin, results in a continuous discussion whether this approach can be useful for the petroleum industry.

6 Summary & conclusions

Active normal faulting along the Wasatch Mountains created an extensional basin into which large volumes of sediment, eroded from uplifted footwall mountains were deposited. The climate during the late Pleistocene shifted from cold and dry towards wetter and warmer resulting in significant lake level rise and subsequent fall that temporarily created accommodation space for number of coarse fan deltas along the basin margin. These highstand and forced regressive fan delta systems can provide good case study in sequence stratigraphy.

Source-sink studies in the major catchments along the Salt Lake City segment combined with calculations of associated fan volumes highlight the role of a number of controlling factors. Fig.6.1 summarizes the main suggested controls on sediment discharge and fan volumes deposited within the Salt Lake Basin during Lake Bonneville times.

●Sediment volumes in the basin are calculated to be highest in the fan deltas associated with relative resistant metamorphic and igneous catchment lithologies (fans 6-7), whereas catchments underlain by more erodible and younger sedimentary lithologies contributed with significant lower fan volumes (fans 1-5). This is counter-intuitive to most of the existing models for fan size.

●The relative resistant catchments correspond to the highest topography in the segment, which underwent glaciation during the Last Glacial Maximum. Glacial processes in these catchments, Mill Creek Canyon, Big Cottonwood Canyon and Little Cottonwood Canyon, have been suggested to be a great contributor of the large amount (77 % of the total basin volume) of sediment deposited in the Salt Lake Basin.

●A glacial control of the system could be a factor explaining, as estimated from the BQART model, the large differences in the calculated fan volumes and sediment discharge from the catchments associated with glaciation. Even though the BQART model considers glacial erosion in the equation, the model is suggested to be underestimating sediment erosion from the glaciated catchments, especially associated with relative resistant catchment lithology. The BQART model also underestimated the volumes of sediments eroded from the non-

glaciated catchments suggesting that some of the parameters within the equation may need to be reviewed.

●Transport of sediments along the basin by longshore currents is indicated to be a contributing factor for higher sediment volumes deposited in the fan deltas located in the southern parts of the study area (fans 6-7). Furthermore, longshore currents are also suggested to be instrumental for explaining the significant larger disparity in estimated sediment discharge and calculated fan volumes for the Big Cottonwood Canyon and Little Cottonwood Canyon drainage systems.

●Source-sink studies can be useful for the petroleum industry by improving the understanding of the complete sedimentary system, especially where little data exists. Further, source-sink studies can provide essential information regarding sediment portioning and presentation in the depositional basin for predicting possible reservoir units, sources and seals.
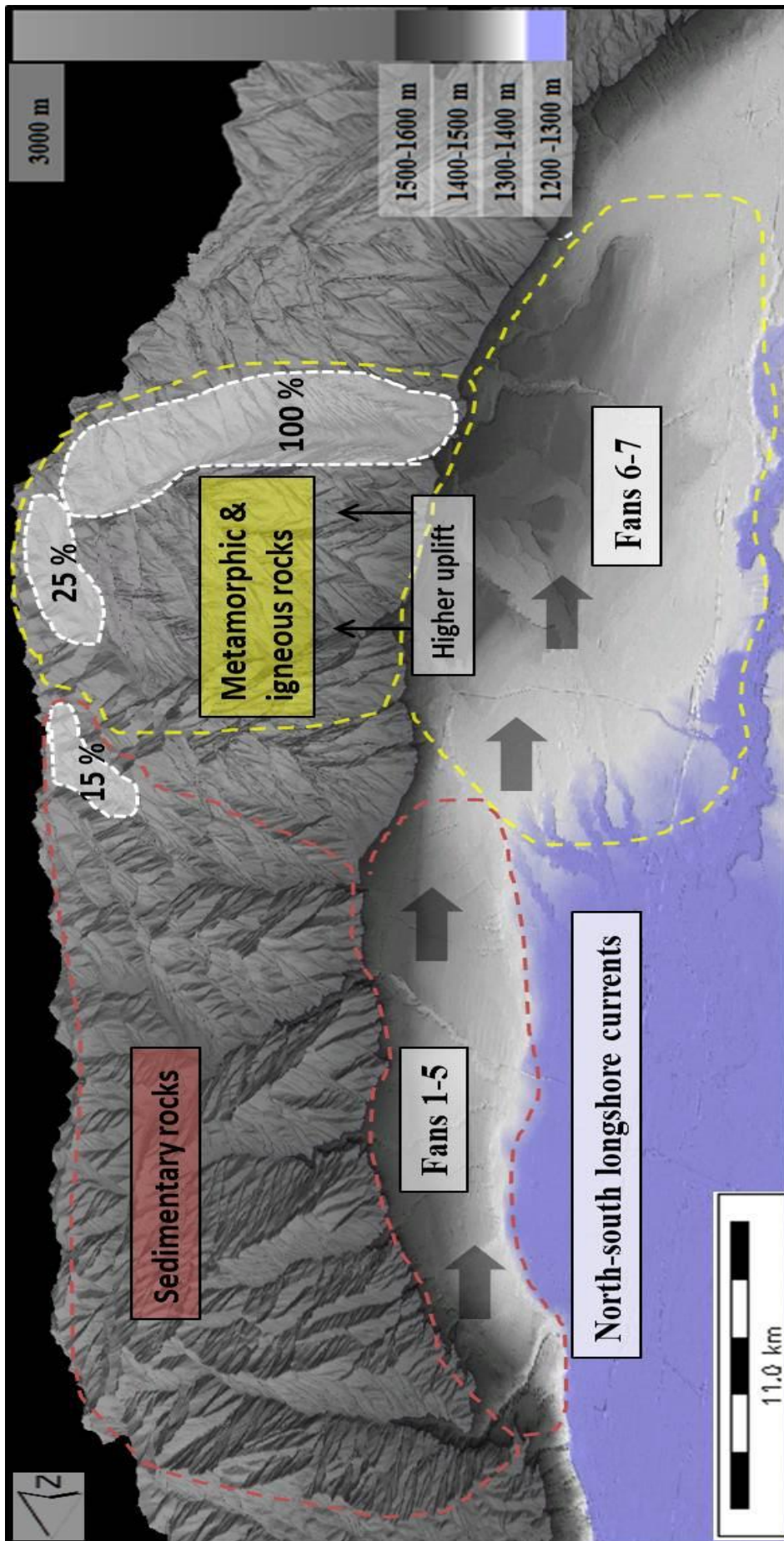
Figure 6.1: *Summarazies the suggested main controls of sediment volumes produced in the catchment areas and deposited in the Salt Lake Basin. Differences in uplift rate resulted in Pleistocene glacial cover (30-12.000 years B.P.) in the highest, most resistant peaks giving higher erosion and higher sediment discharge and hence depositional volumes. Arrows indicates a north-south direction of the longshore system, which have been suggested to be an instrumental factor contributing to higher sediment volumes in fans 6-7. Yellow dotted line represents resistant catchment lithology and fan 6-7, red dotted line represent erosive catchment lithology and fans 1-5.*

7 References

Allen, P. A., et al. (2013). The Qs problem: Sediment volumetric balance of proximal foreland basin systems. *Sedimentology, 60***,** 102-130.

Allen, P. A. & Densmore, A. L. (2000). Sediment flux from an uplifting fault block. *Basin Research,* 12**,** 367-380.

Armstrong, P. A, Taylor, A. R & Ehlers, T. A (2004). Is the Wasatch fault footwall (Utah, United States) segmented over million-year time scales? *Geology,* 32**,** 385-388.

Arzani, N. (2012). Catchment lithology as a major control on alluvial megafan development, Kohrud Mountain range, central Iran. *Earth Surface Processes and Landforms,* 37**,** 726-740.

Atwood, W. W. (1909). Glaciation of the Uinta and Wasatch mountains, US Government Printing Office.

Bills, B. G., Currey, D. R. & Marshall, G. A. (1994). Viscosity Estimates for the Crust and Upper-Mantle from Patterns of Lacustrine Shoreline Deformation in the Eastern Great-Basin. *Journal of Geophysical Research-Solid Earth,* 99**,** 22059-22086.

Black, B. D., et al. (1996). Paleoseismic investigation on the Salt Lake City segment of the Wasatch fault zone at the South Fork Dry Creek and Dry Gulch sites, Salt Lake County, Utah, Salt Lake City, UT, United States (USA), Utah Geological and Mineral Survey, Salt Lake City, UT.

Blair, T. C. & McPherson, J. G. (1994a). Alluvial fan processes and 14 forms. *Geomorphology of desert environments***,** 354.

Blair, T.C. & McPherson, J. G. (1994b). Alluvial fans and their natural distinction from rivers based on morphology, hydraulic processes, sedimentary processes, and facies assemblages. *Journal of Sedimentary Research,* 64**,** 450-489.

Blum, M. D. & Hattier-Womack, J. (2009). Climate change, sea-level change, and fluvial sediment supply to deep-water depositional systems. *Special Publication - Society for Sedimentary Geology,* 92**,** 15-39.

Blum, M. D. & Tornqvist, T. E. (2000). Fluvial responses to climate and sea-level change: a review and look forward. *Sedimentology,* 47**,** 2-48.

Boggs, S. (1995). *Principles of sedimentology and stratigraphy*, Prentice Hall Englewood Cliffs.

Bruhn, R. L., Gibler, P. R. & Parry, W.T. (1987). Rupture characteristics of normal faults: an example from the Wasatch fault zone, Utah. *Geological Society, London, Special Publications,* 28**,** 337-353.

Bruhn, R.L. and Anguita, D.(2013). Earthquake geology in the Neffs Canyon area, Salt Lake City, Department of Geology and Geophysics, The University of Utah. http://www.utah.edu/research/Anguita.DanielaPDF.pdf. [retrieved 23.03.2013].

Bryant, B. & Nichols, D. J. (1990). Geologic Map of the Salt Lake City 30′ X 60′ Quadrangle, North-central Utah, and Uinta County, Wyoming, US Geological Survey.

Bull, W. B. (1962). Relations of alluvial fan size and slope to drainage basin size and lithology in western Fresno County, CA. *US Geological Survey Professional Paper***,** 51-53.

Bull, W. B. (1964). Alluvial fans and near surface subsidence in Western Fresno County, California. *Profess. Papers, U. S. Geol. Survey.*, 1-71.

Bull, W. B. (1972). Recognition of alluvial fan deposits in the stratigraphic record. *Recognition of Ancient Sedimentary Environments* 16, 63-83. Society of Economic Paleontologists and Mineralogists.

Bull, W. B. (1977). The alluvial-fan environment. *Progress in physical geography,* 1, 222-270.

Case, F.W. (1990). Engineering Geology of the Salt Lake City Metropolitan Area, Utah.

Case, W.F., et al. (2005). Geological Guide to the Central Wasatch Front Canyons, Salt Lake County, Utah. *Public Information Series 87.* Utah Geological Survey.

Chan, M. A. & Milligan, M. R. (1994). Gilbert's vanishing deltas; a century of changes in Pleistocene deposits of N. Utah. *Geological Society of America,* 26, 318-318.

Cluff, Lloyd S., et al. (1975). Recent activity of the Wasatch fault, Northwestern Utah U.S.A. *Tectonophysics,* 29, 161-168.

Cook, K. L. & Berg, J. W. (1961). Regional Gravity Survey Along the Central and Southern Wasatch. Front, Utah. *Geological Survey Professional Paper 316-E.*

Cook, K. R., et al. (1984). Trihalomethane Compounds and Their Precursors in Salt Lake County: Evaluation of Trihalomethane Source and Production http://digitalcommons.usu.edu/water_rep/524 [retrieved 01.03.2013].

Cowie, P. A. , et al. (2006). Investigating the surface process response to fault interaction and linkage using a numerical modelling approach. *Basin Research,* 18, 231-266.

Crittenden, M. D. (1963). New data on the isostatic deformation of Lake Bonneville, US Government Printing Office.

Currey, D. R., et al. (1985). Durations, average rates, and probable causes of Lake Bonneville expansions, stillstands, and contractions during the last deep-lake cycle, 32,000 to 10,000 years ago, United States (USA), Univ. Utah, Cent. Public Aff. Adm.

Currey, D.R., Atwood, G. & Mabey, D.R. (1984). Major Levels of Great Salt Lake and Lake Bonneville, May 1984. Utah Geological and Mineral Survey.

Densmore, A. L., Allen, P. A. & Simpson, G. (2007). Development and response of a coupled catchment fan system under changing tectonic and climatic forcing. *J. Geophys. Res.,* 112, F01002.

Driscoll, N. & Nittrouer, C. (2000). Source to sink studies. *Margins,* 11, 14.

DuRoss, C. B. (2008) Holocene Vertical Displacement on the Central Segments of the Wasatch Fault Zone, Utah. *Bulletin of the Seismological Society of America,* 98, 2918-2933.

DuRoss, C.B., et al. (2012). Paleoseismic investigation to compare surface faulting chronologies of the west Valley Fault and Salt Lake City segment of the Wasatch Fault Zone, Salt Lake Conuty.

Ehlers, T. A. & Farley, K. A. (2003). Apatite (U–Th)/He thermochronometry: methods and applications to problems in tectonic and surface processes. *Earth and Planetary Science Letters,* 206, 1-14.

Eldredge, S. (2010). Glacial Landforms in Big and Little Cottonwood Canyons, Salt Lake County, Utah. *Geosights article, Survey Notes,* 42.

Eppes, M. C. & McFadden, L. (2008). The influence of bedrock weathering on the response of drainage basins and associated alluvial fans to Holocene climates, San Bernardino Mountains, California, USA. *Holocene,* 18**,** 895-905.

Evans, O. F. (1942). The Origin of Spits, Bars, and Related Structures. *The Journal of Geology,* 50**,** 846-865.

Gawthorpe, R. L. & Hurst, J. M. (1993). Transfer Zones in Extensional Basins - Their Structural Style and Influence on Drainage Development and Stratigraphy. *Journal of the Geological Society,* 150**,** 1137-1152.

Gawthorpe, R.L. & Leeder, M.R. (2000). Tectono sedimentary evolution of active extensional basins. *Basin Research,* 12**,** 195-218.

Gilbert, G.K. (1890). Lake Bonneville, United States Geological Survey.

Godsey, H. S. , et al. (2011). Stratigraphy and chronology of offshore to nearshore deposits associated with the Provo shoreline, Pleistocene Lake Bonneville, Utah. *Palaeogeography, Palaeoclimatology, Palaeoecology,* 310**,** 442-450.

Godsey, H. S., et al. (2005a). Don R. Currey Memorial Field Trip to the shores of Pleistocene Lake Bonneville. *Field Guides,* 6**,** 419-448.

Godsey, H. S., Currey, D. R. & Chan, M. A. (2005b). New evidence for an extended occupation of the Provo shoreline and implications for regional climate change, Pleistocene Lake Bonneville, Utah, USA. *Quaternary Research,* 63**,** 212-223.

Granger, A.E. , et al. (1952). Geology of the Wasatch Mountains East of Salt Lake City 1.

Hallet, B., Hunter, L. & Bogen, J. (1996). Rates of erosion and sediment evacuation by glaciers: A review of field data and their implications. *Global and Planetary Change,* 12**,** 213-235.

Hampel, A., Hetzel, R. & Maniatis, G. (2010). Response of faults to climate-driven changes in ice and water volumes on Earth's surface. *Philos Transact A Math Phys Eng Sci,* 368**,** 2501-17.

Harvey, A. M. (2002). Effective timescales of coupling within fluvial systems. *Geomorphology,* 44**,** 175-201.

Harvey, A. M., Mather, A. E. & Stokes, M. (2005). Alluvial fans: geomorphology, sedimentology, dynamics—introduction. A review of alluvial-fan research. *Geological Society, London, Special Publications,* 251**,** 1-7.

Harvey, A.M. (2005). Differential effects of base-level, tectonic setting and climatic change on Quaternary alluvial fans in the northern Great Basin, Nevada, USA. *Geological Society, London, Special Publications,* 251**,** 117-131.

Hebdon, N. J., Atkinson, T. C., Lawson, T. J., Young, I. R. (1997). Rate of Glacial Valley Deepening During the Late Quaternary in Assynt, Scotland. *Earth Surface Processes and Landforms,* 22**,** 307-315.

Helland-Hansen, W. & Mart, O.J. (1996). Shoreline Trajectories and Sequences: Description of Variable Depositional-Dip Scenarios. *SEPM Journal of Sedimentary Research,* Vol. 66**,** 670-688.

Hintze, F. F. (1914). A Contribution to the Geology of the Wasatch Mountains, Utah. *Annals of the New York Academy of Sciences,* 23**,** 85-143.

Hintze, L. F. (1988). Geologic history of Utah, Department of Geology, Brigham Young University.

Hintze, L. F. (2005). Utah's spectacular geology: how it came to be, Department of Geology, Brigham Young University.

Hintze, L. F. , et al. (2000). Digital Geologic Map of Utah. Utah Geological Survey, Utah Geological Survey, Department of natural resources, in cooperation with the United States Geological Survey Map 179DM.

Hooke, R. L. B. (1968). Steady-state relationships on arid-region alluvial fans in closed basins. *American Journal of Science,* 266**,** 609-629.

Hooke, R. L. B. & Rohrer, W. L. (1977). Relative erodibility of source-area rock types, as determined from second-order variations in alluvial-fan size. *Geological Society of America Bulletin,* 88**,** 1177-1182.

Ives, R. L. (1950). Glaciations in Little Cottonwood Canyon, Utah. *The Scientific Monthly,* 71**,** 105-117.

James, L. P. (1979). Geology, ore deposits, and history of the Big Cottonwood mining district, Salt Lake County, Utah, Utah Geological Survey.

Jewell, P. W. (2010). River incision, circulation, and wind regime of Pleistocene Lake Bonneville, USA. *Palaeogeography Palaeoclimatology Palaeoecology,* 293**,** 41-50.

Jewell, P.W. (2007). Morphology and paleoclimatic significance of Pleistocene Lake Bonneville spits. *Quaternary Research,* 68**,** 421-430.

Jones, D. J. & Marsell, R. E. (1955). Pleistocene sediments of lower Jordan Valley, Utah.

Karow, T. & Hampel, A. (2010). Slip rate variations on faults in the Basin-and-Range Province caused by regression of Late Pleistocene Lake Bonneville and Lake Lahontan. *International Journal of Earth Sciences,* 99**,** 1941-1953.

Kaufman, D. S. (2003). Amino acid paleothermometry of quaternary ostracodes from the Bonneville Basin, Utah. *Quaternary Science Reviews,* 22**,** 899-914.

Kirkbride, M. & Mathews, D. (1997). The role of fluvial and glacial erosion in landscape evolution: The Ben Ohau Range, New Zealand. *Earth Surface Processes and Landforms,* 22**,** 317-327.

Kowallis, B. J., Ferguson, J. & Jorgensen, G. J. (1990). Uplift Along the Salt Lake Segment of the Wasatch Fault from Apatite and Zircon Fission-Track Dating in the Little Cottonwood Stock. *Nuclear Tracks and Radiation Measurements,* 17**,** 325-329.

Kutzbach, J. E., et al. (1993). Simulated climatic changes: results of the COHMAP climate-model experiments. *Global climates since the last glacial maximum***,** 24-93.

Laabs, B. J. C., et al. (2011). Chronology of latest Pleistocene mountain glaciation in the western Wasatch Mountains, Utah, U.S.A. *Quaternary Research,* 76**,** 272-284.

Lecce, S. A. (1991). Influence of Lithologic Erodibility on Alluvial-Fan Area, Western White Mountains, California and Nevada. *Earth Surface Processes and Landforms,* 16**,** 11-18.

Leeder, M. R. (1997). Sedimentary basins: Tectonic recorders of sediment discharge from drainage catchments. *Earth Surface Processes and Landforms,* 22**,** 229-237.

Lemons, D. R. , Milligan, M. R. & Chan, M.A. (1996). Paleoclimatic implications of late Pleistocene sediment yield rates for the Bonneville Basin, northern Utah. *Palaeogeography, Palaeoclimatology, Palaeoecology,* 123**,** 147-159.

Lemons, D.R. (1997). Stratigraphy, paleoclimatic implications, and permeability distribution of fine-grained lacustrine deltas along the eastern margin of late Pleistocene Lake Bonneville.

Lemons, D. R. & Chan, M. A. (1999). Facies architecture and sequence stratigraphy of fine-grained lacustrine deltas along the eastern margin of late Pleistocene Lake Bonneville, northern Utah and southern Idaho. *Aapg Bulletin-American Association of Petroleum Geologists,* 83**,** 635-665.

Link, P.K., Kaufman, D.S. & Thackray, G.D. (1999). Field Guide to Pleistocene Lakes Thatcher and Bonneville and the Bonneville Flood, Southeastern Idaho. *Field Guide to Pleistocene Lakes Thatcher and Bonneville***,** 251-266.

Lund, R. W. (1990). Engineering Geology of the Salt Lake City Metropolitan Area, Utah.

Machette, M. N. (1989). Preliminary Surficial Geologic Map of the Wasatch Fault Zone, Eastern Part of Utah Valley, Utah County and Parts of Salt Lake and Juab Counties, Utah, Geological, Survey, The Survey.

Machette, M. N., et al. (1991). The Wasatch fault zone, Utah segmentation and history of Holocene earthquakes. *Journal of Structural Geology,* 13**,** 137-149.

Machette, N.M. (1992). Surficial Geological map of the Wasatch Fault Zone, Eastern parts of Utah Valley, Utah County and parts of Salt Lake and Juab Counties, Utah. *U.S. Department of the Interior U.S Geological Survey* 28.

Madsen, D. B. & Currey, D. R. (1979). Late Quaternary Glacial and Vegetation Changes, Little Cottonwood Canyon Area, Wasatch Mountains, Utah. *Quaternary Research,* 12**,** 254-270.

Martinsen, O. J., et al. (2011). Source-to-sink systems on passive margins: theory and practice with an example from the Norwegian continental margin. *Geological Society, London, Petroleum Geology Conference* 7**,** 913-920.

Mattson, A. & Bruhn, R. L. (2001). Fault slip rates and initiation age based on diffusion equation modeling: Wasatch Fault Zone and eastern Great Basin. *Journal of Geophysical Research-Solid Earth,* 106**,** 13739-13750.

McCalpin, J.P (2002). Post-Bonneville paleoearthquake chronology of the Salt Lake City segment, Wasatch fault zone, from the 1999" Megatrench" site, Utah Geological Survey.

Mcpherson, J. G., Shanmugam, G. & Moiola, R. J. (1987). Fan-Deltas and Braid Deltas - Varieties of Coarse-Grained Deltas. *Geological Society of America Bulletin,* 99**,** 331-340.

Mears, B. Jr. (1981). Periglacial wedges and the late Pleistocene environment of Wyoming's intermontane basins. *Quaternary Research,* 15**,** 171-198.

Menacherry, S. (2008). "Source to sink" Sedimentology and Petrology of a Dryland Fluvial System, and Implications for Reservoir Quality, Lake Eyre Basin, Central Australia. *Australian School of Petroleum, Faculty of Science.* The University of Adelaide.

Milligan, M. R. & Lemons, D. R. (1998). A sequence stratigraphic overview of sandy and gravelly lacustrine deltas deposited along the eastern margin of late Pleistocene Lake Bonneville, northern Utah and southern Idaho.

Milliman, J. D. & Meade, R. H. (1983). World-Wide Delivery of River Sediment to the Oceans. *Journal of Geology,* 91**,** 1-21.

Milliman, J. D. & Syvitski, J. P. M. (1992). Geomorphic Tectonic Control of Sediment Discharge to the Ocean - the Importance of Small Mountainous Rivers. *Journal of Geology,* 100**,** 525-544.

Montgomery, D. R. (2002). Valley formation by fluvial and glacial erosion. *Geology,* 30**,** 1047-1050.

Muto, T. & Steel, R.J. (2002). In Defense of Shelf Edge Delta Development during Falling and Lowstand of Relative Sea Level. *The Journal of Geology,* 110**,** 421-436.

Oviatt, C. G. (1997). Lake Bonneville fluctuations and global climate change. *Geology,* 25**,** 155-158.

Oviatt, C. G., Currey, D. R. & Sack, D. (1992). Radiocarbon Chronology of Lake Bonneville, Eastern Great-Basin, USA. *Palaeogeography Palaeoclimatology Palaeoecology,* 99**,** 225-241.

Pack, F. J. (1939). Lake Bonneville: A popular treatise dealing with the history and physical aspects of Lake Bonneville, The University of Utah press.

Parry, W. T. (2005). A Hiking Guide to the Geology of the Wasatch Mountains: Mill Creek and Neffs Canyons, Mount Olympus, Big and Little Cottonwood and Bells Canyons, University of Utah Press.

Parry, W. T. & Bruhn, R. L. (1987). Fluid Inclusion Evidence for Minimum 11-Km Vertical Offset on the Wasatch Fault, Utah. *Geology,* 15**,** 67-70.

Patrickson, S. J., et al. (2010). Late Pleistocene to early Holocene lake level and paleoclimate insights from Stansbury Island, Bonneville basin, Utah. *Quaternary Research,* 73**,** 237-246.

Personius, S. F. & Scott, W. E. (1992). Surficial geologic map of the Salt Lake City segment and parts of adjacent segments of the Wasatch fault zone, Davis, Salt Lake, and Utah counties, Utah. *Miscellaneous Investigations Series - U. S. Geological Survey.* Reston, VA, United States (USA), U. S. Geological Survey, Reston, VA.

Postma, G. & Roep, T. B. (1985). Resedimented Conglomerates in the Bottomsets of Gilbert-Type Gravel Deltas. *Journal of Sedimentary Petrology,* 55**,** 874-885.

Reading, H. G (2009). Sedimentary environments: processes, facies and stratigraphy, Wiley-Blackwell.

Richmond, G. M. (1964). Glaciation of Little Cottonwood and Bells Canyons, Wasatch Mountains, Utah, US Government Printing Office.

Sack, D. (1999). The composite nature of the Provo level of Lake Bonneville, Great Basin, western North America. *Quaternary Research,* 52**,** 316-327.

Schofield, I., et al. (2004). Shoreline development, longshore transport and surface wave dynamics, Pleistocene Lake Bonneville, Utah. *Earth Surface Processes and Landforms,* 29**,** 1675-1690.

Schwartz, D. P. & Coppersmith, K. J. (1984). Fault Behavior and Characteristic Earthquakes - Examples from the Wasatch and San-Andreas Fault Zones. *Journal of Geophysical Research,* 89**,** 5681-5698.

Smith, R. B. & Bruhn, R. L. (1984). Intraplate extensional tectonics of the Eastern basin Range: Inferences on structural style from seismic reflection data, regional tectonics, and thermal mechanical models of brittle ductile deformation. *Journal of Geophysical Research: Solid Earth (1978–2012),* 89**,** 5733-5762.

Somme, T. O., et al. (2011). Linking Onshore-Offshore Sediment Dispersal in the Golo Source-to-Sink System (Corsica, France) During the Late Quaternary. *Journal of Sedimentary Research,* 81**,** 118-137.

Spencer, R. J. , et al. (1984). Great Salt Lake, and precursors, Utah: the last 30,000 years. *Contributions to Mineralogy and Petrology*.

Stock, G.M., et al. (2009). Spatial and temporal variations in denudation of the Wasatch Mountains, Utah, USA. *Lithosphere,* 1**,** 34-40.

Summerfield, M. A. & Hulton, N. J. (1994). Natural controls of fluvial denudation rates in major world drainage basins. *Journal of Geophysical reasearch* 99**,** 13-13.

Summerfield, M. A. & Kirkbride, M. P. (1992). Climate and Landscape Response. *Nature,* 355**,** 306-306.

Syvitski, J. P. M. & Milliman, J.D (2007). Geology, Geography, and Humans Battle for Dominance over the Delivery of Fluvial Sediment to the Coastal Ocean. *The Journal of Geology,* 115**,** 1-19.

Sømme, T.O., et al. (2009). Relationships between morphological and sedimentological parameters in source-to-sink systems: a basis for predicting semi-quantitative characteristics in subsurface systems. *Basin Research,* 21**,** 361-387.

Thompson, R. S., et al. (1993). Climatic changes in the western United States since 18,000 yr BP. *Global climates since the last glacial maximum***,** 468-513.

Vezzoli, G. (2004). Erosion in the Western Alps (Dora Baltea Basin): 2. Quantifying sediment yield. *Sedimentary Geology,* 171**,** 247-259.

Viseras, C., et al. (2003). Differential features of alluvial fans controlled by tectonic or eustatic accommodation space. Examples from the Betic Cordillera, Spain. *Geomorphology,* 50**,** 181-202.

Whipple, K. X. & Trayler, C. R. (1996). Tectonic control of fan size: The importance of spatially variable subsidence rates. *Basin Research,* 8**,** 351-366.

Appendix A: Source to sink analysis

City Creek Canyon analysis
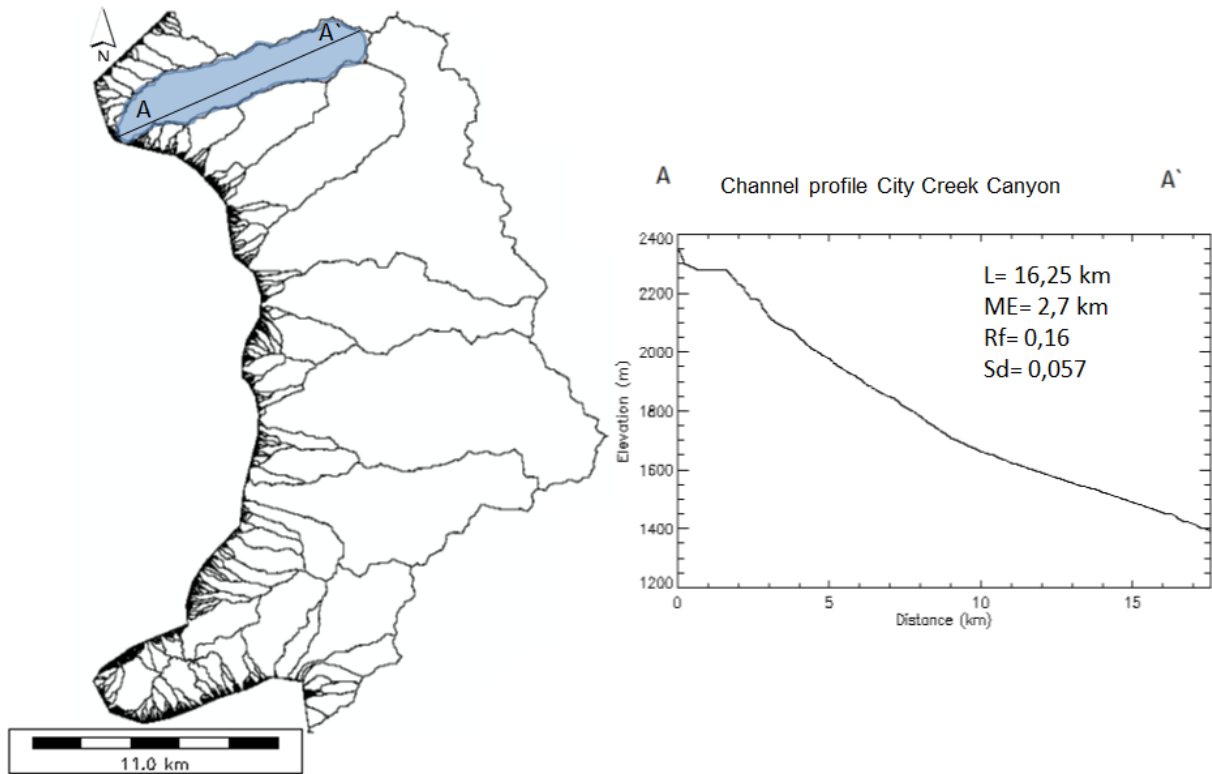
Catchment characteristics

Figure A.1: *City Creek Canyon catchment and basin profile L (basin length); ME (maximum basin elevation); Rf (basin shape); Sd (basin stream slope). Characteristics extracted from RiverTools software.*
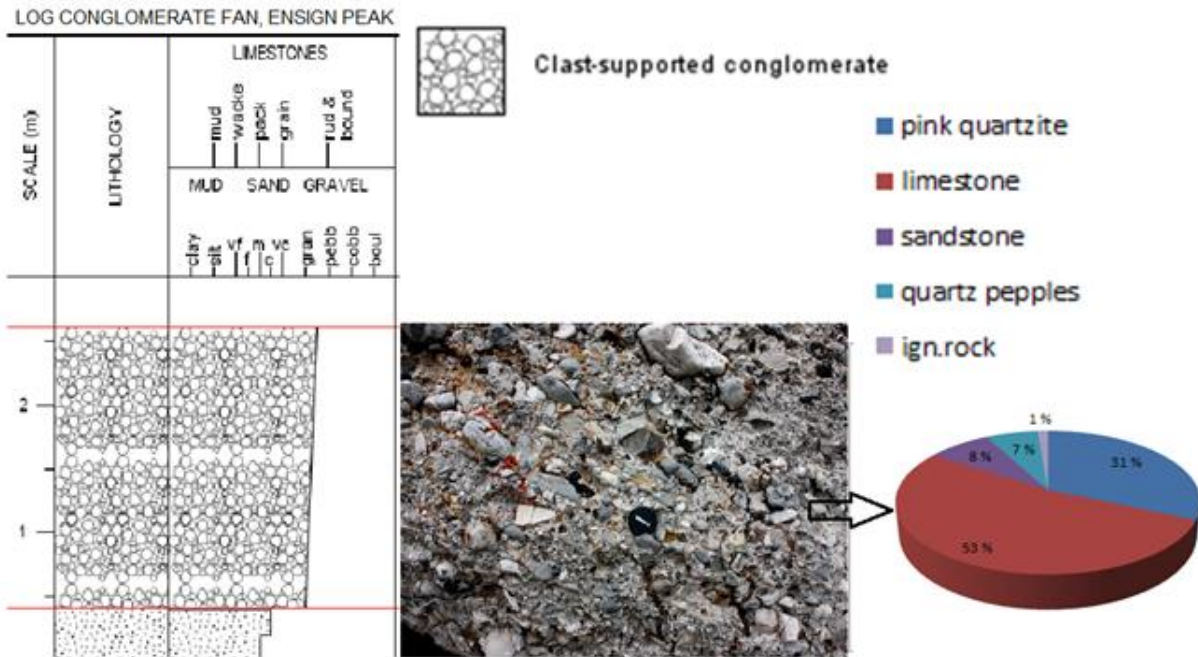
Figure A.2: *Logged section and lithology pie-chart of the City Creek conglomeratic bedrock No.1 located near Ensign Peak (40°47'39.11"N, 111°53'25.96"W).*

100×100 cm^2 sink analysis, fan 1

100x100 cm^2 sink analysis, City Creek Canyon, fan 1

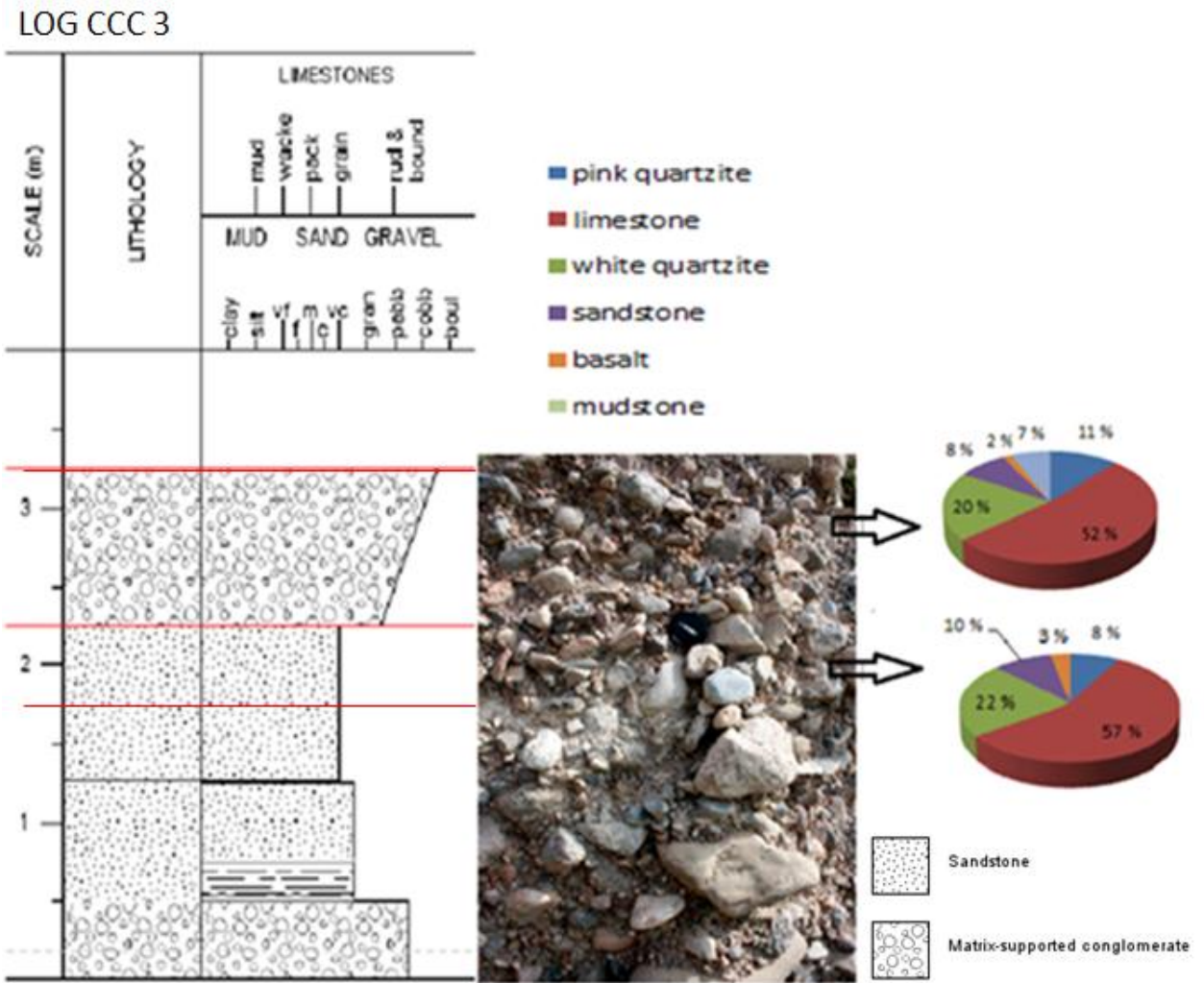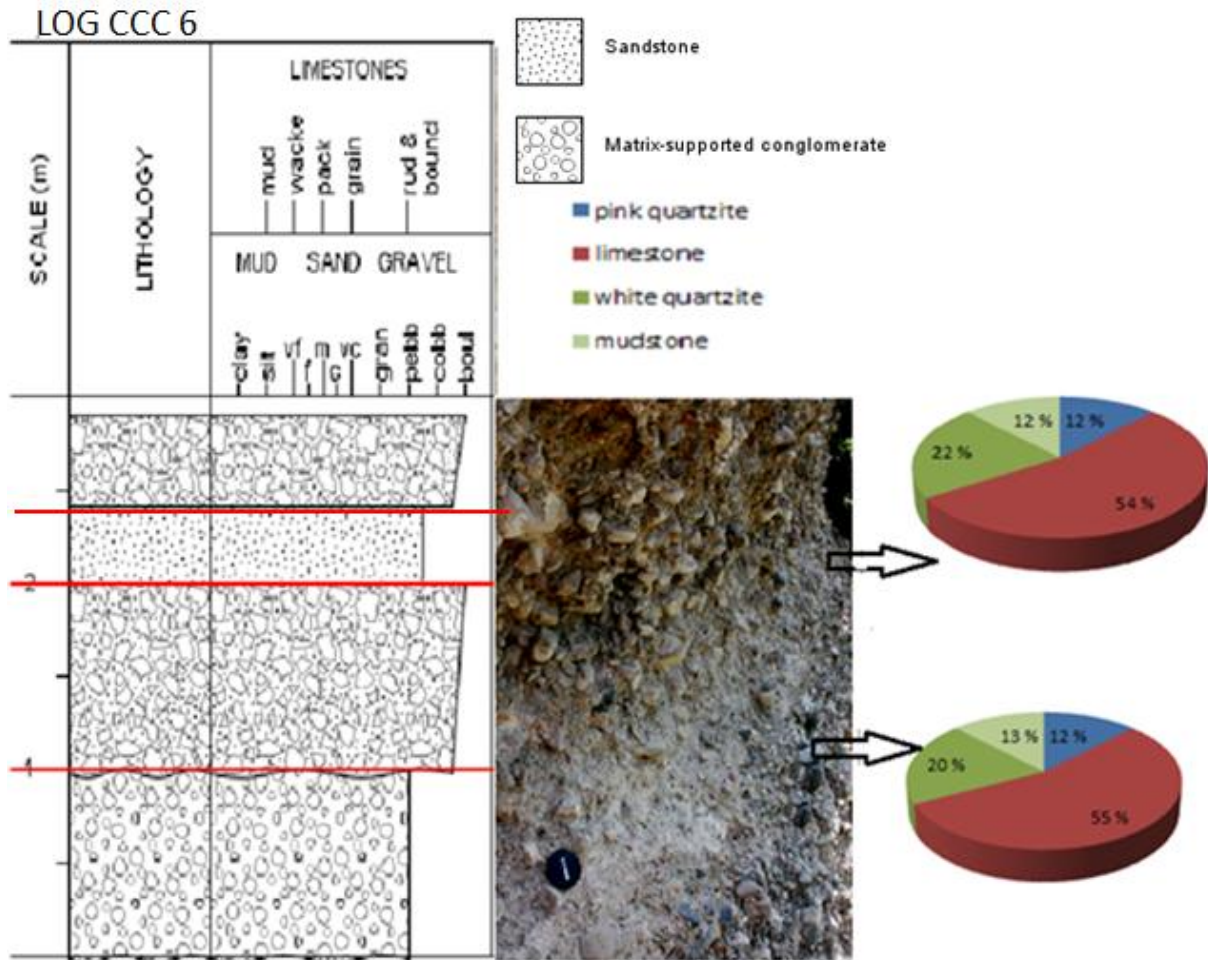|	CCC	Mean grain size, cm	Largest measured clast, cm	Sorting	Rounding	Matrix	Dominant lithology	Shoreline level	Facies Association
40°47'30.42"N, 111°52'40.90"W	1	5-6	15	Poorly	Subrounded	Silt	Quartzite, limestone	Bonneville	A
40°47'10.15"N, 111°53'0.74"W	2	5-7	25	Poorly	Subrounded	Sand	Limestone	Bonneville	A
40°47'8.69"N, 111°53'1.01"W	3	5-6	35	Poorly	Subangular	Coarse sand	Limestone	Bonneville	A
40°47'7.01"N, 111°53'0.44"W	4	5-7	12	Poorly	Subrounded	Carbonate cement	Limestone	Provo	A
40°47'7.36"N, 111°52'59.78"W	5	3-4	10	Poorly	Subangular-subrounded	Carbonate cement	Limestone	Provo	A
40°47'11.32"N, 111°52'56.55"W	6	12-15	30	Poorly	Subrounded	Carbonate cement	Limestone	Provo	A
40°47'13.34"N, 111°52'52.26"W	7	6-7	10	Poorly	Subrounded	Sand	Limestone, pink quartzite	Bonneville	A
40°47'23.47"N, 111°51'58.76"W	8	3-4	40	Poorly	Subrounded	Medium-coarse sand	Limestone, basalt	Bonneville	A

Figure A.3: *Logged section of facies association A, fan delta deposits location CCC 3, Bonneville level. Dominating clast lithology is limestone.*

Figure A.4: *Logged section of facies association A, fan delta deposits location CCC 6, Provo level. Dominating clast lithology is limestone.*

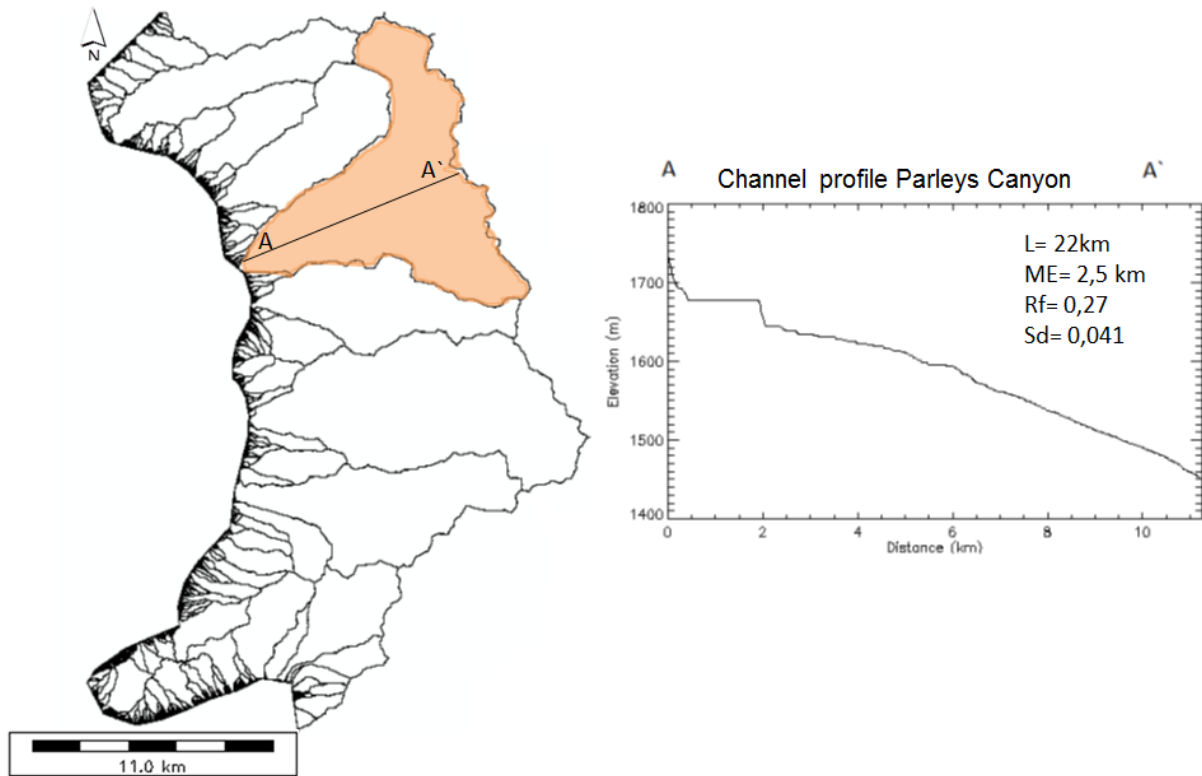## Parleys Canyon analysis

Catchment characteristics

Figure A.5: *Parleys Canyon catchment area and basin profile; L (basin length); ME (maxiumum basin elevation); Rf (basin shape); Sd (basin stream slope). Characteristics extracted from RiverTools software.*

100×100 cm² sink analysis, fan 4

100x100 cm² sink analysis, Parley Canyon, fan 4

	PCC	Mean grain size, cm	Largest measured clast, cm	Sorting	Rounding	Matrix	Dominant lithology	Shoreline level	Facies Association
40°42'37.28"N, 111°48'32.77"W	1	4-5	30	Poorly	Subrounded	Sand	Red sandstone	Bonneville	A
40°42'34.42"N, 111°48'26.87"W	2	3-4	8	Moderate	Subrounded	Silt-fine sand	Pink quartzite	Provo	A
40°42'31.37"N, 111°48'30.11"W	3	5-6	30	Poorly	Subrounded	Clast-supported	Limestone	Provo	A
40°42'29.16"N, 111°48'25.47"W	4	5-6	20	Poorly	Subrounded	Medium sand	Pink quartzite	Bonneville	A
40°42'29.65"N, 111°48'8.87"W	5	5-7	25	Poorly	Subrounded	Medium sand	Red sandstone	Bonneville	A
40°42'34.44"N, 111°48'21.18"W	6	10-15	45	Poorly	Subrounded	Clast-supported	Pink quartzite	Provo	A
40°42'33.46"N, 111°48'34.90"W	7	4-5	40	Poorly	Subrounded	Medium sand	Quartzite, sandstone	Provo	A
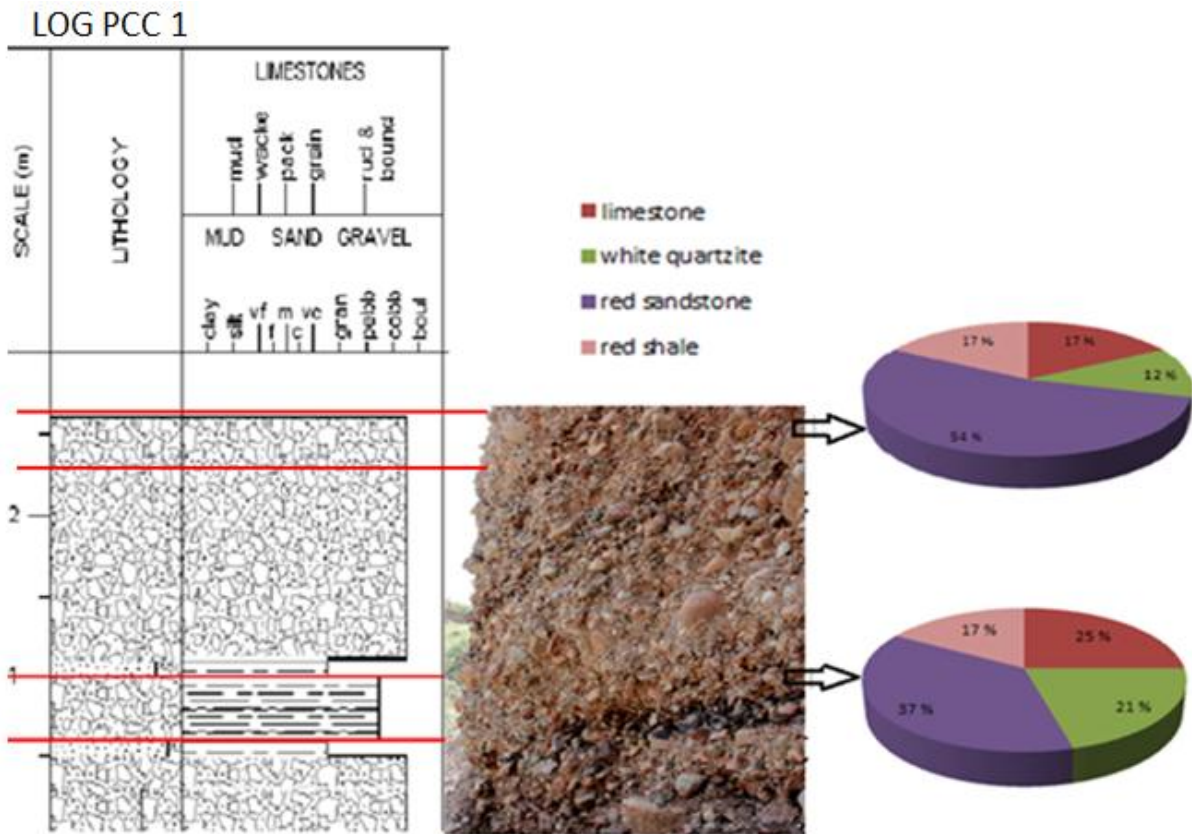
Figure A.6: *Logged section of facies association A, fan delta deposits, location PCC 1, Bonneville level. Dominating clast lithologies are red sandstone /shale, limestone and white quartzite.*
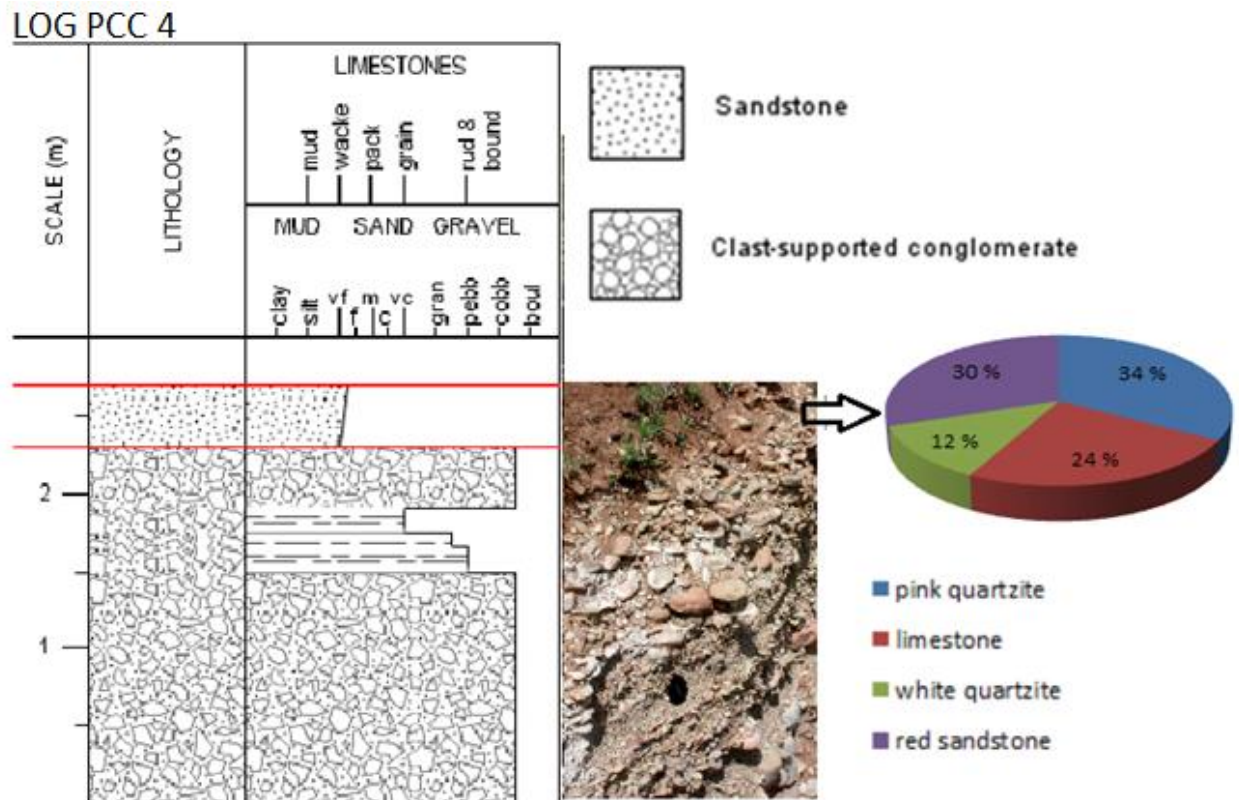
Figure A.7: *Logged section of facies association A, fan delta deposits, location PCC 4, Provo level. Dominating clast lithologies are pink quartzite, red sandstone and limestone.*

Mill Creek Canyon analysis

Catchment characteristics

Figure A.8: *Mill Creek Canyon catchment area and basin profile; L (basin length); ME (maximum basin elevation); Rf (basin shape); Sd (basin stream slope). Characteristics extracted from RiverTools software.*

100×100 cm² sink analysis, fan 5

100x100 cm² sink analysis, Mill Creek Canyon, fan 5

|	MCC	Mean grain size, cm	Largest measured clast, cm	Sorting	Rounding	Matrix	Dominant lithology	Shoreline level	Facies Association
40°41'31.89"N, 111°47'26.83"W	1	5-10	20	Poorly	Subrounded	Carbonate cement	White quartzite	Bonneville	A
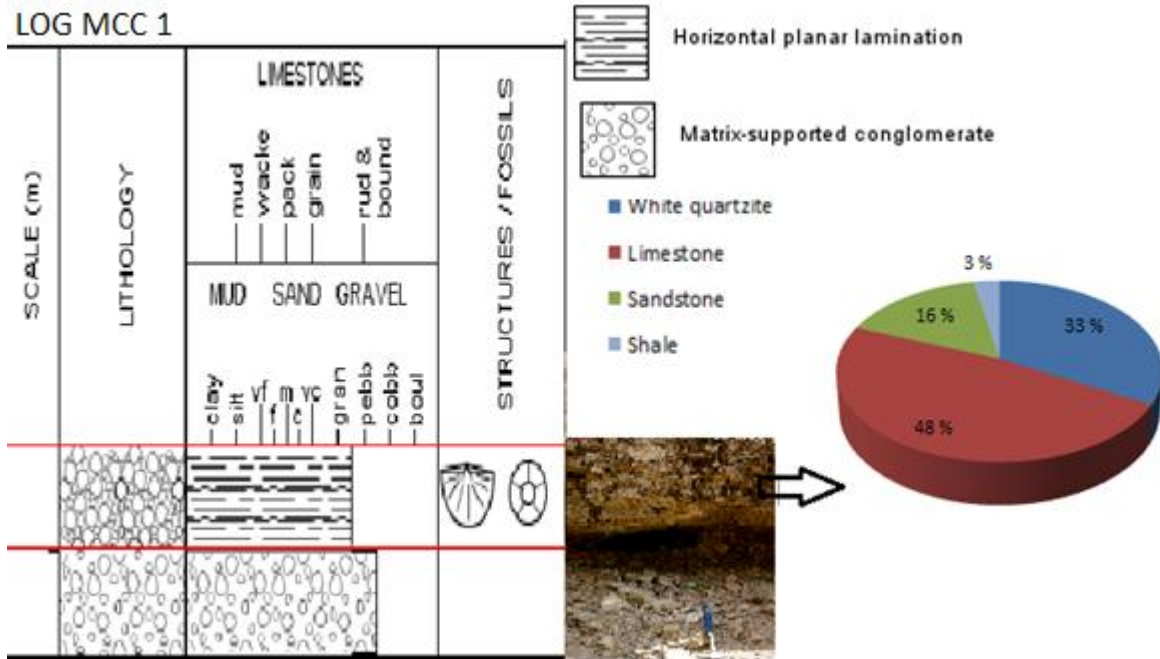
Figure A.9: *Logged section of facies association A, fan delta deposits, location MCC 1, Bonneville level. Dominating clast lithologies are limestone and white quartzite.*

Big Cottonwood Canyon analysis

Catchment characteristics
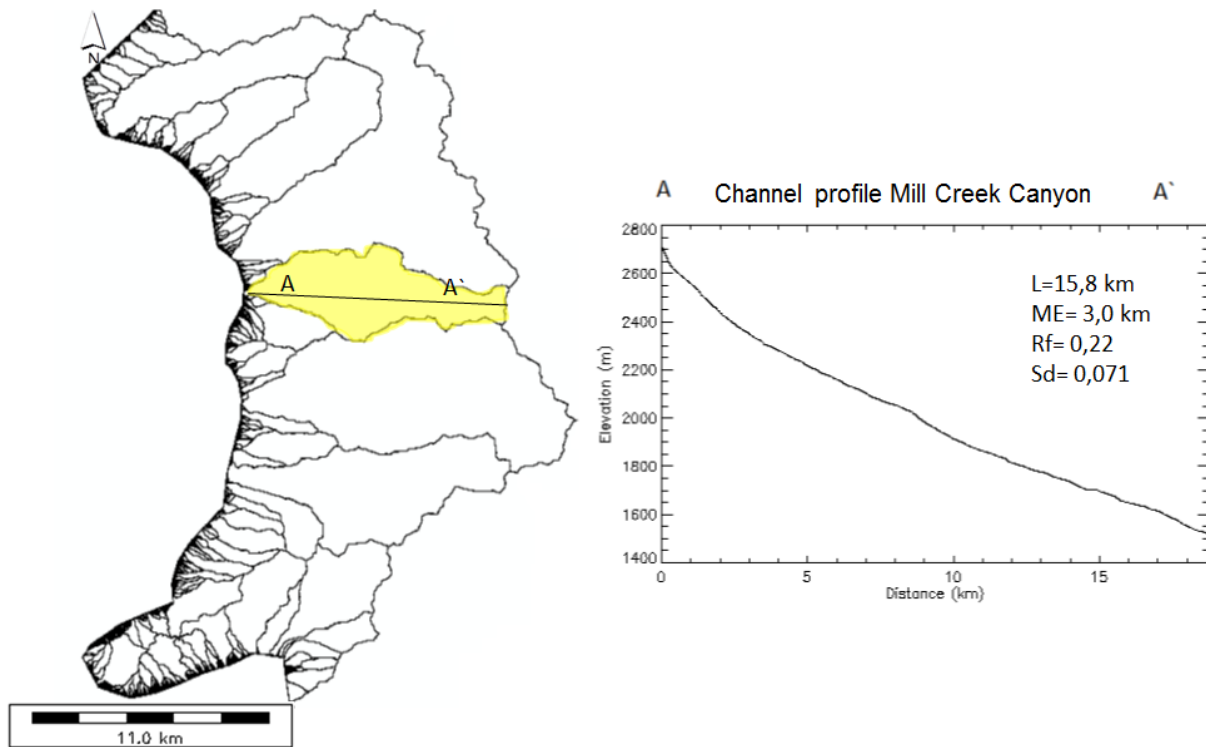

L= 20 km
ME= 3,3 km
Rf= 0,32
Sd= 0,054

Figure A.10: *Big Cottonwood Canyon catchment area and basin profile, L (basin length), ME (maxiumum basin elevation), Rf (basin shape), Sd (basin stream slope). Characteristics extracted from RiverTools software.*

100×100 cm^2 sink analysis, fan 6

100x100 cm^2 sink analysis, Big Cottonwood Canyon, fan 6

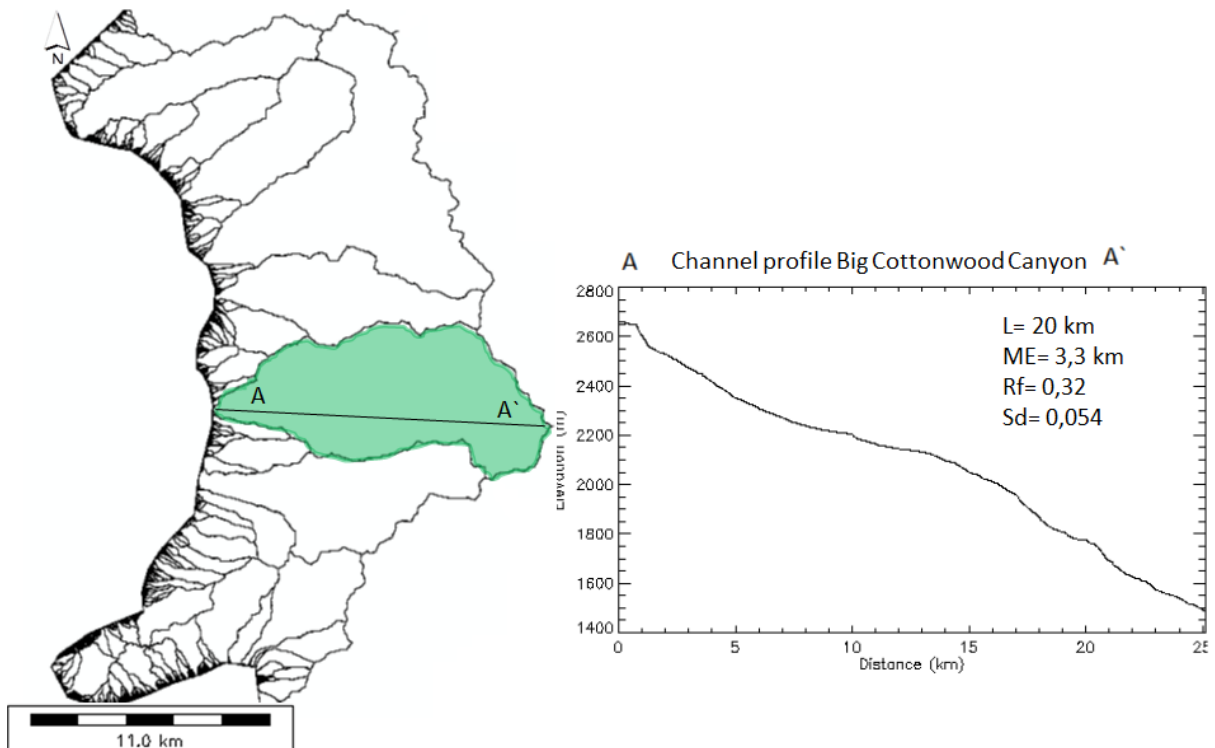|	BCC	Mean grain size, cm	Largest measured clast, cm	Sorting	Rounding	Matrix	Dominant lithology	Shoreline level	Facies Association
40°37'51.52"N, 111°47'49.87"W	1	5-7	25	Poorly	Subrounded	Sandy matrix	Quartzite	Bonneville	A
40°37'44.13"N, 111°47'41.28"W	2	10-12	35	Poorly	Subrounded	Sandy matrix, silt on top	Sandstone	Bonneville	A
40°37'44.57"N, 111°47'41.57"W	3	4-5	25	Poorly	Subrounded	Sandy matrix	Limestone	Bonneville	A
40°37'51.45"N, 111°47'48.46"W	4	6-7	18	Poorly	Subangular-subrounded	Sandy matrix	Quartzite	Bonneville	A
40°37'40.21"N, 111°48'40.35"W	5	8-10	35-40	Poorly	Subrounded	Sandy matrix	Limestone	Provo	B

Figure A.11: *Logged section of facies association A, fan delta deposits, location BCC 3, Bonneville level. Dominating clast lithologies are limestone, quartzite and monzogranite.*

Little Cottonwood Canyon analysis

Catchment characteristics
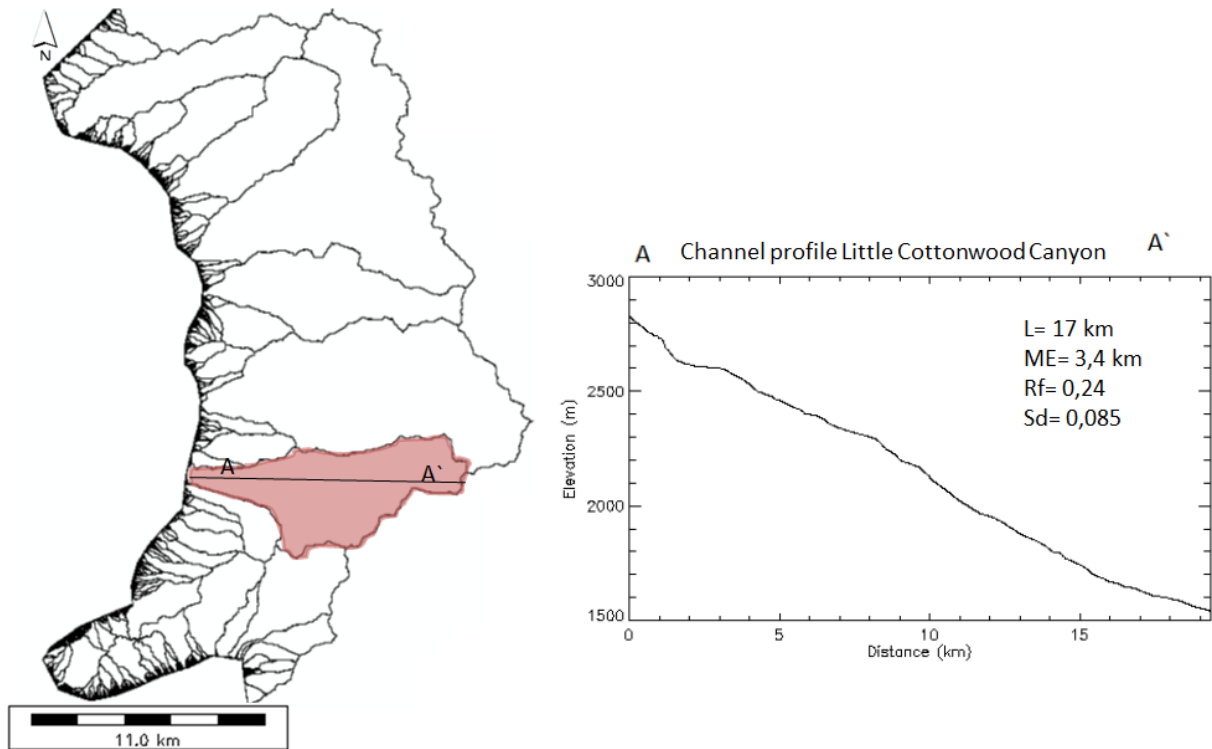
Figure A.12: *Little Cottonwood Canyon catchment area and basin profile; L (basin length); ME (maximum basin elevation); Rf (basin shape); Sd (basin stream slope). Characteristics extracted from RiverTools software.*

100×100 cm^2 sink analysis, fan 7

100x100 cm^2 sink analysis, Little Cottonwood Canyon, fan 7

	LCC	Mean grain size, cm	Largest measured clast, cm	Sorting	Rounding	Matrix	Dominant lithology	Shoreline level	Facies Association
40°31'30.46"N, 111°51'3.14"W	1	5-6	25	Poorly	Subrounded	Fine-medium sand	Quartz monzonite	Provo	A
40°33'56.96"N, 111°50'59.23"W	2	10-12	45	Poorly	Subrounded	Coarse sand	Quartz monzonite	Provo	B
40°33'28.57"N, 111°49'14.42"W	3	3-5	10	Poorly	Subrounded	Medium-coarse sand	Quartz monzonite	Bonneville	A
40°33'28.57"N, 111°49'14.42"W	4	3-5	12	Poorly	Subrounded	Medium-coarse sand	Quartz monzonite	Bonneville	A
40°33'29.44"N, 111°49'12.34"W	5	3-4	8	Poorly	Subrounded	Clay	Quartz monzonite	Bonneville	A
40°33'29.63"N, 111°49'17.16"W	6	5-10	25	Poorly	Subrounded	Fine-medium sand	Quartz monzonite	Bonneville	A
40°33'29.78"N, 111°49'17.25"W	7	2-3	7	Moderate	Subrounded	Silt-very fine sand	Quartz monzonite	Bonneville	A

Figure A.13: *Logged section of facies association B, glacial deposits, location LCC 2, Provo level. Dominating clast lithologies are monzo-granite and white quartzite.*
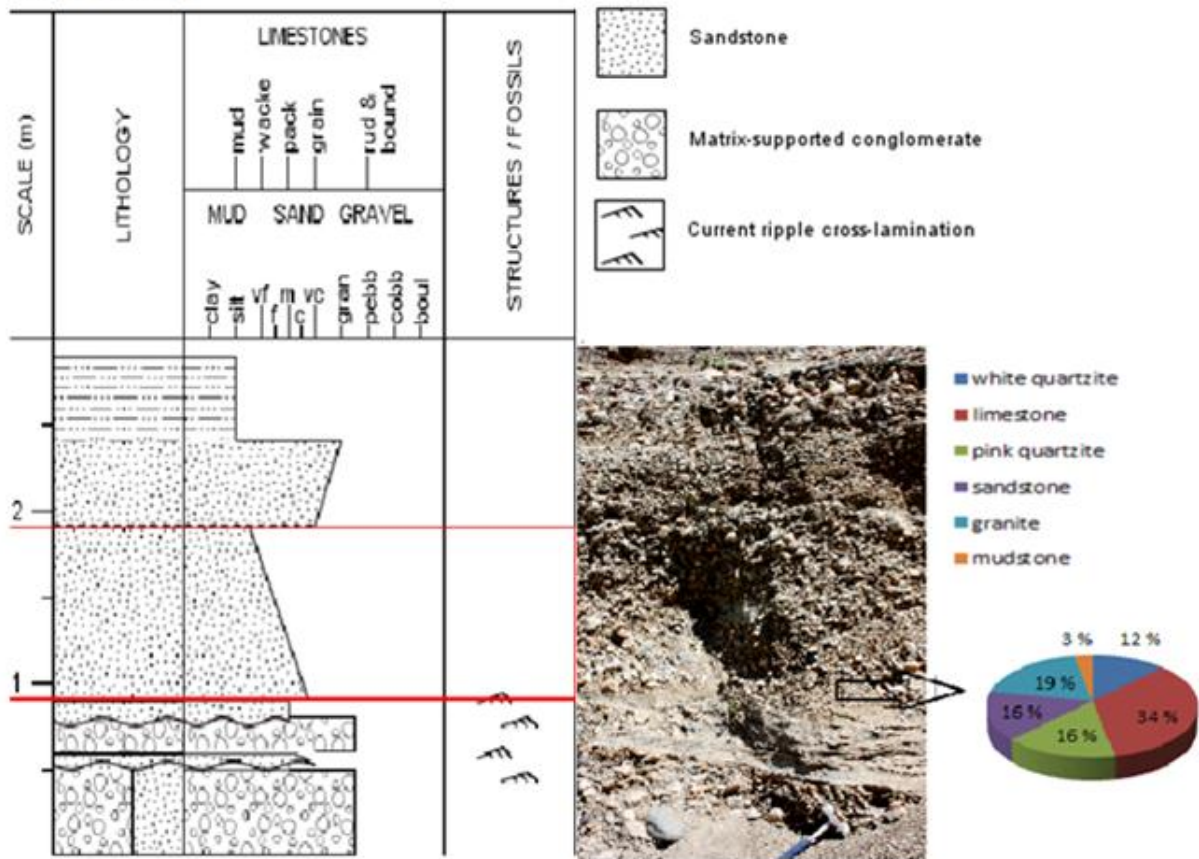

Figure A.14: *Logged section of facies association A, fan delta deposits, location LCC 3, Bonneville level. Dominating clast lithologies are monzo-granite and pink quartzite.*
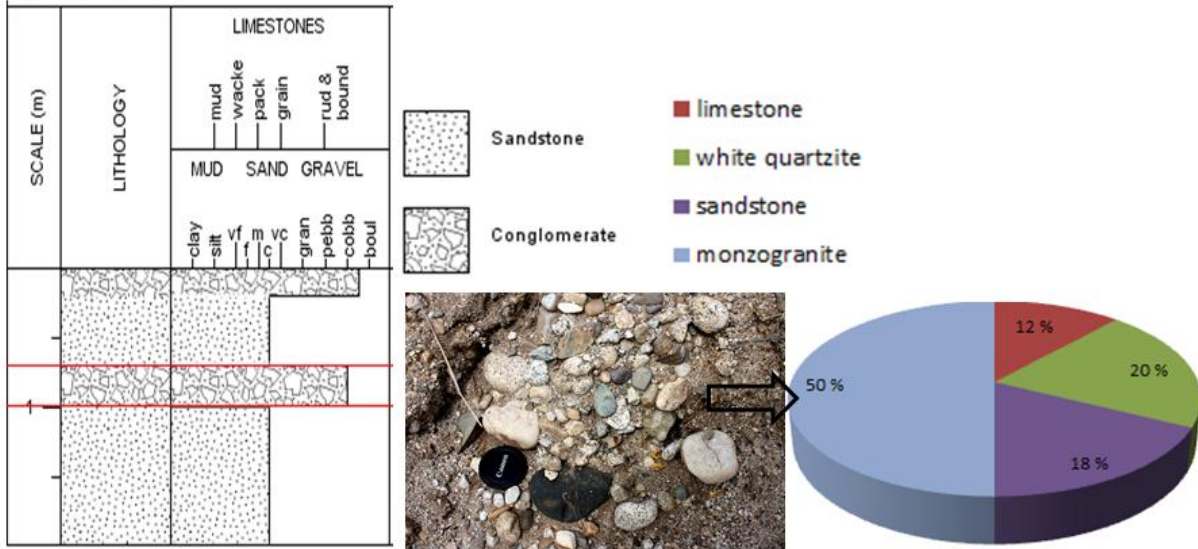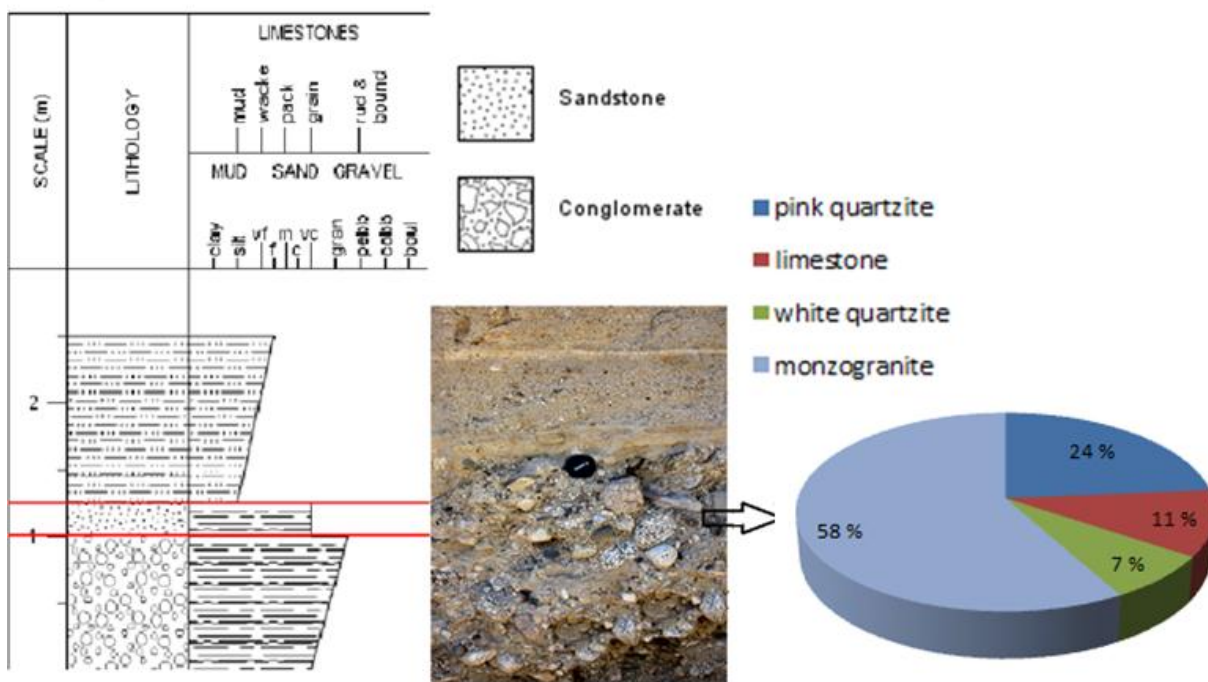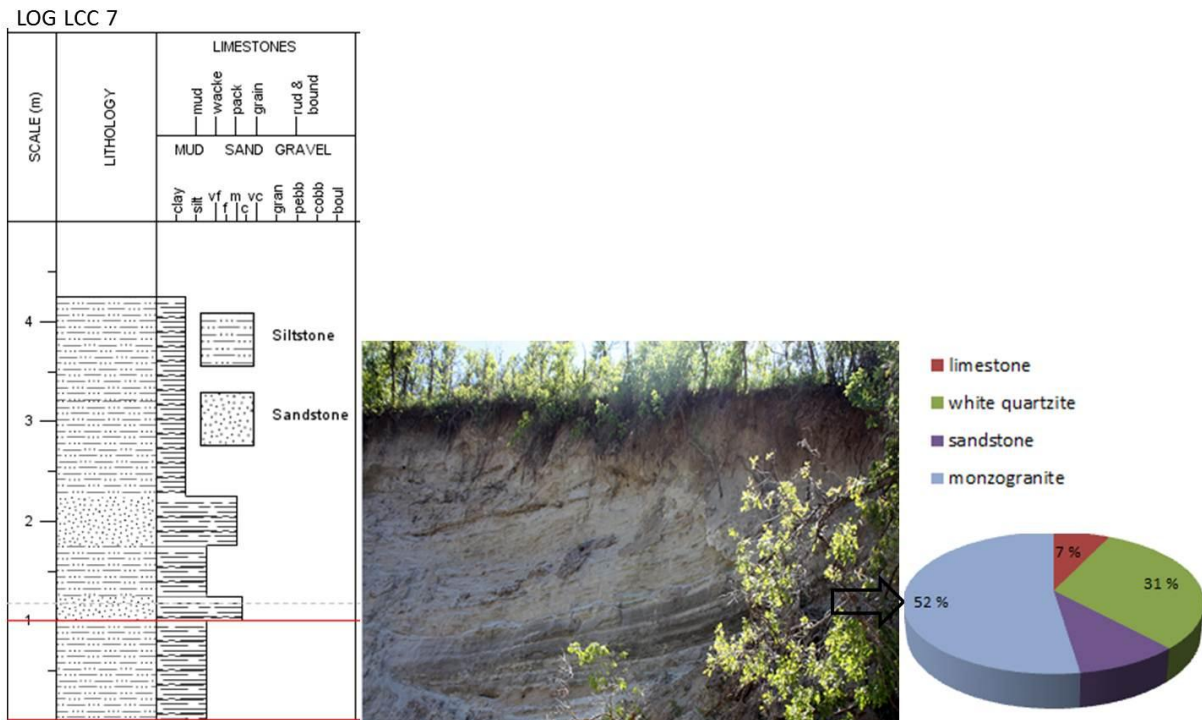
Figure A.15: *Logged section of facies association A, fan delta, location LCC 7, Bonneville level. Dominating clast lithologies are monzo-granite and white quartzite.*

Point of Mountain spit & Draper area analysis

Catchment characteristics
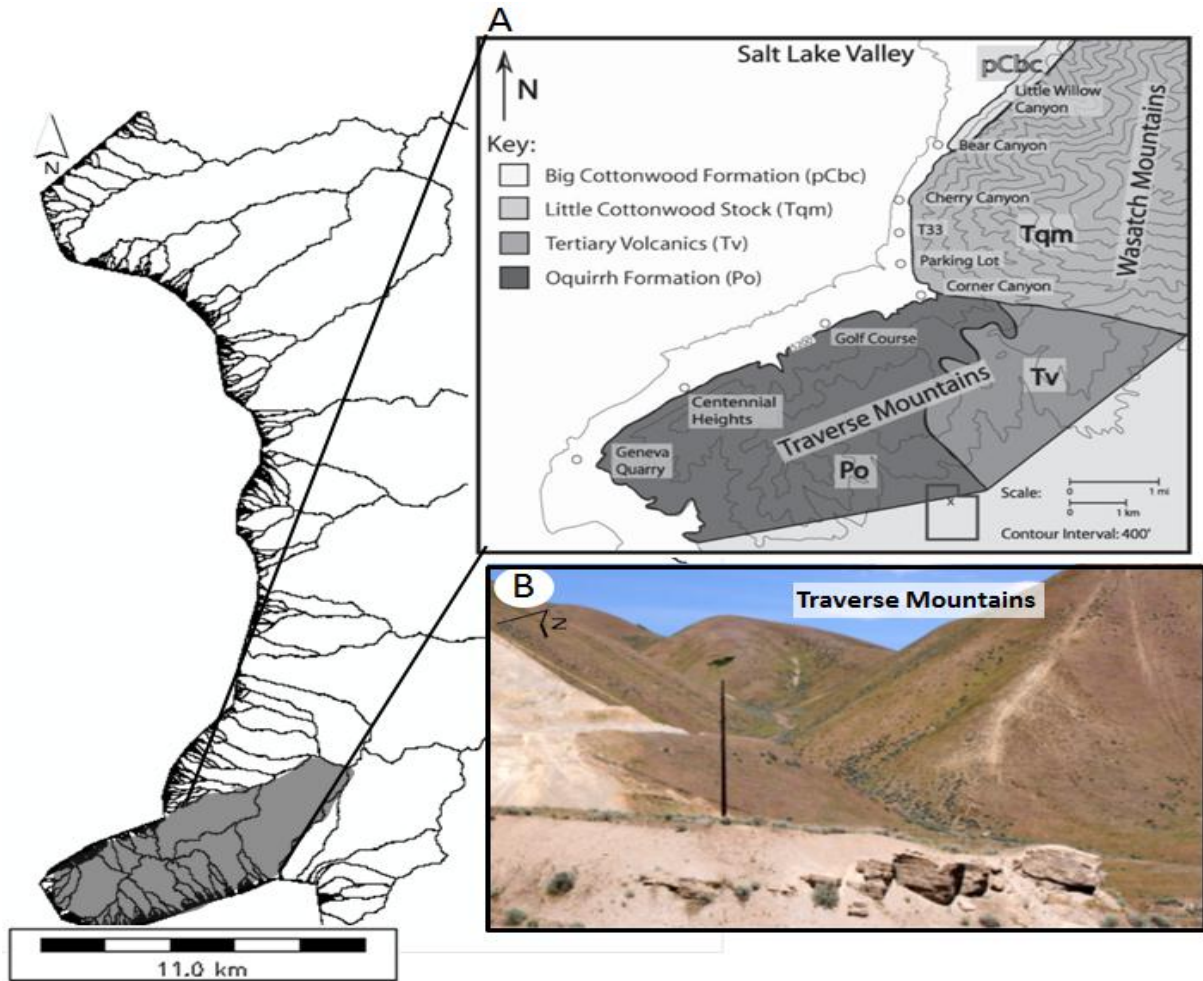
Figure A.16: A) *Catchment lithology and location of the Traverse Mountains, from (Schofield et al., 2004); B) The Traverse Mountains catchment area.*

100×100 cm² sink analysis, the Point of Mountain

100x100 cm² sink analysis, Point of Mountain spit & Draper area

	POM	Mean grain size, cm	Largest measured clast, cm	Sorting	Rounding	Matrix	Dominant lithology	Shoreline level	Facies Association
40°27'27.42"N, 111°53'59.44"W	1	0,5-1	5	Moderate-good	Subrounded-well rounded	Clast-supported	Sandstone	Bonneville	C
40°27'28.72"N, 111°53'55.72"W	2	1-3	5	Moderate-good	Subrounded-well rounded	Clast-supported	Quartzite	Bonneville	C
40°27'26.25"N, 111°54'4.00"W	3	1-2	15	Moderate	Subrounded-well rounded	Clast-supported	Quartzite	Bonneville	C
40°28'42.55"N, 111°55'53.65"W	4	10-15	50	Subangular-subrounded	Poorly	Fine-coarse sand	Quartzite	Provo	A
40°27'28.99"N, 111°54'28.88"W	5	2-3	5	Subangular-subrounded	Poorly	Coarse sand	Quartzite	Bonneville	A

Figure A.17: *Logged section of facies association A, fan delta deposits location POM 4, Provo level. Dominating clast lithologies are quartzite and limestone clasts.*

Figure A.18: *Logged section of facies association C, wave-dominated deposits, location POM 3, Bonneville level. Dominating clast lithologies are quartzite, limestone and sandstone.*
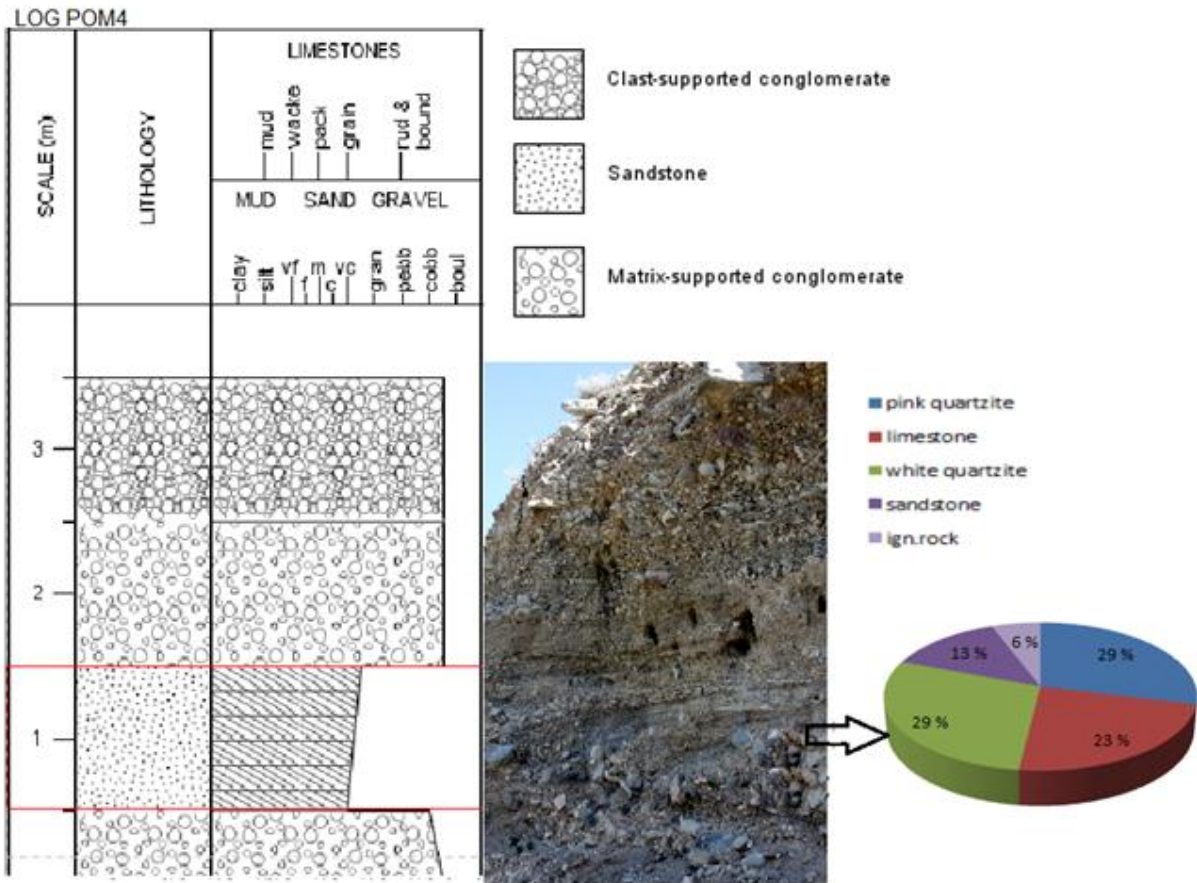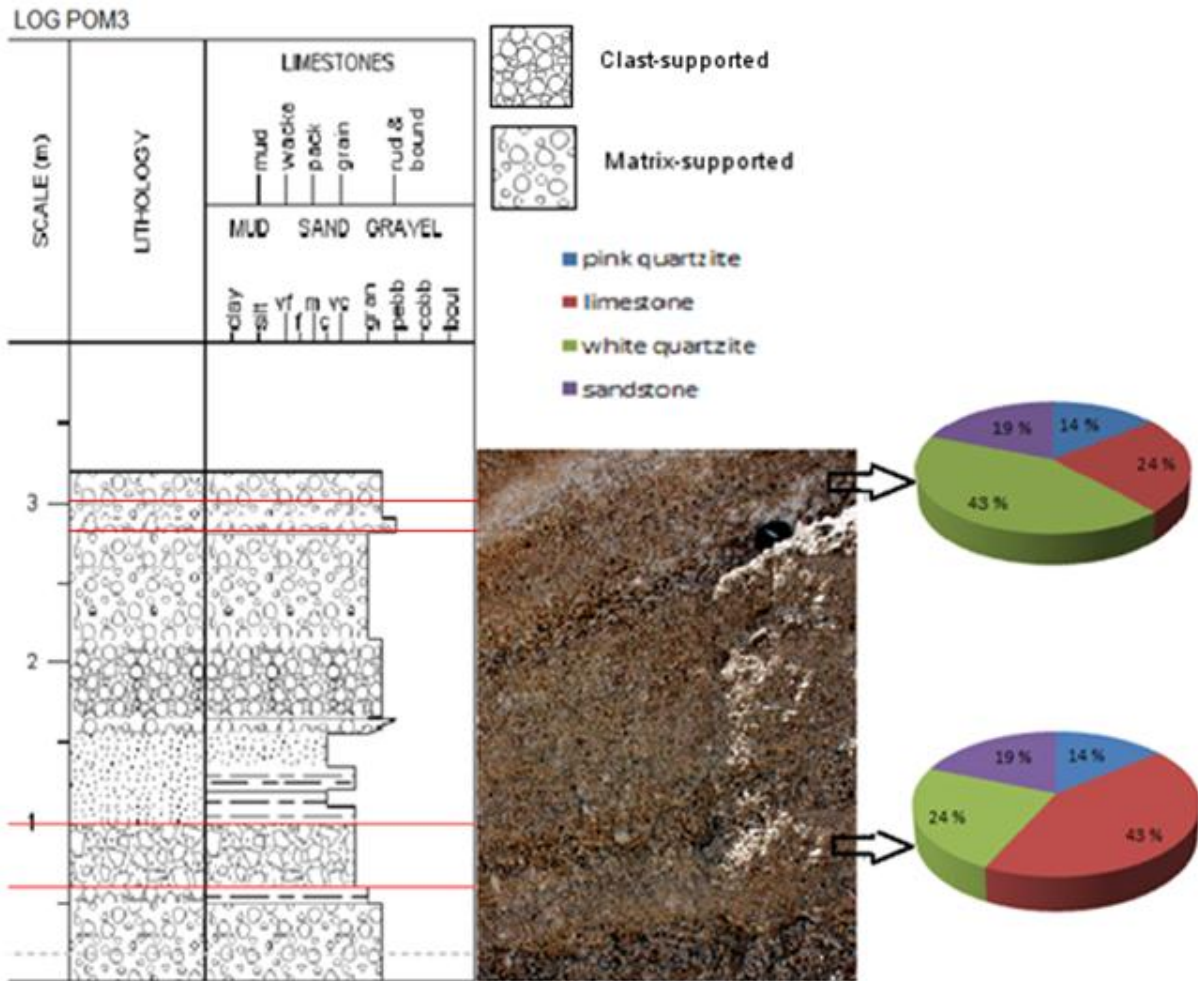
Appendix B: Sediment volume calculations

Sediment volumes calculations for Bonneville fan deltas

	Bonneville	CCC fan delta	RBC fan delta	EMC fan delta	PCC fan delta	MCC fan delta	BCC fan delta	LCC fan delta
Volume inputs								
Total area of delta top m²	61800000	2550000	1930000	4380000	2750000	6890000	11900000	21000000
Height (m) above datum (Stansbury)	180	180	180	180	180	180	180	180
Dip angle for top Stansbury								
0°	11.124	0.459	0.3474	0.7884	0.495	1.2402	2.142	3.78
7.5°	10.45656	0.43146	0.326556	0.741096	0.4653	1.165788	2.01348	3.5532
15°	9.78912	0.40392	0.305712	0.693792	0.4356	1.091376	1.88496	3.3264
Results								
High Case volume km³	11.12	0.46	0.35	0.79	0.50	1.24	2.14	3.78
Mid Case volume km³	10.46	0.43	0.33	0.74	0.47	1.17	2.01	3.55
Low Case volume km³	9.79	0.40	0.31	0.69	0.44	1.09	1.88	3.33

Sediment volumes calculations for Provo fan deltas

	Provo area	CCC fan delta	RBC fan delta	EMC fan delta	PCC fan delta	MCC fan delta	BCC fan delta	LCC fan delta
Volume inputs								
Total area of delta top m²	91300000	1870000	4280000	5260000	8880000	8960000	14700000	36400000
Height (m) above datum (Stansbury)	73	73	73	73	73	73	73	73
Dip angle for top Stansbury								
0°	6.665	0.137	0.312	0.384	0.648	0.654	1.073	2.657
7.5°	6.265	0.128	0.294	0.361	0.609	0.615	1.009	2.498
15°	5.865	0.120	0.275	0.338	0.570	0.576	0.944	2.338
Results								
High Case Volumes (km³)	6.66	0.14	0.31	0.38	0.65	0.65	1.07	2.66
Mid Case Volumes (km³)	6.27	0.13	0.29	0.36	0.61	0.61	1.01	2.50
Low Case Volumes (km³)	5.87	0.12	0.27	0.34	0.57	0.58	0.94	2.34

Appendix C: The BQART model calculations

$$Q_s = wBQ^{0,31}A^{0,5}RT$$

City Creek Canyon

Time (years)	T°C	Flux pr.yr.	Total flux	
6000	10.9	0,089	534	
6000	6.6	0,053	318	
18000	1.1	0,00899	161.82	
30000			1013.82	10^6 t

Red Butte Canyon

Time	T°C	Flux pr.yr.	Total flux	
6000	10.9	0,047	282	
6000	6.6	0,028	168	
18000	1.1	0,00477	85.86	
30000			535.86	10^6 t

Emigration Canyon

Time (years)	T°C	Flux pr.yr.	Total flux	
6000	10.9	0,089	534	
6000	6.6	0,053	318	
18000	1.1	0,00899	161.82	
30000			1013.82	10^6 t

Parleys Canyon

Time	T°C	Flux pr.yr.	Total flux	
6000	10.9	0,191	1146	
6000	6.6	0,115	690	
18000	1.1	0,019	342	
30000			2178	10^6 t

Mill Creek Canyon

Time (years)	T°C	Flux pr.yr.	Total flux	
6000	10.9	0,123	738	
6000	6.6	0,074	444	
18000	1.1	0,09	1620	
30000			2802	10^6 t

Big Cottonwood Canyon

Time	T°C	Flux pr.yr.	Total flux	
6000	10.9	0,093	558	
6000	6.6	0,056	336	
18000	1.1	0,03	540	
30000			1434	10^6 t

Little Cottonwood Canyon

Time (years)	T°C	Flux pr.yr.	Total flux	
6000	10.9	0,082	492	
6000	6.6	0,049	294	
18000	1.1	0,082	1476	
30000			2262	10^6 t

Converting from weight (t) to volume (km³)

Converting sediment flux from 10^6 t to km³	
Porosity %	30
Density (kg/m³)	2700

Catchments:	Sediment flux km³ /30.000 yrs.
City Creek Canyon	0.5
Red Butte Canyon	0.3
Emigration Canyon	0.5
Parleys Canyon	1.0
Mill Creek Canyon	1.3
Big Cottonwood Canyon	0.7
Little Cottonwood Canyon	1.1
Total discharge volume km³/30.000 years	**5.4**